Biomedicine & Pharmacotherapy 100 (2018) 221–225

Contents lists available at ScienceDirect

Biomedicine & Pharmacotherapy

journal homepage: www.elsevier.com/locate/biopha

Swertisin ameliorates diabetes by triggering pancreatic progenitors for islet neogenesis in Streptozotocin treated BALB/c mice

Abhay Srivastava, Nidheesh Dadheech[1], Mitul Vakani, Sarita Gupta*

Molecular Endocrinology and Stem Cell Research Lab, Department of Biochemistry, Faculty of Science, The Maharaja Sayajirao University of Baroda, Vadodara, Gujarat, 390002, India

ARTICLE INFO

Keywords:
Islet neogenesis
Pancreatic progenitors
Diabetes mellitus
Swertisin

ABSTRACT

In the present study, Swertisin's role in triggering resident pancreatic progenitors for islet neogenesis in Streptozotocin (STZ) diabetic mice was explored. STZ diabetic mice when treated with Swertisin demonstrated reversion to normoglycemia and significant elevation of fasting serum insulin levels. On screening the pancreatic tissue post Swertisin treatment in the STZ diabetic mice, we observed significant up-regulation of key transcription factors viz. Pdx1, Neurog3, MafA and Nkx6.1 required for islet neogenesis and beta cell homeostasis. We further observed increase in expression of Nestin and Neurog3 positive population; Nestin and Glut2 positive population and increase in c-peptide and Glucagon positive population within the Islets of Langerhans indicating increased pancreatic progenitor activity and their differentiation into Insulin producing beta cells in Swertisin treated STZ diabetic mice. Thus, this short study highlights pancreatic innate capability to regenerate and recover using its own resident progenitors upon appropriate stimulus, which could culminate into an effective diabetic therapy.

1. Introduction

The hallmark of diabetes is loss of insulin producing beta cells leading to hyperglycaemia due to insufficient insulin production [1]. Various therapies have evolved till date for the amelioration of diabetic condition including pancreatic regenerative therapy [2].

The origin of the newly created islets or the pancreatic progenitor source or their exact characteristics has been a highly controversial topic in the field of islet biology. Hence, existing reports suggest that pancreatic progenitors can have either acinar, ductal and/or islet source within the pancreatic tissue [3]. Popular convection although still controversial, suggests that there exists pancreatic progenitors that migrate and differentiate into islets when required [4]. The advantage of pancreatic progenitors is to differentiate very efficiently and very quickly into islets or insulin producing beta cells [5].

In recent years various stem cell sources have been identified to produce insulin producing beta cells and different stem cells require different induction along with culture media conditions to be differentiated into functional islet clusters. There are many molecules that have been previously reported for islet neogenesis e.g. Activin-A, Betacellulin, KGF, Exendin-4, Nicotinamide etc. [6]. In the present study, we have used Swertisin, which was isolated from an Indian herb *Enicostemma littorale* (EL). EL is an anti-diabetic plant used in traditional Indian medicine and swertisin has been characterised as a potent islet differentiating agent. Our group have previously reported Swertisin's islet neogenic potential on NIH3T3 and PANC1 cell lines in vitro and in pancreatectomised mice model in vivo. Swertisin in these studies successfully induced differentiation into insulin producing islets which responded to glucose challenge. Further, when these islets were transplanted in the type 1 diabetic mice model, they were able to ameliorate the diabetic condition effectively [7,8]. Here, we have tried to emphasize that a small molecule Swertisin can trigger pancreatic progenitors by up-regulating key transcription factors essential for replenishment of lost beta cells and recovery of pancreatic endocrine function, thus providing an incredible therapeutic intervention in the treatment for diabetes mellitus.

2. Material and methods

2.1. Chemicals

All chemicals, culture media and molecular biology reagent used in this study were purchased from Sigma Aldrich and Invitrogen, ThermoFisher Scientific. The details of the antibodies used are given in

* Corresponding author.
E-mail address: sarita.gupta-biochem@msubaroda.ac.in (S. Gupta).
[1] Current affiliation: Dr. Jean Buteau Laboratory, Alberta Diabetes Institute, University of Alberta, Edmonton T6G 2E1, Alberta, Canada.

https://doi.org/10.1016/j.biopha.2018.01.096
Received 29 November 2017; Received in revised form 16 January 2018; Accepted 24 January 2018

Table 1
List of Antibodies.

Sr. No.	Antibody	Company & Catalog No.	Isotype IgG	Mono/ Polyclonal Ab	Mol. Weight (kDa)	Application	Dilution
1	Pdx-1	BD#554655	Mouse	Mono	40	Immunoblotting/ Immunofluorescence	1:1000/ 1:200
2	Neurogenin-3	Sigma #SAB1306585	Rabbit	Poly	23	Immunoblotting/ Immunofluorescence	1:1000/ 1:100
3	MAFA	Sigma #SAB2105099	Rabbit	Mono	40	Immunoblotting	1:1000
4	Nkx 6.1	DSHB #F64A6B4	Mouse	Poly	40	Immunoblotting/ Immunofluorescence	1:40/1: 20
5	GLUT2	Sigma #SAB1303865	Rabbit	Mono	61	Immunoblotting/ Immunofluorescence	1:1000/ 1:100
6	β-Actin	BD#612657	Mouse	Mono	42	Immunoblotting	1:10000
7	Nestin-PE	BD#561230	Mouse	Mono	177	Immunofluorescence	1:100
8	Glucagon	Sigma#G 2654	Mouse	Mono	3.48	Immunofluorescence	1:100
9	C-Peptide	CST#4593	Rabbit	Mono	5	Immunofluorescence	1:100
10	Anti-Mouse-IgG-	Jackson ImmunoResearch #115-035-003	Goat	Poly		Immunoblotting	1:5000
11	Anti-Rabbit-IgG-HRP	Jackson Immuno Research #111-035-003	Goat	Poly		Immunoblotting	1:5000
12	Anti-Rabbit-IgG-FITC	Sigma#F9887	Goat	Poly		Immunofluorescence	1:200
13	Anti-Mouse-IgG-CF555	Sigma#SAB4600299	Goat	Poly		Immunofluorescence	1:100

Table 1.

2.2. Isolation and characterization of Swertisin

Swertisin was isolated and purified from the whole dried plant of *Enicostemma littorale* as previously described [7].

2.3. Animal selection and induction of diabetes and in vivo experimental design

Adult virgin female BALB/c mice weighing 20–25 g aged 6–8 weeks were kept at animal house with 12 h light and dark cycle with water and pellet diet *ad libitum*. Gender was selected as per the availability of mice at the animal house at the time of the study. Diabetes was induced with STZ injection (65 mg/kg body weight) intraperitoneally for 5 days with overnight fasting. Diabetic status of animals was confirmed by monitoring Fasting Blood Glucose (FBG) using Accu-check Performa glucometer (Accu-check, Roche, USA) at regular intervals as shown in Fig. 1A. Eight animals were distributed per group.

Swertisin treatment Design: The STZ diabetic mice were treated with Swertisin (2.5 mg/kg body wt.) from 14th day of experiment till 30th day after which the mice were sacrificed. Swertisin was administered with saline intravenously through tail vein. Fasting serum insulin was estimated and compared within the groups on the day of sacrifice.

These studies were carried out in strict accordance as per the guidelines and approval of institutional Committee for the Purpose of Control and Supervision on Experiments on Animals, India (CPCSEA). Post experiment animals were euthanatized using xylazine (10 mg/kg) and ketamine (150 mg/kg) injection followed by cervical dislocation ensuring death.

2.4. Insulin ELISA

Fasting serum Insulin was analyzed using mouse-insulin ELISA (Mercodia Inc., USA) as per manufacturer's protocol.

2.5. Protein extraction and western blotting

Tissue were harvested and kept on ice. Tissues were minced with the help of a mortar and pestle in liquid nitrogen on ice. The mashed tissue powder was resuspended in Laemmli buffer with 4 M urea and sonicated on ice for 7 cycles of 20 s with 2 s on and 0.2 s off sequence with 2 min on ice between every cycle at 45% amplitude. 20 µg of total protein as estimated by Bradford's method was resolved on SDS-PAGE Tris-glycine gels and transferred to nitrocellulose membrane. Non-specific binding was blocked by incubating the membranes in 5% fat free skimmed milk with 0.1% Tween-20 in PBS/TBS for 1 h at RT. The blots were subsequently incubated overnight with primary antibodies against the following proteins: PDX-1, NEUROG-3, NKX6.1, MAFA, GLUT2 and β-ACTIN at 4 °C, with gentle agitation. Blots were washed with TBS/PBS containing 0.1% Tween (TBS/PBS-T) (4 × 15 min) and then incubated with respective secondary antibodies conjugated with HRP for 1 h at RT with gentle agitation (Table 1). After four washes with PBS/TBS-T and two washes with PBS/TBS; specific bands of immune-reactive proteins were visualized using Ultrasensitive enhanced chemiluminiscence reagent (Millipore, USA) and images were captured on chemigenious gel documentation system (Uvitech, Cambridge).

2.6. Cryosectioning & immunohistochemistry

After treatment period when mice were sacrificed, splenic pancreas were dissected out and fixed by immersion in 4% paraformaldehyde overnight at 4 °C and then cryo-protected in 15% and 30% sucrose solutions in 0.1 M sodium phosphate buffer (pH 7.4). These tissues were then embedded in tissue freezing medium (OCT, Leica), and frozen. Pancreatic tissue sections were mounted on Poly-L -lysine coated slides. Cryosectioning was performed on a cryostat (Leica CM1520) at 20 µm intervals. Sections were incubated in blocking buffer [2% fetal bovine serum, 2% bovine serum albumin, 0.1% Triton X-100 in Phosphate Buffer Saline (PBS) with pH 7.4] followed by incubation in primary antibody overnight at 4 °C (Table 1). After incubation, sections were rinsed in washing buffer (ten times diluted blocking buffer in PBS) and then incubated respective secondary antibody (Table 1). Further, sections were counterstained with the DNA stain DAPI, washed with PBS, mounted with coverslips and finally sealed with transparent nail paint. Immunostained sections were viewed under confocal microscope (Zeiss LSM 710) and the fluorescence above the negative slides (only secondary antibody treated) was captured.

2.7. Statistical analysis

The data is presented as mean ± SEM. The significance of difference was evaluated by the paired Student's *t*-test. When more than one group was compared with one control, significance was evaluated

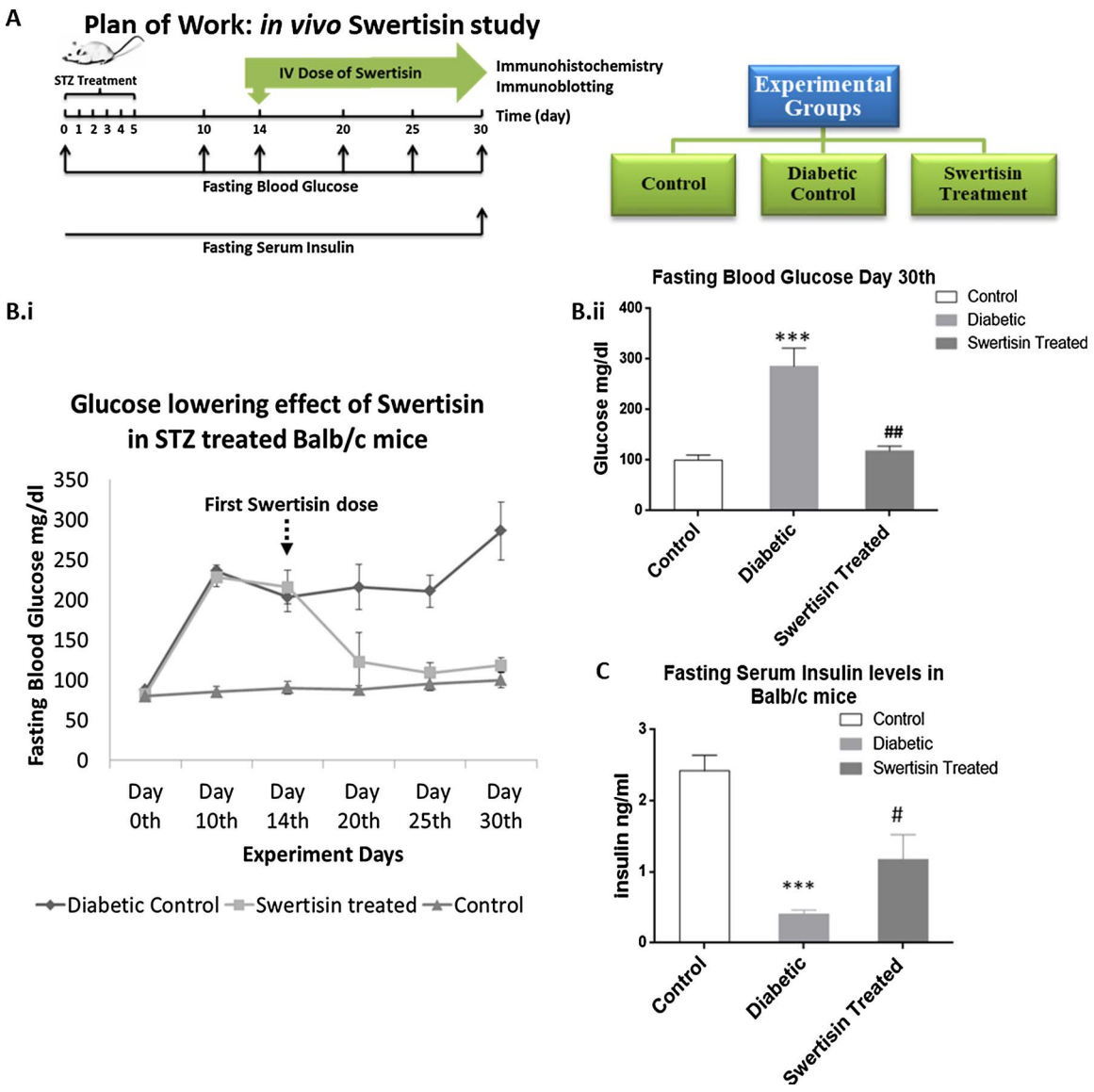

Fig. 1. Assessment of Fasting blood glucose and serum insulin levels post Swertisin treatment in STZ diabetic BALB/c mice: (A) Experimental design for Swertisin treatment for extended time period: Schematic representation of the work flow for the in vivo Swertisin treatment in STZ diabetic BALB/c mice (n = 8). (Bi & ii) Graph represents fasting blood glucose level at regular time intervals for control, diabetic and Swertisin treated STZ diabetic BALB/c mice. The graphs are plotted with mean values ± SEM. ***p ≤ 0.001 Control vs Diabetic. ##p ≤ 0.01 Diabetic vs Swertisin Treated (n = 5/6). (C) Here, graph represents comparative fasting serum insulin level after Swertisin treatment to STZ induced diabetic BALB/c mice. The graphs are plotted with mean values ± SEM. ***p ≤ 0.001 Control vs Diabetic. #p ≤ 0.05 Diabetic vs Swertisin Treated (n = 3).

according to one-way analysis of variance (ANOVA).

3. Results

3.1. Assessment of Fasting blood glucose and serum insulin levels post Swertisin treatment in STZ diabetic BALB/c mice

STZ treatment caused a significant increase in the FBG levels and decrease in Fasting serum insulin levels in the diabetic BALB/c mice. We observed that with the treatment of Swertisin there was a decrease in the FBG levels, which came back to normal range in a week's time and persisted till the end of Swertisin treatment after which the mice were sacrificed. Further, the fasting serum insulin levels were significantly increased after the Swertisin treatment. Acquiring normoglycemia and increase in the insulin levels were clear indication of ameliorated endocrine pancreatic function (Fig. 1B.i and ii, and C).

3.2. Assessment of islet neogenesis by analysing pancreatic protein expression post Swertisin treatment in STZ diabetic BALB/c mice

Protein expression data gave us a comprehensive understanding with respect to recovery of diabetic mice post Swertisin treatment. We observed that the key transcription factors viz. PDX1, NEUROG3, MAFA, NKX6.1 and GLUT2 essential for endocrine pancreatic development, regeneration and function were significantly elevated in the Swertisin treated group compared to diabetic condition. This suggested that the diabetic pancreas when treated with Swertisin was able to recover its function. β Actin served as endogenous control (Fig. 2A.i–vi).

Finally, in the immunohistochemistry data we compared the diabetic mice pancreas to the Swertisin treated mice pancreas. Here, we observed an increased expression of NESTIN, NEUROG3 and GLUT2 positive cells compared to the islets in the diabetic mice. Also, the islets in the diabetic pancreas appeared to be hollowed due to the impact of STZ whereas there was significant recovery in Swertisin treated mice

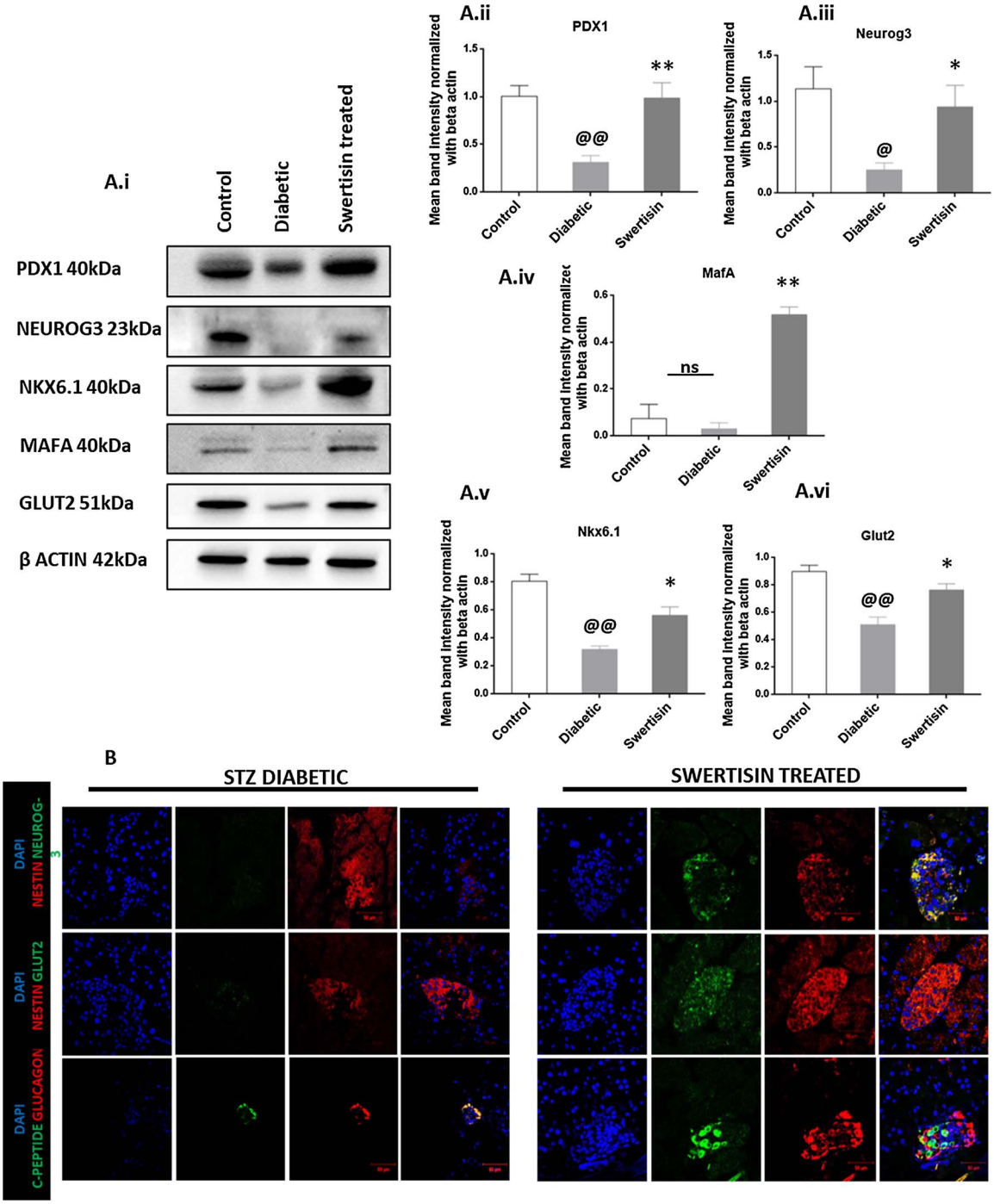

Fig. 2. Pancreatic Protein expression in Swertisin treated STZ diabetic mice: (Ai) Comparative protein profile for the key transcription factors and markers essential for endocrine pancreatic regeneration using immunoblotting has been demonstrated. The transcription factors are as follows: PDX1, NEUROG3, MAFA, NKX6.1, GLUT2 and BETA ACTIN as endogenous control. (Aii–vi) Densitometric graphs are plotted with mean ± SEM band intensity normalized with BETA ACTIN levels for respective proteins, @ = Control vs Diabetic (@@ ≤ 0.005 p value and @ ≤ 0.05 p value) and * = Diabetic vs Swertisin (** ≤ 0.005 p value and * ≤ 0.05 p value) (n = 3). (B) Comparative immunohistochemistry of Diabetic mice pancreas and Diabetic mice treated with Swertisin. A combination of NEUROG3 (green) along with NESTIN (red), GLUT2 (green) along with NESTIN (red) and C-PEPTIDE (green) along with GLUCAGON (red) were observed to focus on pancreatic resident endocrine progenitors and endocrine pancreas. Nuclei were stained with DAPI (blue) (n = 3).

pancreas. Presence of c-peptide was observed more prominently in the Swertisin treated mice pancreas. This data suggested that Swertisin treatment was capable of triggering the resident progenitor population within the pancreas to regenerate the damaged beta cells and thus recover the endocrine pancreatic function (Fig. 2B).

4. Discussion

Limitations of donor islets have prompted renewed interest in islet regeneration as a source of new islets [9]. In this study, we tested whether diabetic adult BALB/c mice can stimulate Islet regeneration by administration of exogenous Swertisin. The aim of the present study was to trigger pancreatic progenitors in STZ treated diabetic mice model so that they can stimulate the pancreatic endocrine recovery thereby ameliorating pancreatic endocrine regeneration and function. Mice were confirmed for hyperglycaemia and administered with Swertisin. Swertisin administration systematically brought the mice FBG levels back to normoglycaemic values by tenth day of Swertisin

treatment. We simultaneously monitored the fasting serum insulin levels which had also recovered significantly compared to diabetic mice. There have been other studies with naturally occurring compounds like Pterosin A and Conophyllin, that effectively reversed pancreatic endocrine function in STZ induced diabetic mice model [10,11]. It has been previously reported that STZ treatment result in partial beta cell death in a dose dependent manner [12]. Hence, to negate the effect of surviving beta cell population post STZ treatment, appropriate diabetic control group had been kept and all the respective parameters for diabetes and regeneration were monitored under similar conditions. Hence, all the improved effects that were observed with respect to serum fasting blood glucose, insulin level and the molecular profile in the pancreatic tissue is solely due to the administration of Swertisin.

We observed a significant increase in the protein expression of GLUT2 in Swertisin treated diabetic mice. GLUT2 positive progenitor population has been previously reported in the regenerating mice pancreas, post STZ treatment. Also, Pancreatic progenitor population expressing GLUT2 were not as susceptible to STZ exposure as beta cells and were able to survive and retain their potential of islet neogenesis [13,14]. In another study, GLUT2 was identified for enriching pancreatic progenitor population [15]. Hence, a significant rapid rise in the GLUT2 levels could be an indication of increased pool of pancreatic progenitor population triggered by Swertisin treatment in diabetic mice.

There was an increased up-regulation of other key transcription factors such as PDX1, NEUROG3, MAFA and NKX6.1 suggesting increase in pancreatic endocrine progenitor population and increased endocrine differentiation and function, which was visible phenotypically with respect to fasting blood glucose and fasting serum insulin. These transcription factors are also expressed after E9.5 followed by expression of GLUT2 at E10.5, prerequisite for the formation of the endocrine pancreas [16]. We observed similar results in the immunohistochemistry sections of Swertisin treated diabetic mice. We also observed NESTIN and NEUROG3 dual positive cells along with increased expression of GLUT2 and NESTIN positive cells in the islets of Langerhans indicating increased progenitor population and activity. An increased c-peptide expression within the islets further suggested increased differentiation with endocrine recovery and function.

5. Conclusion

Swertisin dose triggered islet neogenesis replenishing the insulin producing cells within pancreas in STZ diabetic mice model, thus ameliorating the diabetic condition. Hence, this study further strengthens our claim for Swertisin as a novel therapeutic intervention in effectively treating diabetes.

Author contribution

A.S.: Conception and design, Collection and/or assembly of data, Data analysis and interpretation and Manuscript writing; N.D.: Conception and design and assembly of data; M.V.: Collection and/or assembly of data and Data analysis and interpretation; S.G.: Conception and design, Financial support, Provision of study material, Data analysis and interpretation, Manuscript writing and Final approval of manuscript.

Disclosure statement

We wish to confirm that there is no potential conflict of interests.

Acknowledgements

We acknowledge the Department of Biotechnology for establishing Instrumentation facility under DBT-MSUB-ILSPARE program, which allowed us to have access to the Confocal microscopy facility and other instruments. We also acknowledge CSIR-UGC-NET Fellowship for providing fellowship to the First author.

References

[1] N.S. Wilcox, J. Rui, M. Hebrok, K.C. Herold, Life and death of β cells in type 1 diabetes: a comprehensive review, J. Autoimmun. 71 (2016) 51–58.
[2] F. Yi, G.-H. Liu, Stem cell therapy for diabetes: a call for efficient differentiation of pancreatic progenitors, J. Regenerat. Med. 2 (1) (2013).
[3] S. Afelik, M. Rovira, Pancreatic beta-cell regeneration: facultative or dedicated progenitors? Mol. Cell. Endocrinol. 445 (2017) 85–94.
[4] Y. El-Gohary, J. Wiersch, S. Tulachan, X. Xiao, P. Guo, C. Rymer, S. Fischbach, K. Prasadan, C. Shiota, I. Gaffar, Intraislet pancreatic ducts can give rise to insulin-positive cells, Endocrinology 157 (1) (2016) 166–175.
[5] H. Noguchi, Pancreatic stem/progenitor cells for the treatment of diabetes, Rev. Diabet. Stud. 7 (2) (2010) 105–111.
[6] R.S. Wong, Extrinsic factors involved in the differentiation of stem cells into insulin-producing cells: an overview, Exp. Diabet. Res. 2011 (2011) 406182.
[7] N. Dadheech, S. Soni, A. Srivastava, S. Dadheech, S. Gupta, R. Gopurappilly, R.R. Bhonde, S. Gupta, A small molecule swertisin from enicostemma littorale differentiates NIH3T3 cells into islet-like clusters and restores normoglycemia upon transplantation in diabetic Balb/c mice, Evid. Based Comp. Alternat. Med. eCAM 2013 (2013) 280392.
[8] N. Dadheech, A. Srivastava, N. Paranjape, S. Gupta, A. Dave, G.M. Shah, R.R. Bhonde, S. Gupta, Swertisin an anti-diabetic compound facilitate islet neogenesis from pancreatic stem/progenitor cells via p-38 MAP kinase-SMAD pathway: an in-vitro and in-vivo study, PloS One 10 (6) (2015) e0128244.
[9] A.M. Shapiro, M. Pokrywczynska, C. Ricordi, Clinical pancreatic islet transplantation, Nat. Rev. Endocrinol. 13 (5) (2017) 268–277.
[10] I. Kojima, K. Umezawa, Conophylline: a novel differentiation inducer for pancreatic beta cells, Int. J. Biochem. Cell Biol. 38 (5–6) (2006) 923–930.
[11] F.L. Hsu, C.F. Huang, Y.W. Chen, Y.P. Yen, C.T. Wu, B.J. Uang, R.S. Yang, S.H. Liu, Antidiabetic effects of pterosin A, a small-molecular-weight natural product, on diabetic mouse models, Diabetes 62 (2) (2013) 628–638.
[12] W.J. Schnedl, S. Ferber, J.H. Johnson, C.B. Newgard, STZ transport and cytotoxicity. specific enhancement in GLUT2-expressing cells, Diabetes 43 (11) (1994) 1326–1333.
[13] Y. Guz, I. Nasir, G. Teitelman, Regeneration of pancreatic beta cells from intra-islet precursor cells in an experimental model of diabetes, Endocrinology 142 (11) (2001) 4956–4968.
[14] M. Banerjee, R.R. Bhonde, Islet generation from intra islet precursor cells of diabetic pancreas: in vitro studies depicting in vivo differentiation, JOP J. Pancreas 4 (4) (2003) 137–145.
[15] H. Segev, B. Fishman, R. Schulman, J. Itskovitz-Eldor, The expression of the class 1 glucose transporter isoforms in human embryonic stem cells, and the potential use of GLUT2 as a marker for pancreatic progenitor enrichment, Stem Cells Dev. 21 (10) (2012) 1653–1661.
[16] L.C. Murtaugh, Pancreas and beta-cell development: from the actual to the possible, Development 134 (3) (2007) 427–438.

Received: 12 January 2018 | Accepted: 13 September 2018

DOI: 10.1002/jcp.27568

ORIGINAL RESEARCH ARTICLE

WILEY Journal of Cellular Physiology

Pancreatic resident endocrine progenitors demonstrate high islet neogenic fidelity and committed homing towards diabetic mice pancreas

Abhay Srivastava[1] | Nidheesh Dadheech[2] | Mitul Vakani[1] | Sarita Gupta[1]

[1]Molecular Endocrinology and Stem Cell Research Lab, Department of Biochemistry, Faculty of Science, The Maharaja Sayajirao University of Baroda, Vadodara, India

[2]Dr. AM James Shapiro Laboratory, Alberta Diabetes Institute, University of Alberta, Edmonton, AB, Canada

Correspondence
Sarita Gupta, Molecular Endocrinology and Stem Cell Research Lab, Department of Biochemistry, Faculty of Science, The Maharaja Sayajirao University of Baroda, Vadodara, Gujarat 390002, India.
Email: saritagupta9@gmail.com; sglmescrl@gmail.com

Funding information
Department of Biotechnology, Ministry of Science and Technology, Government of India, Grant/Award Number: BT/PR3564/BRB/10/975/2011

Abstract

Pancreatic progenitors have been explored for their profound characteristics and unique commitment to generate new functional islets in regenerative medicine. Pancreatic resident endocrine progenitors (PREPs) with mesenchymal stem cell (MSC) phenotype were purified from BALB/c mice pancreas and characterized. PREPs were differentiated into mature islet clusters in vitro by activin-A and swertisin and functionally characterized. A temporal gene and protein profiling was performed during differentiation. Furthermore, PREPs were labeled with green fluorescent protein (GFP) and transplanted intravenously into streptozotocin (STZ) diabetic mice while monitoring their homing and differentiation leading to amelioration in the diabetic condition. PREPs were positive for unique progenitor markers and transcription factors essential for endocrine pancreatic homeostasis along with having the multipotent MSC phenotype. These cells demonstrated high fidelity for islet neogenesis in minimum time (4 days) to generate mature functional islet clusters (shortest reported period for any isolated stem/progenitor). Furthermore, GFP-labeled PREPs transplanted in STZ diabetic mice migrated and localized within the injured pancreas without trapping in any other major organ and differentiated rapidly into insulin-producing cells without an external stimulus. A rapid decrease in fasting blood glucose levels toward normoglycemia along with significant increase in fasting serum insulin levels was observed, which ameliorated the diabetic condition. This study highlights the unique potential of PREPs to generate mature islets within the shortest period and their robust homing toward the damaged pancreas, which ameliorated the diabetic condition suggesting PREPs affinity toward their niche, which can be exploited and extended to other stem cell sources in diabetic therapeutics.

KEYWORDS
cellular homing, diabetes mellitus, islet differentiation, pancreatic progenitors

1 | INTRODUCTION

Glucose homeostasis is tightly regulated by the hormones of the endocrine pancreas and any disturbance in its function can lead to metabolic disorders causing diabetes mellitus, with the loss of pancreatic β cells as its hallmark (Edlund, 2001; S. K. Kim & Hebrok, 2001). Even after decades of extensive research, there is no cure for diabetes. Available drugs can only manage the progression of the diabetic condition. In recent years, islet transplantation has become a hopeful therapeutic intervention. However, the limitation of

cadaveric donor islets has created a dilemma for its therapeutic clinical transition for diabetic patients. Hence, it is here that regenerative medicine and cell therapy renders excellent promise for providing pancreatic islet differentiation using various stem cell sources (Staels et al., 2016).

Embryonic stem cells (ESCs) and induced pluripotent stem cells (iPSCs) have been explored widely for generating functional islet clusters but there have been distinct hurdles, such as the absence of certain essential pancreatic markers, having a low index for glucose-stimulated insulin secretion (GSIS) and the vast amount of time taken for producing the insulin-producing cells. This has compelled researchers to look into other stem cell sources and adult stem cells provide a better platform in terms of clinical and ethical acceptability and availability for islet neogenesis. Adult stem cells, both pancreatic and nonpancreatic, have been successfully differentiated into functional islet clusters. Nonpancreatic adult stem cells mainly mesenchymal stem cells (MSCs) from various sources such as bone marrow, umbilical cord, adipose tissue, dental pulp, and so forth have been used in in vitro studies to increase the islet mass. The literature suggests that there are mainly three distinct sources of pancreatic adult stem cells or pancreatic progenitors that is progenitors from an acinar origin, the ductal progenitors and the intra-islet progenitors which have the potential to generate new insulin-producing cells (Afelik & Rovira, 2017; Jiang & Morahan, 2014; Wen, Chen, & Ildstad, 2011). Here, in this study, we have focused on adult stem cells from the pancreas and have extensively characterized them as pancreatic resident endocrine progenitors (PREPs) having MSC characteristics along with their extraordinary islet neogenic and pancreatic homing properties.

Different types of stem cells require different induction and culture media conditions to be differentiated into functional islet clusters, there are many molecules that can be used for islet neogenesis, for example, activin-A, β-cellulin, keratinocyte growth factor, exendin-4, nicotinamide, and so forth (Wong, 2011). In the current study, we have used activin-A and Swertisin, two potent islet differentiating agents. Swertisin, a flavone has been derived from an Indian herb, *Enicostemma littorale* (a perennial herb), whose potent islet neogenic potential has been well characterized by our research group. Our group has previously reported their islet neogenic potential on NIH3T3 and PANC1 cell lines in vitro and in the pancreatectomised mice model in vivo (Dadheech et al., 2013, 2015). We have further demonstrated that swertisin can stimulate pancreatic progenitors in diabetic mice to recover its lost endocrine pancreatic function (Srivastava, Dadheech, Vakani, & Gupta, 2018).

A series of investigations have evaluated the MSCs migratory property toward damaged tissues known as homing (Chamberlain, Fox, Ashton, & Middleton, 2007; Henschler, Deak, & Seifried, 2008; Karp & Teo, 2009; Yagi et al., 2010). Homing is the *trans*-endothelial migration of the MSCs after getting localized into the vasculature of damaged/target tissue (Karp & Teo, 2009). Previous reports on transplantation of MSCs to manage diabetes also showed homing of these cells in the pancreas but with very little efficacy (Deans & Moseley, 2000; Ezquer et al., 2008; Hess et al., 2003; Lee et al., 2006). Furthermore, chemokine-mediated homing of MSCs has been exploited in the paradigm of wound healing in diabetic and obese conditions (Hocking, 2015). Researchers have also being focusing on stimulation of MSCs in different conditions for increased homing and participation for regeneration in skeletal diseases, heart regeneration, arthritis, and cancer (Eseonu & De Bari, 2015; Kristocheck et al., 2018; Lin et al., 2017; Xie et al., 2017).

The ideal scenario in treating diabetes mellitus would be complete replacement of damaged β cells within islets and the ideal candidate to perform this task would be inherent pancreatic progenitors. Although, the notion of stimulating pancreatic progenitors and increasing β-cell mass is being explored extensively by several groups, there exists a large void in understanding the origin, identity and potential of these cells (Jiang & Morahan, 2015). In the present investigation, we have explored the robust homing demonstrated by unique characteristics of PREPs, which is clinically relevant for diabetes therapeutics. This homing property can be exploited by other stem cells like ESCs, iPSCs, and MSCs from various sources, which can be differentiated into the pancreatic progenitor state and then transplanted for improved clinical and therapeutic efficacy, thus developing a personalized cell-based treatment (Aigha, Memon, Elsayed, & Abdelalim, 2018; Faleo, Lee, Nguyen, & Tang, 2016; Memon, Karam, Al-Khawaga, & Abdelalim, 2018; Rezania et al., 2013).

2 | MATERIALS AND METHODS

2.1 | Chemicals and other material

All chemicals and culture media used in this study were purchased from Sigma Aldrich and Invitrogen, Thermo Fisher Scientific. The details of the antibodies used are given in the Supporting Information Table S6. Molecular biology reagents and complementary DNA (cDNA) and polymerase chain reaction (PCR) kits were procured from Invitrogen, Thermo Fisher Scientific. The C2C12 cell line, a muscle progenitor cell line was procured from the National Centre For Cell Sciences, Pune (The National Animal Cell Repository).

2.2 | Islet isolation and culturing

Islets were isolated from healthy (6 weeks) male BALB/c mice maintaining sterile conditions by the method of Xia and Laychock (1993).

2.3 | Isolation and establishment of mouse PREPs

Mouse pancreatic resident endocrine progenitors were isolated from a fresh islet preparation followed by digestion of whole mouse pancreas as previously described (Dadheech et al., 2015; Joglekar & Hardikar, 2012; Srivastava et al., 2016). Two pancreata were used per isolation. Islet preparation was confirmed with 90% dithizone (DTZ) positive structures. Freshly isolated islets (5,000 islets per 25 cm^2 flask; Nunc, Thermo Fisher Scientific, India) were placed and

cultured in Roswell Park Memorial Institute 1640 complete media with 10% serum (Gibco, Thermo Fisher Scientific, India) for 24 hr and then shifted to Dulbecco's modified Eagle's medium (DMEM) high glucose complete media with 10% serum (Gibco, Fisher Scientific, India) to promote monolayer formation. Cultures were maintained in 95% air/5% CO_2 at 37°C, and the medium was renewed every alternate days. Islets in these conditions slowly disintegrate to form a monolayer of cells. The monolayers were subcultured when the cells had grown to 70% confluence. Gradually, the terminally differentiated cells undergo senescence following the survival of a homogenous cell population. The derived monolayers were characterized at passage-10 of the culture period before utilizing in the subsequent investigations.

2.4 | Immunocytochemistry (ICC)

Undifferentiated PREPs and functional islets were characterized using ICC. Briefly, growing cells or clusters were fixed with 4% paraformaldehyde (PFA) for 10 min at 4°C (islets were further incubated with chilled absolute methanol for 10 min at room temperature) and proceeded with ICC as discussed in our previous reports (Dadheech et al., 2015).

2.5 | Cryosectioning and ICC

The splenic pancreas were dissected out, and cryosectioning was performed as discussed in the supplementary data of our previous report (Chruvattil et al., 2016). Sections were incubated in blocking buffer (2% fetal bovine serum, 2% bovine serum albumin [BSA], and 0.1% Triton X-100 in phosphate-buffered saline [PBS] with pH 7.4) followed by steps similar to the ICC described above.

2.6 | Surface marker and intracellular marker staining by flow cytometry

Cells were trypsinized, resuspended 0.5×10^6 cells/tube in 100 µl of staining media (PBS with 1% BSA) and stained with the respective primary and secondary antibodies (fixed for intracellular marker staining with 4% PFA and chilled absolute methanol). They were washed and analyzed on BD FACS ARIAIII with a 70 µM nozzle and 70 PSI pressure conditions. For green fluorescent protein (GFP) and GFP-insulin dual positive acquisition, 100,000 cells were acquired on a flow cytometer per tube and 30,000 for the rest. Flowjo™ was used for data analysis.

2.7 | Trilineage differentiation

The cells were plated into a six-well plate at 10^5 cells/well in the presence of osteocyte reagents (20 mM B-glycerol phosphate, 50 µg/ml ascorbic acid, and 10 mM dexamethasone) for 10 days. The culture medium was replaced every third day. Adipogenesis was induced by treatment with IBMax (10 mg/ml), 10 mM dexamethasone, and 10 mg/l insulin for 8 days. The culture medium was replaced every third day. Chondrocyte differentiation was induced by treatment with 10 mM dexamethasone and 10 mg/L insulin for 20 days. The culture medium was replaced every fifth day.

2.8 | Islet differentiation

The cells were allowed to differentiate in the presence of serum-free DMEM knockout media (Invitrogen, ThermoFisher Scientific), activin-A (Sigma-Aldrich), and Swertisin, stock concentration of 30 mg/ml in dimethyl sulphoxide was added into the growth media to a final concentration of 15 µg/ml (Dadheech et al., 2013, 2015). PREPs were differentiated using activin-A at 20 ng/ml and swertisin at 15 µg/ml concentrations as differentiating agents in a 4-day differentiation protocol with insulin (5 µg/ml), transferrin (5 µg/ml), and selenite (5 ng/ml) cocktail.

2.9 | Protein extraction and western blot analysis

Protein samples from cells, differentiated clusters, and dissected pancreatic tissue after PREP transplantation and swertisin treatment was harvested and homogenized. Immunoblotting was performed as described in our previous reports (Dadheech et al., 2015).

2.10 | RNA extraction, first strand cDNA synthesis and real-time quantitative PCR (qRT-PCR)

RNA was harvested from the C2C12 cell line, undifferentiated PREPs, and clusters at every time point during islet differentiation across groups followed by cDNA preparation and qRT-PCR, as described in our previous report (Dadheech et al., 2015). The primers used for the RT-PCR are given in Supporting Information Table S7.

2.11 | Insulin and c-peptide ELISA

Glucose-stimulated c-peptide release assay: Differentiated islet clusters were challenged with 5.5 and 20 mM glucose in KRBH, respectively, as discussed in our previous report (Dadheech et al., 2013). Serum insulin and c-peptide were analyzed using mouse-insulin ELISA (Mercodia Inc.) and mouse-c-peptide ELISA (ALPCO Immunoassays), respectively, as per the manufacturer's protocol.

2.12 | Transfection and GFP labeling

Transfection of PREPs (passage #12) with p-eGFPN1 (Clontech) was performed by using a Neon electroporation system (Invitrogen) with one pulse at a pulse voltage of 1300 mV with a pulse width of 40 ms and plating the cells on a 3.5 cm^2 dish, according to the manufacturer's protocol. Stable GFP expressing clones were selected by growing them in media containing G418 at 300 µg/ml. Clones were purified from isolated colonies using clonal discs and scaled up for transplantation in BALB/c mice.

2.13 | Animal selection and Induction of diabetes and in vivo experimental design

Adult virgin female mice of BALB/c strain weighing 20–25 g aged 6–8 weeks were kept at an animal house with a 12 hr light and dark cycle with water and pellet diet ad libitum. Gender was selected as per the availability of mice at the animal house at the time of the study. Diabetes was induced with streptozotocin (STZ) injection (65 mg/kg body weight) intraperitoneally for 5 days with overnight fasting. The diabetic status of animals was confirmed by monitoring fasting blood glucose (FBG) using an Accucheck Performa glucometer (Accucheck, Roche) at regular intervals as shown in Figures 4a. Eight animals were distributed per group.

PREP transplantation design, 2×10^6 GFP-labeled PREPs per mice were transplanted in the diabetic mice intravenously through the tail vein with normal saline on Day 10 of the experiment. Animals were sacrificed and analyzed for various parameters on Day 15 of the

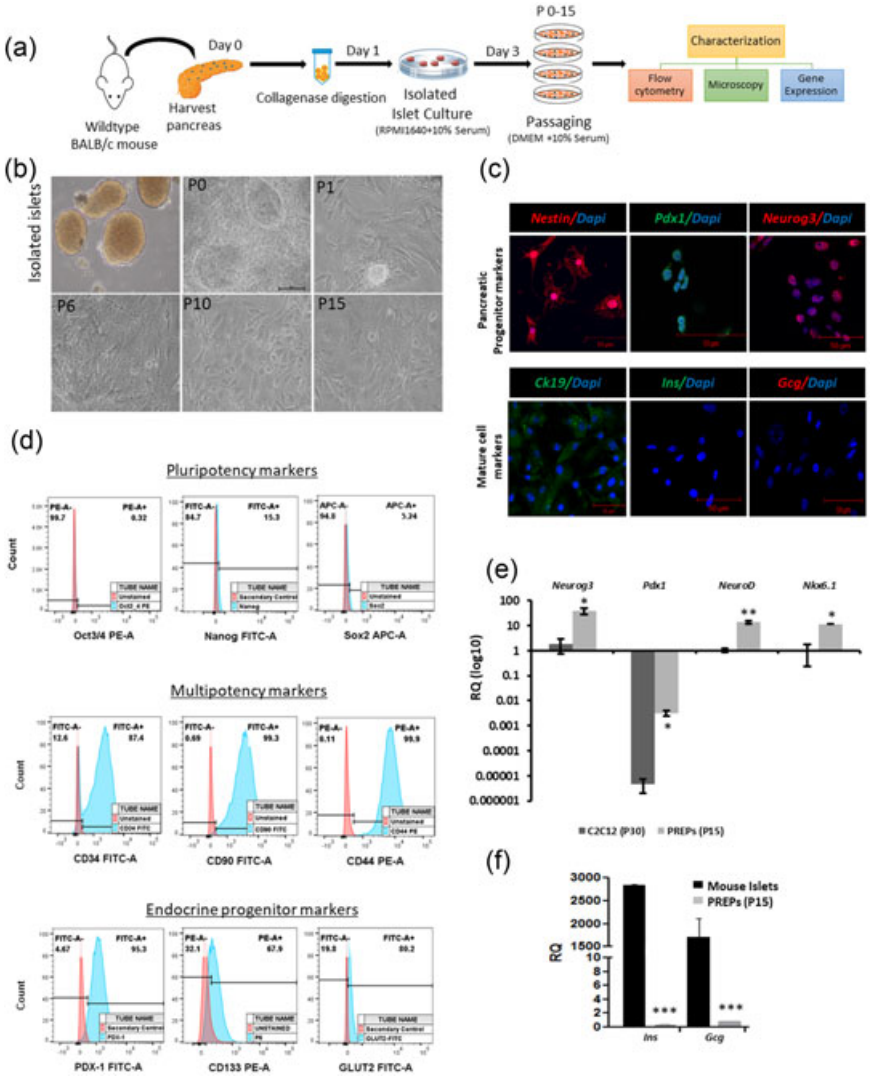

FIGURE 1 Isolation and characterization of pancreatic resident endocrine progenitors. (a) Schematic summary of work flow for purification and characterization of PREPs from BALB/c mice. (b) Culturing of mice islet of Langerhans and purification of PREPs by sequential passaging of endocrine pancreas from P_0 to P_{15}, where a homogeneous population of mesenchymal cells was observed to be purified with sequential passaging (scale bar = 100 μm; magnification: ×20). (c) Characterization of PREPs using immunocytochemistry was performed to identify their endocrine pancreatic stem cell origin and to confirm the absence of pancreatic hormones. Here the markers are as follows: Nestin (red), PDX1 (green), Neurog3 (red), CK19 (green), insulin (green), and glucagon (red). Nucleus is stained by DAPI, blue in color (scale bar = 50 μm, magnification: ×63; $N = 3$). (d) Characterization of PREPs using flow cytometry into mesenchymal stem cells was performed using various surface CD markers along with markers like GLUT2 and PDX1 ($N = 3$). (e) Gene expression using qRT-PCR of essential TFs (Neurog3, Pdx1, NeuroD1, and Nkx6.1) was screened in PREPs and compared with C2C12 muscle progenitor cell line taken as negative control. The graphs are plotted with mean ± *SEM*. $^*p \le 0.05$ and $^{**}p \le 0.01$ C2C12 versus PREPs ($N = 3$). (f) Comparison between PREPs' and mice pancreas insulin and glucagon transcript levels. The graphs are plotted with mean ± *SEM*. $^{***}p \le 0.001$ undifferentiated versus mice pancreas ($N = 3$). CD: cluster of designation; DAPI: 4′,6-diamidino-2-phenylindole; Gcg: glucagon; Ins: insulin; PREP: pancreatic resident endocrine progenitor; qRT-PCR: quantitative real-time polymerase chain reaction; TF: transcription factors [Color figure can be viewed at wileyonlinelibrary.com]

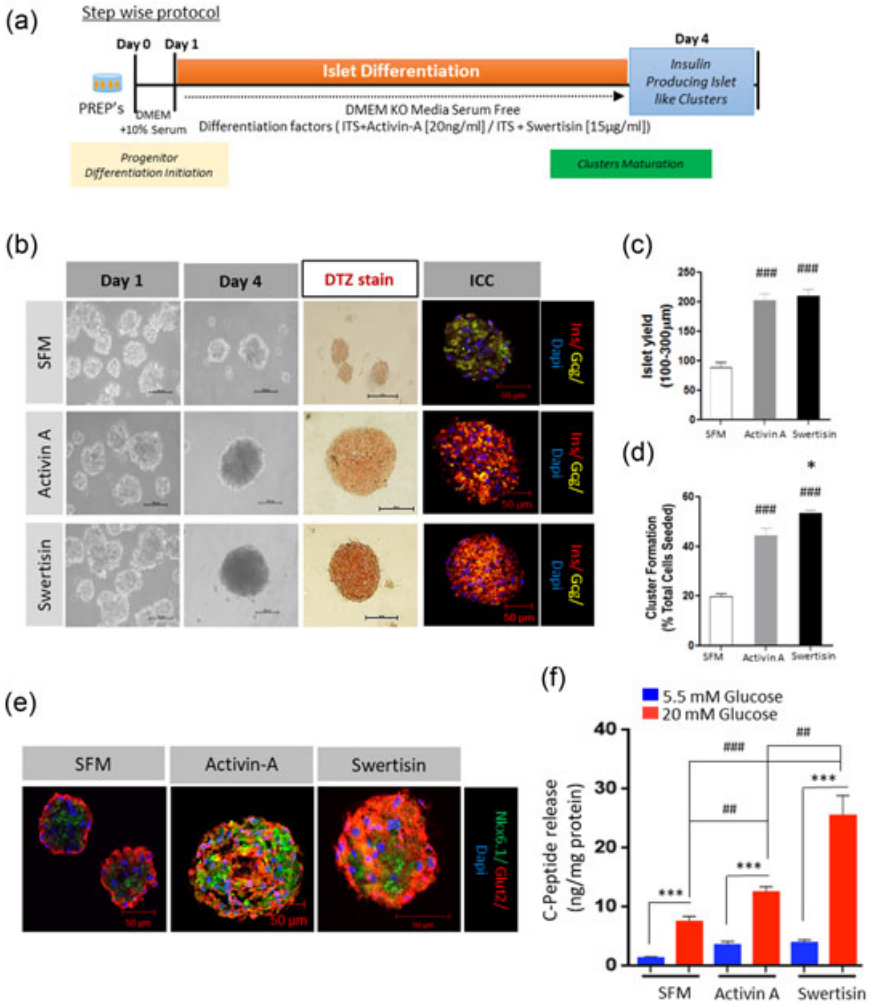

FIGURE 2 Islet differentiation from PREPs and their functional characterization. (a) Schematic representation of islet differentiation timeline and stepwise protocol from PREPs. (b) Microscopic morphological changes were observed during islet differentiation by using both activin-A and swertisin as differentiating agents. It can be observed that islet clusters begin to form from Day 1 itself, which are then allowed to mature till Day 4 of differentiation. To confirm mature islet formation DTZ staining was performed. Islets generated in the activin-A and swertisin groups stained positive for DTZ confirming the presence of insulin within, whereas SFM islets were negatively stained for DTZ suggesting incomplete or no differentiation. The scale bar at Day 0 represents 10 µm and differentiation is 100 µm (magnification: ×20). This was further confirmed by the immunocytochemistry of mature islets demonstrating the presence of insulin (red) along with glucagon (yellow-pseudocolor). Nuclei were stained with DAPI (blue) and the scale bar represents 50 µm (magnification: ×63; $N = 3$). (c) A comparison between total number of islet clusters formed between 100 and 300 µM diameter across the groups was made, to understand the effective islet yield after differentiation. (d) The graph signifies the percentage efficiency of islet formation across groups. The graph plotted is with mean ± *SEM*. $^{###}p \leq 0.001$ SFM versus activin-A and swertisin; $^{*}p \leq 0.05$ Activin versus swertisin ($N = 3$). (e) Immunocytochemistry of mature islet clusters, which were positive for nkx6.1 (green) along with Glut2 (red) in SFM, activin-A, and swertisin groups. Nuclei were stained with DAPI (blue; scale bar = 50 µm; magnification: ×63; $N = 3$). (e) C-peptide release assay was performed to confirm the responsiveness of differentiated islets to the presence of glucose. The graphs are plotted with mean ± *SEM*. $^{***}p \leq 0.001$ 5.5 mM SFM/activin-A/swertisin versus 20 mM SFM/activin-A/swertisin. $^{##}p \leq 0.01$ 20 mM SFM versus 20 mM activin-A and 20 mM activin-A versus 20 mM swertisin; $^{###}p \leq 0.001$ 20 mM SFM versus 20 mM swertisin ($N = 3$). DAPI: 4′,6-diamidino-2-phenylindole; DTZ: dithizone; ICC: immunocytochemistry; PREP: pancreatic resident endocrine progenitor; SFM: serum-free media [Color figure can be viewed at wileyonlinelibrary.com]

experiment that is on the fifth day post-PREPs transplantation. Fasting serum insulin along with other parameters were estimated and compared within the groups.

This study was carried out in strict accordance as per the guidelines and approval of the institutional Committee for the Purpose of Control and Supervision on Experiments on Animals, India. Post experiment animals were euthanized using xylazine (10 mg/kg) and ketamine (150 mg/kg) injection followed by cervical dislocation ensuring death.

2.14 | Statistical analysis

The data are presented as mean ± *SEM*. The significance of difference was evaluated by the paired Student's *t* test. When more than one

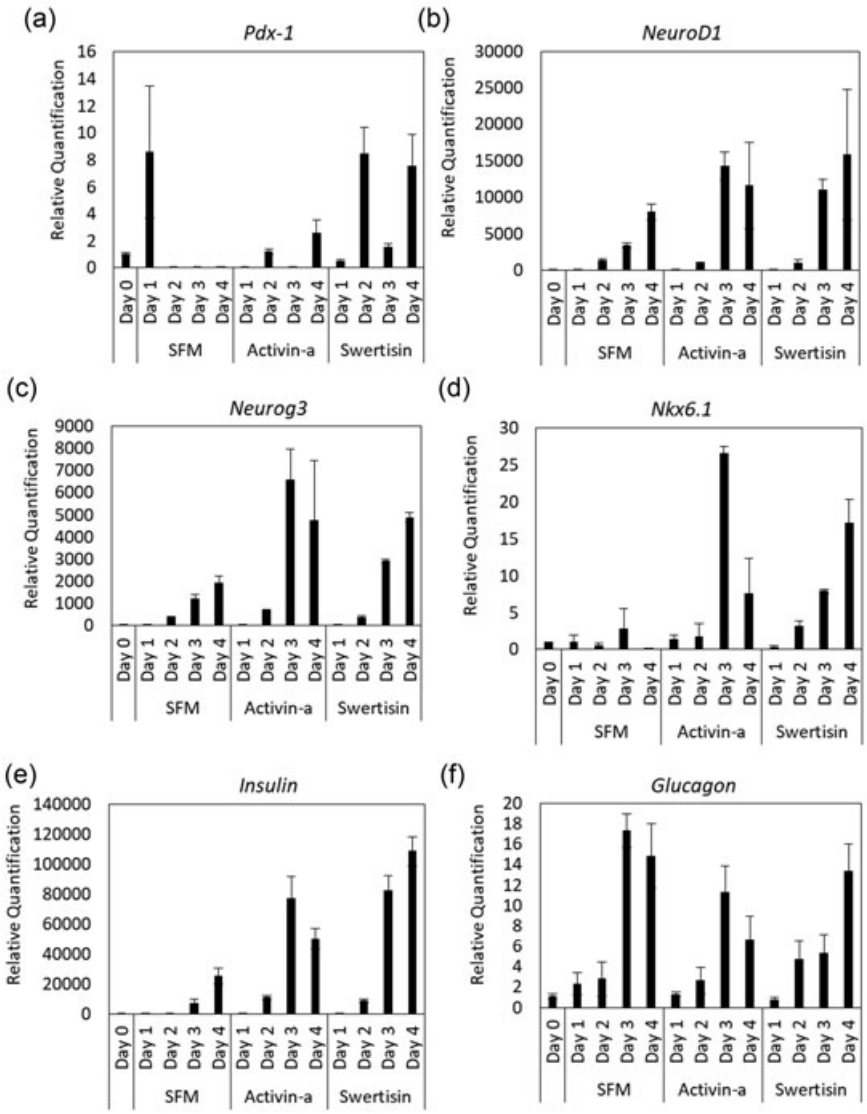

FIGURE 3 Temporal gene profiling in islet differentiation from PREPs. (a) Temporal day wise *Pdx1* expression during islet differentiation from PREPs for SFM, activin-A, and swertisin groups ($N = 3$). (b) Temporal day wise *NeuroD1* expression during islet differentiation from PREPs for SFM, activin-A, and swertisin groups ($N = 3$). (c) Temporal day wise *Neurog3* expression during islet differentiation from PREPs for SFM, activin-A, and swertisin groups ($N = 3$). (d) Temporal day wise *Nkx6.1* expression during islet differentiation from PREPs for SFM, activin-A, and swertisin groups ($N = 3$). (e) Temporal day wise *insulin* expression during islet differentiation from PREPs for SFM, activin-A, and swertisin groups ($N = 3$). (f) Temporal day wise *Glucagon* expression during islet differentiation from PREPs for SFM, activin-A, and swertisin groups ($N = 3$). PREP: pancreatic resident endocrine progenitor; SFM: serum-free media

group was compared with one control, significance was evaluated according to one-way analysis of variance.

3 | RESULTS

3.1 | PREPs were isolated and purified from the endocrine pancreas of BALB/c mice

Mice pancreas was harvested and chemically digested to isolate islet of Langerhans. These islet clusters disaggregated into a monolayer culture, which further leads to isolation and culturing of pancreatic progenitors. We obtained a homogenous population of cells with sequential passaging (Figure 1a,b). The purified cells were extensively passaged and characterized between passage 12–15 for stemness markers, pancreatic endocrine transcription factors (TFs) and MSC phenotype.

3.2 | PREPs demonstrated pancreatic endocrine progenitor nature with MSC phenotype

The ICC panel in Figure 1c defines these cells for their pancreatic neuroendocrine lineage by identifying the respective protein markers (Supporting Information Table S6). These cells were positive for markers like NESTIN, PDX1, NEUROG3, CK19, and negative for INSULIN and GLUCAGON in ICC (Figure 1c). These cells were further characterized for pluripotency markers namely, OCT3/4, SOX2, and NANOG, which were not expressed in these cells. They were then screened for a cluster of designation (CD) surface markers for the MSC phenotype. We observed the cells to be highly positive for CD90, CD44, CD34, CD133 along with PDX-1 and GLUT2. This confirmed their pancreatic endocrine progenitor and MSC phenotype (Figure 1d). These cells were screened for expression of TF genes essential for endocrine pancreas homeostasis namely, *Neurog3*, *Pdx1*, *NeuroD1*, and *Nkx6.1* which was compared with the C2C12 muscle

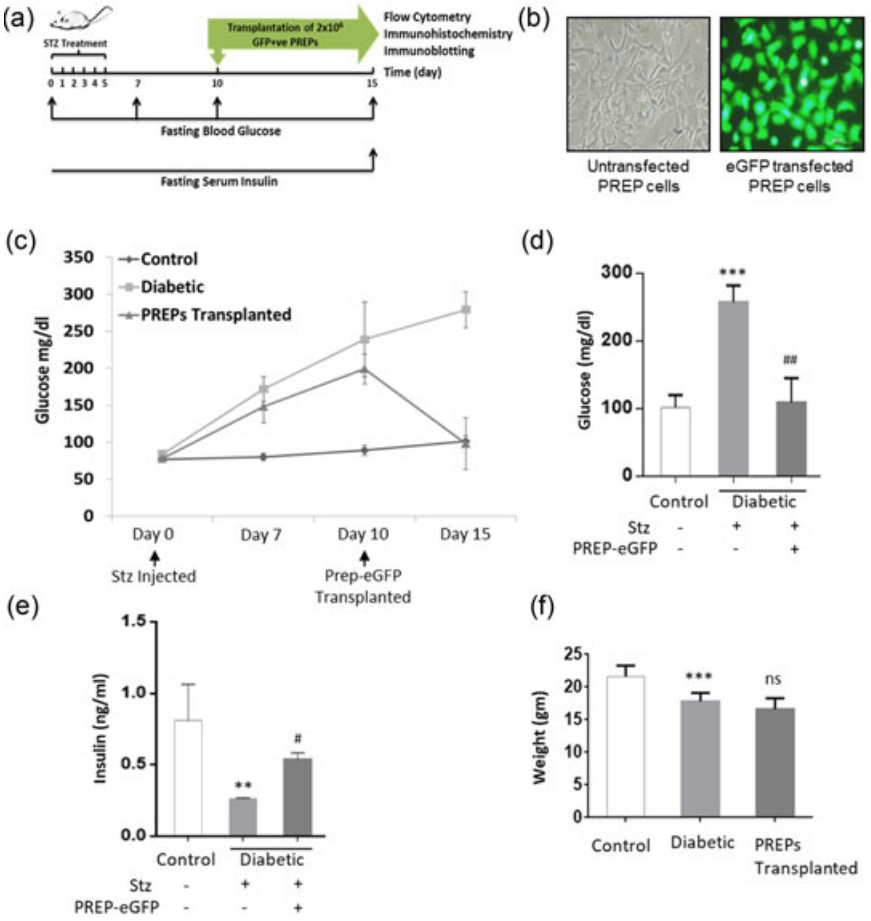

FIGURE 4 Evaluation of PREPs transplantation in STZ diabetic BALB/c mice. (a) Schematic representation of the plan of work for the transplantation study explaining the methodology and parameters. (b) Labeling of PREPs with peGFPN1 vector (scale bar = 100 μm; magnification: ×20). (c) Fasting blood glucose levels in control, diabetic, and PREP transplanted mice at regular time intervals ($N = 6$). (d) Comparative fasting blood glucose after PREP transplantation. $^{***}p \leq 0.001$ control versus diabetic. $^{\#\#}p \leq 0.01$ diabetic versus PREP transplanted. (e) Comparative fasting insulin after PREP transplantation ($N = 3$). $^{**}p \leq 0.001$ control versus diabetic. $^{\#}p \leq 0.01$ diabetic versus PREP transplanted. The graphs are plotted with mean ± *SEM*. (f) Body weight comparison between control, diabetic, and PREP-transplanted mice ($N = 6$). $^{***}p \leq 0.001$ control versus diabetic. $^{ns}p \geq 0.05$ Diabetic versus PREP transplanted. PREP: pancreatic resident endocrine progenitor; STZ: streptozotocin [Color figure can be viewed at wileyonlinelibrary.com]

progenitor cell line taken as negative control using RT-PCR. We observed a significantly higher expression of all the above genes in the isolated progenitor population (Figure 1e). Similarly, insulin and glucagon expression were observed to be significantly downregulated in the progenitor population when compared with isolated mice islets confirming their progenitor phenotype (Figure 1f).

3.3 | PREPs demonstrated multipotency via successful trilineage differentiation

MSC nature of PREPs was confirmed by performing Trilineage differentiation.

3.3.1 | Adipocyte differentiation

PREPs differentiated into adipocytes with oil droplet formation in the cytoplasm. These oil droplets were stained red in color with the oil Red O staining, which was highly significant when compared with undifferentiated PREPs (Supporting Information Figure S1A and Bi).

3.3.2 | Osteocyte differentiation

PREPs differentiated into osteocytes that became more compact along with considerable mineralization around the cell surface. This mineralization was confirmed by staining with Alizarin Red S dye, which stains the calcium deposited by osteocytes (Supporting Information Figure S1A and Bii).

3.3.3 | Chondrocyte differentiation

PREPs were differentiated into chondrocytes, which was confirmed by alcian blue staining. Alcian blue stains positive for proteoglycan aggrecan, an indicator of cartilage formation (Supporting Information Figure S1A and Biii).

3.4 | PREPs demonstrated high fidelity for differentiation into islet cell clusters

PREPs were differentiated into islet clusters using Activin-A and Swertisin as described in the schematic stepwise protocol (Figure 2a). Mature islets were observed at Day 4 of differentiation in both groups, whereas the serum-free media group (SFM) resulted in immature loose small-cell clusters. To confirm islet differentiation, these clusters were stained with DTZ, which stains the zinc present within the mature islets bound to insulin. We observed a positive staining of DTZ in the islet clusters in both swertisin and activin-A groups but not in the SFM group. This observation confirmed the formation of mature islets in both Activin-A- and Swertisin-treated groups and incomplete differentiation with immature islets in the SFM group (Figure 2b and Supporting Information Figure S2A).

We observed that the clusters formed in both the islet differentiating groups were well compact and spherical with their size mainly between 100 and 300 μm, whereas, in comparison with the SFM group, which displayed mostly smaller and loose clusters, the islet number was significantly low in the range of 100–300 μm but high in smaller sized clusters that is less than 100 μm, which suggested that the SFM group alone was insufficient to completely differentiate PREPs into Islet of Langerhans (Figure 2c,d).

3.5 | PREP-differentiated islet clusters were confirmed functionally

We observed the presence of INSULIN and GLUCAGON in the differentiated islets of both Activin-A and Swertisin groups. We also observed intense staining for Nkx6.1 (green) and Glut2 (red) in these islet clusters. However, in the SFM group we observed much less INSULIN, NKX6.1, and GLUT2, and more of GLUCAGON suggesting incomplete differentiation. These observations confirmed the formation of mature islet clusters in the Activin-A and Swertisin groups (Figure 2e and Supporting Information Figure S2B). Normal mice islets were stained as the reference standard for INSULIN, GLUCAGON and C-PEPTIDE (Supporting Information Figure S2C).

Finally, we challenged these islet clusters with 5 and 20 mM glucose concentrations and measured their C-PEPTIDE release using C-PEPTIDE ELISA. We observed significantly more C-PEPTIDE release in 20 mM glucose exposure compared with 5 mM across all groups. Activin-A and Swertisin groups exposed to 20 mM glucose released more C-PEPTIDE with respect to the SFM group. Hence, this collectively confirmed that the islets generated using Activin-A and Swertisin were mature and functional (Figure 2f).

3.6 | Time-dependent gene and protein profiling of islet clusters differentiated from PREPs demonstrated the kinetics of TFs between the progenitor and mature islets

PREPs were introduced to islet differentiation media with the respective differentiating agents. The differentiated islet samples were harvested every day across groups for 4 days, which were analysed for their gene and protein expression by qRT-PCR and western blot analysis, respectively (Supporting Information Tables S6 and S7).

Temporal gene expression profiling for the important TFs namely, *Pdx1*, *Neurog3*, *NeuroD*, and *Nkx6.1* along with hormones *Insulin and Glucagon* were performed. With respect to TFs, a general pattern was observed from the undifferentiated PREPs at Day 0 to the mature islets at Day 4. A gradual increase in all the TFs and the two hormones were observed throughout the gene expression plots. Also, the expression of TFs in the SFM group was lower than that of Activin-A and Swertisin. Furthermore, we observed an increase in the insulin transcript levels in the Swertisin group compared with Activin-A and SFM groups on Day 4 (Figure 3a–f).

The western blot analysis answered the question as to why PREPs differentiate so rapidly and take the shortest route to islet differentiation. We observed the presence of pancreatic TFs like PDX1, NEUROG3, NEUROD, MAFA, PAX4, and NKX6.1 in the undifferentiated PREPs along with the basal amount of phosphorylated SMAD3. Secondly, expression of stem cell markers both Nestin and CD133 for Activin-A and Swertisin-treated groups decreased significantly, which ultimately by day four was completely abolished. This confirmed PREPs losing their progenitor phenotype and becoming terminally differentiated. However, in the SFM group, we observed persistent expression of Nestin and CD133 suggesting PREPs inability to differentiate into islet clusters complementing the microscopic and DTZ staining data. Thirdly, the signaling molecules in the AKT-MEPK-TKK pathway were activated upon induction with Activin-A and Swertisin. In both these groups, we observed elevated phosphorylation of SMAD3 and increased expression of SMAD4 along with decreased expression of inhibitory SMAD7. Phosphorylation of p38MAPK was also observed to be elevated. All these regulatory signaling protein activations were observed to be elevated in the Activin-A and Swertisin group when compared with the SFM group. Finally, all the TFs namely, PDX1, NEUROG3, NEUROD, PAX4, MAFA, and NKX6.1, which are absolutely necessary for the development of the endocrine pancreas and its functioning, were temporally upregulated in the course of islet differentiation. Also, if we focus on Nkx6.1 alone, which is the marker for terminally differentiated insulin-producing β cells, it was observed to be weakly expressed in the SFM group suggesting poor or incomplete differentiation, whereas its expression is significantly elevated in the other two groups. The endogenous control taken was β-actin (Supporting Information Figure S3).

3.7 | In vivo assessment of amelioration of STZ-treated diabetic BALB/c mice on transplanting PREPs

GFP-labeled PREPs were transplanted in the STZ diabetic mice through the tail vein. After four days of transplantation, the mice were sacrificed on the fifth day that is the 15th experimental day. Homing of these GFP-labeled PREPs was monitored in the major organs. FBG and insulin was monitored in mice (Figure 4a).

3.7.1 | Labeling of PREPs with GFP

PREPs were transfected with pEGFPN1 vector using the NEON electroporation system to generate a stable GFP-positive PREP clone for transplantation studies (Figure 4b).

3.7.2 | Diabetic condition in BALB/c mice was confirmed by monitoring FBG, serum insulin, and pancreatic histology

FBG levels were monitored at four time points as per Figure 4a. A significant increase in the blood glucose was observed in the experimental groups showing that they have become diabetic. Also,

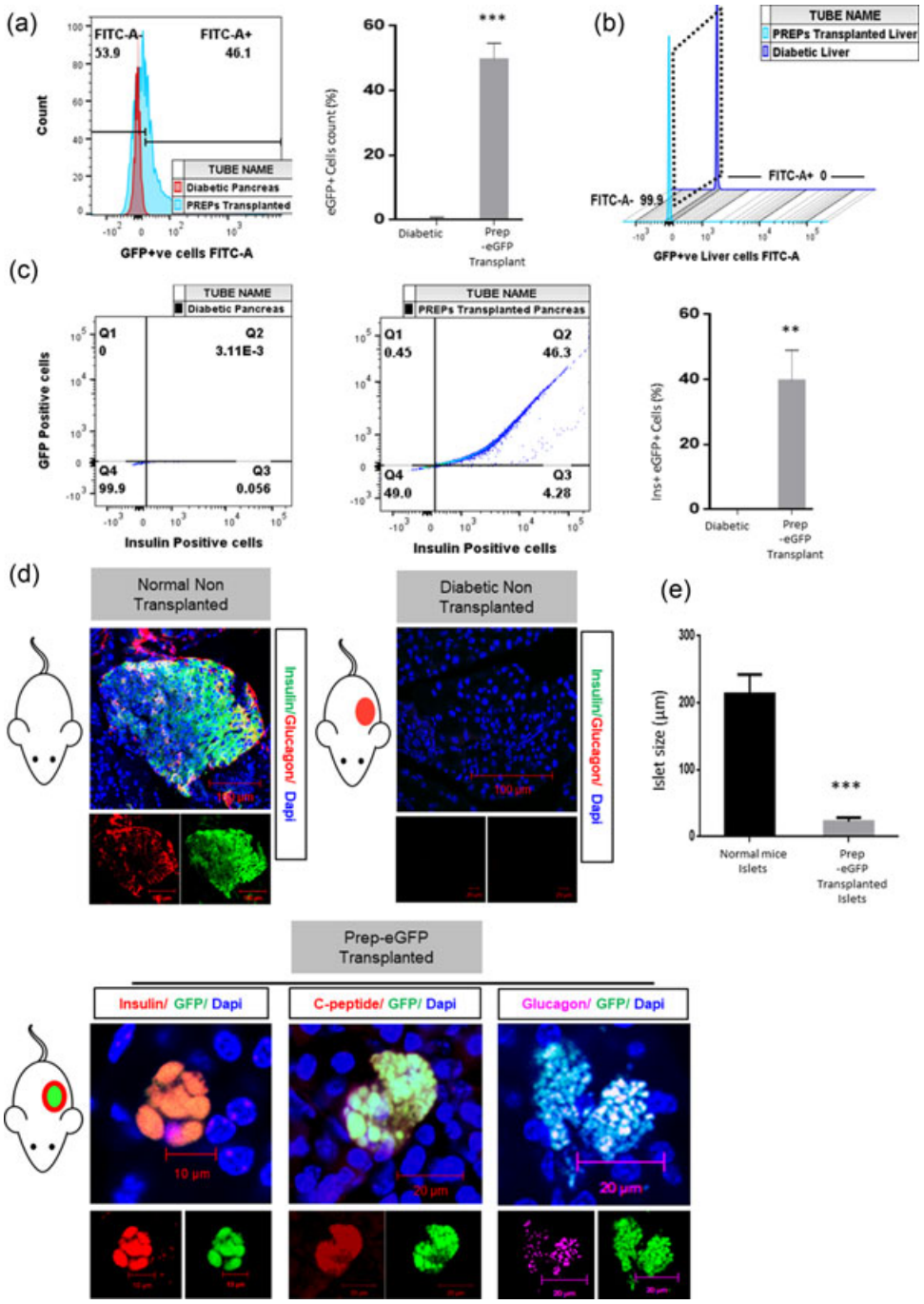

FIGURE 5 Evaluation of PREPs homing in STZ Diabetic BALB/c mice. (a) Flow cytometric analysis of percentage composition of GFP-positive PREPs in mice pancreas, that is homing of PREPs into mice pancreas. ***$p \leq 0.001$ diabetic pancreas versus PREP-transplanted pancreas ($N = 3$). (b) Flow cytometric analysis of percentage composition of GFP-positive PREPs in mice liver that is homing of PREPs into mice liver ($N = 3$). (c) Functional characterization of GFP-positive PREPs transplanted in diabetic mice for their differentiation into insulin-positive cells within mice pancreas by flow cytometry, that is identifying dual-positive GFP + insulin population within PREP transplanted mice pancreas. The graphs are plotted with mean ± *SEM*. **$p \leq 0.001$ Diabetic pancreas versus PREP transplanted pancreas ($N = 3$). (d) Functional characterization of PREPs transplanted in STZ diabetic mice pancreas by immunohistochemistry, which demonstrated localization of GFP-positive cells within mice pancreas and their colocalization with insulin (red), c-peptide (red; and/or glucagon [magenta-pseudocolor]). Normal mice pancreatic section was taken as standard and was stained with insulin (green) and glucagon (red; scale bar = 100, 20, and 10 µm; magnification: ×63; $N = 3$). (e) Size distribution analysis between normal mice islets and PREPs generated islets in diabetic mice. The graphs are plotted with mean ± *SEM*. ***$p \leq 0.001$ Normal islets versus PREP-transplanted islets ($N = 10$). GFP: green fluorescent protein; PREP: pancreatic resident endocrine progenitor; STZ: streptozotocin [Color figure can be viewed at wileyonlinelibrary.com]

the islets in the STZ-treated diabetic mice pancreas had shrunken due to β-cell death (Supporting Information Figure S4A). PREPs GFP-positive were transplanted in diabetic mice. After transplantation, it was observed (Figure 4c–e) that the group transplanted with PREPs reverted back to the normoglycaemic condition in 4 days (100 ± 20 mg/dl) along with significant recovery in their fasting serum insulin. However, there was no significant recovery in the body weight of diabetic mice post-PREPs transplantation, which was recorded on the fifth day posttransplantation (Figure 4f).

3.7.3 | GFP-labeled PREPs demonstrated robust homing into STZ diabetic mice pancreas posttransplantation

The pancreas and liver of the diabetic mice were harvested after transplantation and their single cell suspension was screened for GFP-positive PREPs through flow cytometry. The graphs determine the percentage of the GFP-positive population in the pancreatic and liver single cell suspension. The *X*-axis depicts the intensity of GFP fluorescence and the *Y*-axis gives the cell count. The graphs of flow cytometry analysis demonstrated that the localization of GPF-positive cells was observed in the pancreas of diabetic groups transplanted with PREPs (~46%; Figure 5a). However, no GFP-positive population was observed in the liver of transplanted diabetic mice (Figure 5b). Also, for PREPs when transplanted into normal mice without STZ treatment, we observed that in contrast to the situation in diabetic mice, PREPs homed into not only pancreas (~21%) but a significant quantity of PREPs were trapped in the liver (~25%) and lungs (~11%), respectively (Supporting Information Figure S5 A). Also, there was a reduction in the FBG level and an increase in the serum c-peptide level indicating an increase in functional insulin-producing cells within the pancreas (Supporting Information Figure S5B,C). However, there was no hypoglycemia observed in these normal mice.

3.7.4 | Transplanted PREPs differentiated into insulin-positive cells within diabetic mice pancreas

Flow cytometry was performed to verify whether the GFP-positive PREP population differentiated into insulin-producing cells. Here the graph was divided into four quadrants: Q1, GFP-positive; Q2, GFP and insulin that is dual-positive; Q3, insulin-positive; and Q4, dual-negative population. We observed that almost the entire GFP population was also positive for insulin (~40%) confirming the differentiation of transplanted GFP-positive PREPs into functional β cells (Figure 5c). We also confirmed this by ICC, where we observed colocalized GFP-positive population with INSULIN and C-PEPTIDE. Furthermore, we observed that few cells within these clusters were also positive for GLUCAGON. Normal mice pancreatic section stained with INSULIN and GLUCAGON was taken as the reference standard (Figure 5d), thus, confirming that GFP-positive PREPs homed into the pancreas and differentiated into insulin and glucagon-producing islet-like clusters. Furthermore, there was no GFP-positive population observed on screening other major organs namely, lungs, kidney, and spleen by fluorescence microscopy in transplanted diabetic mice (Supporting Information Figure S4B). Also, on analysing the size distribution of transplanted PREP islets, we observed that these islet clusters were significantly smaller when compared with normal mice islet clusters (Figure 5e).

4 | DISCUSSION

Our study here is an attempt to understand the fidelity of pancreatic progenitors in treating β-cell death in diabetes mellitus. In the current study, we have also attempted to comprehend the characteristics of pancreatic resident endocrine progenitors along with exploring the islet neogenic and homing potential of pancreatic resident endocrine progenitors in amelioration of diabetic condition.

PREPs were isolated and purified by sequential passaging from BALB/c mouse pancreas by using a previously described methodology (Joglekar & Hardikar, 2012). These cells exhibited characteristics of previously reported pancreatic progenitors with certain profound discrepancies from the reported literature. PREPs were positive for NESTIN, PDX1, NEUROG3, and negative for INSULIN and GLUCAGON. This is a classical pancreatic progenitor signature (Banerjee & Bhonde, 2003; Ta, Choi, Atouf, Park, & Lumelsky, 2006; Zhang et al., 2005; Zulewski et al., 2001). Furthermore, the presence of CK19 suggested their pancreatic ductal origin. Also, Nestin and CK19 were positive markers on PREPs that suggested their ductal origin, which migrated into an islet niche for neogenesis (Zulewski et al., 2001).

Furthermore, these progenitors were positive for MSC markers like CD44 and CD90, which has been found positive in NESTIN + progenitors. However, these cells were unique in expressing CD34. All the previous data on pancreatic progenitors have suggested its absence but we observed a robust presence of CD34 in these progenitors (Zanini et al., 2011; Zhang et al., 2005). There has been a growing belief among the scientific community that CD34 positivity is a highlighting characteristic of cells with progenitor activity (Sidney, Branch, Dunphy, Dua, & Hopkinson, 2014). CD133 is another progenitor marker present abundantly in these cells. It has been reported as a maker that can be used to enrich the pancreatic progenitor population (Sugiyama & Kim, 2008). Finally, GLUT2 was abundantly present in this population. Presence of GLUT2 in the pancreatic progenitor originating from the duct has been previously reported (Pang, Mukonoweshuro, & Wong, 1994). The presence of GLUT2-positive progenitor population was observed in STZ-treated normoglycaemic mice attained after insulin treatment. This also suggested that hyperglycaemic conditions decrease GLUT2 expression, which was not observed in our case, as we isolated and cultured these cells strictly in proliferative media containing 25 mM glucose (Guz, Nasir, & Teitelman, 2001). Hence, the two unique markers for these cells, CD34 and GLUT2, may be used for enriching and purifying these cells. These cells also demonstrated adipogenic, osteogenic, and chondrogenic differentiation ability establishing their multipotent

characteristics, which was reported previously in pancreatic progenitors and is a criterion to characterize MSCs (Baksh, Song, & Tuan, 2004; Zanini et al., 2011).

It has been previously reported that various antioxidant enzyme levels and their respective gene expressions in β cell were significantly lower than that in other tissues. This lack of effective reactive oxygen species (ROS) scavenging mechanism leads to β-cell death in a glucotoxic environment (Gorasia et al., 2015; Lenzen, Drinkgern, & Tiedge, 1996; Wang & Wang, 2017). PREPs were cultured and differentiated in a media with 25 mM glucose, hence constantly maintained in high glucose conditions mimicking the diabetic sugar environment. There have been reports that suggest that the pancreatic progenitor population not only thrives in the high glucose environment but these conditions stimulate islet neogenesis (H. S. Kim et al., 2013). During islet differentiation in vitro, PREPs started forming clusters from the first day of differentiation and matured into islet clusters in a span of mere four days under serum-free condition and presence of Activin-A/Swertisin. This indicated their predisposition in taking the shortest route to islet differentiation (Venkatesan, Gopurapilly, Goteti, Dorisetty, & Bhonde, 2011). Furthermore, this rapid differentiation was observed in both Activin-A and Swertisin that follow the AKT-MEPK-TKK pathway, elucidated in our previous report (Dadheech et al., 2015). Analysing the temporal protein expression from undifferentiated PREPs at day zero to completely mature islet clusters at day four confirmed high islet cluster forming fidelity. The undifferentiated PREPs demonstrated basal expression of the key TFs namely, PDX1, NEUROG3, NEUROD, MAFA, and NKX6.1 required for endocrine pancreatic development and function along with activation of key signaling molecules like pSMAD3 and pP38MAPK confirming their inherent potential to differentiate into islet clusters, which justifies their nomenclature as PREPs (S. K. Kim & Hebrok, 2001; Murtaugh, 2007). Furthermore, SMAD7, which is an inhibitory SMAD, was expressed highly in the undifferentiated cells thus inhibiting the islet differentiation but with the induction and progression of islet differentiation, its expression subsides while increasing the expression of regulatory SMAD4 and phosphorylation of SMAD3. Phosphorylation of pMAPK also increases, which propelled the differentiation forward by upregulating the above-mentioned key TFs. Since the machinery required for islet differentiation was inherently present in these cells, stimulating them with islet differentiating agents and providing the right conditions induced the shortest route ever reported for any stem/progenitor population for the same (Lina Sui, Yi, & Liu, 2013; Wen et al., 2011).

There have been many protocols developed over the years using ESCs, iPSCs, and various MSCs using various protocols for islet differentiation making the process increasingly complex and cumbersome (Wong, 2011). Therefore, taking into account the process, time taken and results obtained, we describe the shortest differentiation process with an effective and desirable outcome. Complete differentiation was marked by the abatement of stem cell markers namely, NESTIN and CD133 at day four of differentiation. Islet differentiation was significantly more efficient in the Activin-A and Swertisin induced group as compared with the SFM group. However, with SFM stem cell markers were persistent throughout the differentiation indicating incomplete or no differentiation. These islets were further functionally characterized. The islets generated from Activin-A and Swertisin groups were functional that is expressed *Insulin* transcript and positive for hormones including INSULIN and GLUCAGON, expressed GLUT2 and NKX6.1 (β-cell marker) and demonstrated glucose-stimulated c-peptide secretion. We observed that Swertisin-induced islets were significantly superior across all the functional parameters, thus generating a better quality of islet clusters, which could effectively maintain glucose homeostasis (Dadheech et al., 2013, 2015; Lumelsky et al., 2001). We further, wanted to evaluate the efficacy of both PREPs homing toward the damaged pancreas and their islet neogenic potential in the in vivo diabetic mice model. Adult female mice are known to be lesser sensitive for STZ induction, which aided in limiting the heightened morbidity rates in the STZ model (Kolb, 1987). Furthermore, females are more susceptible to metabolic disorder post menopause, which increases the clinical relevance of this study as the onset of chronic type 2 diabetes mainly occurs at a later stage in life (Janssen, Powell, Crawford, Lasley, & Sutton-Tyrrell, 2008).

Reports suggest MSCs' wide participation therapies to manage the diabetic condition. It has been reported previously that $0.5–2 \times 10^6$ MSCs were transplanted intravenously. Hence, taking these values as a reference, we transplanted 2×10^6 GFP-positive PREPs intravenously into the STZ diabetic mouse model (Ezquer et al., 2008; Hess et al., 2003; Lee et al., 2006). STZ enters β cells through Glut2 transporters and causes DNA damage by generating ROS (Bonal, Avril, & Herrera, 2008). Studies have demonstrated that MSCs transplanted intravenously can migrate to the injured tissue but can also get trapped in the lungs and liver, which was observed when PREPs were transplanted in normal mice, but pleasantly, we did not observe any GFP-positive population in lungs, liver, spleen, or kidneys in the diabetic mice transplanted with PREPs (Chamberlain, Fox, Ashton, & Middleton, 2007). Furthermore, it has been observed that MSCs can migrate under the influence of chemokine released from wounds, which could be a reason why PREPs exclusively homed into STZ damaged pancreas in diabetic mice (Hocking, 2015). Previous reports suggest about ~3% homing of bone marrow MSCs when transplanted intravenously to ameliorate diabetes by repairing damaged pancreas (Ezquer et al., 2008; Hess et al., 2003). However, we report a significantly larger amount of GFP percentage composition in the transplanted mice pancreas. Also these GFP PREPs were insulin positive suggesting their differentiation was stimulated by pancreatic niche, which was supported by normoglycemia and increased serum insulin levels in mice. This was probably because we transplanted pancreatic resident endocrine progenitors, which have more affinity toward their own niche and could migrate and differentiate into insulin-producing cells without the need of any external stimulus. Furthermore, it has been observed that MSCs can migrate under the influence of chemokine released from wounds, which could be a plausible reasons why PREPs exclusively homed into STZ damaged pancreas in diabetic mice (Hocking, 2015). This homing affinity of PREPs toward its niche could

be a unique characteristic that can be further explored and extended to other types of stem cells like ESCs, iPSCs, and other MSCs, where the pancreatic progenitor state is a prerequisite and intermediary state for generating islets for diabetes therapeutics.

5 | CONCLUSION

We conclude by stating that PREPs having MSC properties take the shortest route to produce insulin-producing islet clusters as they are equipped with the innate transcription machinery. Furthermore, these cells when transplanted into a STZ diabetic mice model demonstrated robust homing to the pancreas and ameliorated the diabetic condition. This study can be extrapolated to pluripotent stem cells (especially iPSCs) and other MSCs, which on differentiating to the pancreatic progenitor state may highlight similar homing toward damaged pancreas and differentiate into functional islet-like clusters under diabetic conditions. This has clinical relevance in developing personalized tailor-made cell replacement therapy for diabetic patients. Hence, this study opens up new insights into the unique characteristics of PREPs and their advantages in the paradigm of diabetes therapeutics.

ACKNOWLEDGMENTS

We would like to acknowledge Prof. Ramesh R. Bhonde, Director (Research), Dr. D. Y. Patil University, Pune, Maharashtra, Mumbai for his valuable inputs in the preparation of this manuscript. We acknowledge the Department of Biotechnology for establishing the Instrumentation facility under the DBT-MSUB-ILSPARE program, which allowed us to access the FACS, Confocal microscopy facility, and other instruments. Miss Komal Rawal, technical staff at the above facility, has put in a great deal of effort, time and patience for the acquisition of data for this manuscript. We also acknowledge CSIR-UGC-NET for providing fellowship to the first author.

CONFLICTS OF INTEREST

The authors have declared that there are no conflicts of interest.

AUTHOR CONTRIBUTIONS

A. S. Conception and design, collection, assembly of data, data analysis, interpretation, and manuscript writing; N. D. Conception and design, assembly of data, and manuscript writing; M. V. Collection and/or assembly of data and data analysis and interpretation; S. G. Conception and design, financial support, provision of study material, data analysis, interpretation, manuscript writing, and final approval of manuscript.

ORCID

Sarita Gupta http://orcid.org/0000-0002-6097-7767

REFERENCES

Afelik, S., & Rovira, M. (2017). Pancreatic beta-cell regeneration: Facultative or dedicated progenitors? *Molecular and Cellular Endocrinology*, *445*, 85–94.

Aigha, I. I., Memon, B., Elsayed, A. K., & Abdelalim, E. M. (2018). Differentiation of human pluripotent stem cells into two distinct NKX6.1 populations of pancreatic progenitors. *Stem Cell Research & Therapy*, *9*(1), 83.

Baksh, D., Song, L., & Tuan, R. S. (2004). Adult mesenchymal stem cells: Characterization, differentiation, and application in cell and gene therapy. *Journal of Cellular and Molecular Medicine*, *8*(3), 301–316.

Banerjee, M., & Bhonde, R. R. (2003). Islet generation from intra islet precursor cells of diabetic pancreas: In vitro studies depicting in vivo differentiation. *JOP: Journal of the pancreas*, *4*(4), 137–145.

Bonal, C., Avril, I., & Herrera, P. L. (2008). Experimental models of beta-cell regeneration. *Biochemical Society Transactions*, *36*(Pt 3), 286–289.

Chamberlain, G., Fox, J., Ashton, B., & Middleton, J. (2007). Concise review: Mesenchymal stem cells: Their phenotype, differentiation capacity, immunological features, and potential for homing. *Stem Cells*, *25*(11), 2739–2749.

Chruvattil, R., Banerjee, S., Nath, S., Machhi, J., Kharkwal, G., Yadav, M. R., & Gupta, S. (2016). Dexamethasone alters the appetite regulation via induction of hypothalamic insulin resistance in rat brain. *Molecular Neurobiology*, *54*, 7483–7496.

Dadheech, N., Soni, S., Srivastava, A., Dadheech, S., Gupta, S., Gopurappilly, R., … Gupta, S. (2013). A small molecule swertisin from enicostemma littorale differentiates NIH3T3 cells into islet-like clusters and restores normoglycemia upon transplantation in diabetic Balb/c mice. *Evidence-Based Complementary and Alternative Medicine: eCAM*, *2013*, 280392–20.

Dadheech, N., Srivastava, A., Paranjape, N., Gupta, S., Dave, A., Shah, G. M., … Gupta, S. (2015). Swertisin an anti-diabetic compound facilitate islet neogenesis from pancreatic stem/progenitor cells via p-38 MAP kinase-SMAD pathway: An In-Vitro and In-Vivo Study. *PLOS One*, *10*(6), e0128244.

Deans, R. J., & Moseley, A. B. (2000). Mesenchymal stem cells: Biology and potential clinical uses. *Experimental Hematology*, *28*(8), 875–884.

Edlund, H. (2001). Developmental biology of the pancreas. *Diabetes*, *50* (Supp 1), S5–S9.

Eseonu, O. I., & De Bari, C. (2015). Homing of mesenchymal stem cells: Mechanistic or stochastic? Implications for targeted delivery in arthritis. *Rheumatology*, *54*(2), 210–218.

Ezquer, F. E., Ezquer, M. E., Parrau, D. B., Carpio, D., Yañez, A. J., & Conget, P. A. (2008). Systemic administration of multipotent mesenchymal stromal cells reverts hyperglycemia and prevents nephropathy in type 1 diabetic mice. *Biology of Blood and Marrow Transplantation*, *14*(6), 631–640.

Faleo, G., Lee, K., Nguyen, V., & Tang, Q. (2016). Assessment of immune isolation of allogeneic mouse pancreatic progenitor cells by a macroencapsulation device. *Transplantation*, *100*(6), 1211–1218.

Gorasia, D. G., Dudek, N. L., Veith, P. D., Shankar, R., Safavi-Hemami, H., Williamson, N. A., … Purcell, A. W. (2015). Pancreatic beta cells are highly susceptible to oxidative and ER stresses during the development of diabetes. *Journal of Proteome Research*, *14*(2), 688–699.

Guz, Y., Nasir, I., & Teitelman, G. (2001). Regeneration of pancreatic beta cells from intra-islet precursor cells in an experimental model of diabetes. *Endocrinology*, *142*(11), 4956–4968.

Henschler, R., Deak, E., & Seifried, E. (2008). Homing of mesenchymal stem cells. *Transfusion Medicine and Hemotherapy*, *35*(4), 306–312.

Hess, D., Li, L., Martin, M., Sakano, S., Hill, D., Strutt, B., … Bhatia, M. (2003). Bone marrow-derived stem cells initiate pancreatic regeneration. *Nature Biotechnology*, *21*(7), 763–770.

Hocking, A. M. (2015). The role of chemokines in mesenchymal stem cell homing to wounds. *Advances in Wound Care*, *4*(11), 623–630.

Janssen, I., Powell, L. H., Crawford, S., Lasley, B., & Sutton-Tyrrell, K. (2008). Menopause and the metabolic syndrome: The study of women's health across the nation. *Archives of Internal Medicine*, *168* (14), 1568–1575.

Jiang, F. X., & Morahan, G. (2014). Pancreatic stem cells remain unresolved. *Stem Cells and Development*, *23*(23), 2803–2812.

Jiang, F. X., & Morahan, G. (2015). Multipotent pancreas progenitors: Inconclusive but pivotal topic. *World Journal of Stem Cells*, *7*(11), 1251–1261.

Joglekar, M. V., & Hardikar, A. A. (2012). Isolation, expansion, and characterization of human islet-derived progenitor cells. *Methods in Molecular Biology*, *879*, 351–366.

Karp, J. M., & Leng Teo, G. S. (2009). Mesenchymal stem cell homing: The devil is in the details. *Cell Stem Cell*, *4*(3), 206–216.

Kim, H. S., Hong, S. H., Oh, S. H., Kim, J. H., Lee, M. S., & Lee, M. K. (2013). Activin A, exendin-4, and glucose stimulate differentiation of human pancreatic ductal cells. *The Journal of Endocrinology*, *217*(3), 241–252.

Kim, S. K., & Hebrok, M. (2001). Intercellular signals regulating pancreas development and function. *Genes & development*, *15*(2), 111–127.

Kolb, H. (1987). Mouse models of insulin dependent diabetes: Low-dose streptozocin-induced diabetes and nonobese diabetic (NOD) mice. *Diabetes/Metabolism Reviews*, *3*(3), 751–778.

Kristocheck, M., Dias, L. D., Ghem, C., Eibel, B., Kalil, R. A. K., & Markoski, M. M. (2018). The homing of bone marrow stem cells is differentially activated in ischemic and valvular heart diseases and influenced by beta-blockers. *Journal of Translational Medicine*, *16*(1), 133.

Lee, R. H., Seo, M. J., Reger, R. L., Spees, J. L., Pulin, A. A., Olson, S. D., & Prockop, D. J. (2006). Multipotent stromal cells from human marrow home to and promote repair of pancreatic islets and renal glomeruli in diabetic NOD/scid mice. *Proceedings of the National Academy of Sciences of the United States of America*, *103*(46), 17438–17443.

Lenzen, S., Drinkgern, J., & Tiedge, M. (1996). Low antioxidant enzyme gene expression in pancreatic islets compared with various other mouse tissues. *Free Radical Biology & Medicine*, *20*(3), 463–466.

Lin, W., Xu, L., Zwingenberger, S., Gibon, E., Goodman, S. B., & Li, G. (2017). Mesenchymal stem cells homing to improve bone healing. *Journal of Orthopaedic Translation*, *9*, 19–27.

Lina Sui, J. Q., Yi, Fei, & Liu, G.-H. (2013). Stem cell therapy for diabetes: A call for efficient differentiation of pancreatic progenitors. *J Regen Med*, *2*(1), 1–4.

Lumelsky, N., Blondel, O., Laeng, P., Velasco, I., Ravin, R., & McKay, R. (2001). Differentiation of embryonic stem cells to insulin-secreting structures similar to pancreatic islets. *Science*, *292*(5520), 1389–1394.

Memon, B., Karam, M., Al-Khawaga, S., & Abdelalim, E. M. (2018). Enhanced differentiation of human pluripotent stem cells into pancreatic progenitors co-expressing PDX1 and NKX6.1. *Stem Cell Research & Therapy*, *9*(1), 15.

Murtaugh, L. C. (2007). Pancreas and beta-cell development: From the actual to the possible. *Development*, *134*(3), 427–438.

Pang, K., Mukonoweshuro, C., & Wong, G. G. (1994). Beta cells arise from glucose transporter type 2 (Glut2)-expressing epithelial cells of the developing rat pancreas. *Proceedings of the National Academy of Sciences of the United States of America*, *91*(20), 9559–9563.

Rezania, A., Bruin, J. E., Xu, J., Narayan, K., Fox, J. K., O'Neil, J. J., & Kieffer, T. J. (2013). Enrichment of human embryonic stem cell-derived NKX6.1-expressing pancreatic progenitor cells accelerates the maturation of insulin-secreting cells in vivo. *Stem Cells*, *31*(11), 2432–2442.

Sidney, L. E., Branch, M. J., Dunphy, S. E., Dua, H. S., & Hopkinson, A. (2014). Concise review: Evidence for CD34 as a common marker for diverse progenitors. *Stem Cells*, *32*(6), 1380–1389.

Srivastava, A., Bhatt, N. M., Patel, T. P., Dadheech, N., Singh, A., & Gupta, S. (2016). Anti-apoptotic and cytoprotective effect of Enicostemma littorale against oxidative stress in Islets of Langerhans. *Pharmaceutical Biology*, *54*(10), 2061–2072.

Srivastava, A., Dadheech, N., Vakani, M., & Gupta, S. (2018). Swertisin ameliorates diabetes by triggering pancreatic progenitors for islet neogenesis in Streptozotocin treated BALB/c mice. *Biomedicine & Pharmacotherapy*, *100*, 221–225.

Staels, W., De Groef, S., Heremans, Y., Coppens, V., Van Gassen, N., Leuckx, G., … De Leu, N. (2016). Accessory cells for beta-cell transplantation. *Diabetes, Obesity & Metabolism*, *18*(2), 115–124.

Sugiyama, T., & Kim, S. K. (2008). Fluorescence-activated cell sorting purification of pancreatic progenitor cells. *Diabetes, Obesity & Metabolism*, *10*(Supp 4), 179–185.

Ta, M., Choi, Y., Atouf, F., Park, C. H., & Lumelsky, N. (2006). The defined combination of growth factors controls generation of long-term-replicating islet progenitor-like cells from cultures of adult mouse pancreas. *Stem Cells*, *24*(7), 1738–1749.

Venkatesan, V., Gopurapilly, R., Goteti, S. K., Dorisetty, R. K., & Bhonde, R. R. (2011). Pancreatic progenitors: The shortest route to restore islet cell mass. *Islets*, *3*(6), 295–301.

Wang, J., & Wang, H. (2017). Oxidative stress in pancreatic beta cell regeneration. *Oxidative Medicine and Cellular Longevity*, *2017*, 1930261–1930269.

Wen, Y., Chen, B., & Ildstad, S. T. (2011). Stem cell-based strategies for the treatment of type 1 diabetes mellitus. *Expert Opinion on Biological Therapy*, *11*(1), 41–53.

Wong, R. S. Y. (2011). Extrinsic factors involved in the differentiation of stem cells into insulin-producing cells: An overview. *Experimental Diabetes Research*, *2011*, 406182–15.

Xia, M., & Laychock, S. G. (1993). Insulin secretion, myo-inositol transport, and Na(+)-K(+)-ATPase in glucose-desensitized rat islets. *Diabetes*, *42* (10), 1392–1400.

Xie, C., Yang, Z., Suo, Y., Chen, Q., Wei, D., Weng, X., … Wei, X. (2017). Systemically infused mesenchymal stem cells show different homing profiles in healthy and tumor mouse models. *Stem Cells Translational Medicine*, *6*(4), 1120–1131.

Yagi, H., Soto-Gutierrez, A., Parekkadan, B., Kitagawa, Y., Tompkins, R. G., Kobayashi, N., & Yarmush, M. L. (2010). Mesenchymal stem cells: Mechanisms of immunomodulation and homing. *Cell Transplantation*, *19*(6), 667–679.

Zanini, C., Bruno, S., Mandili, G., Baci, D., Cerutti, F., Cenacchi, G., … Forni, M. (2011). Differentiation of mesenchymal stem cells derived from pancreatic islets and bone marrow into islet-like cell phenotype. *PLOS One*, *6*(12), e28175.

Zhang, L., Hong, T. P., Hu, J., Liu, Y. N., Wu, Y. H., & Li, L. S. (2005). Nestin-positive progenitor cells isolated from human fetal pancreas have phenotypic markers identical to mesenchymal stem cells. *World Journal of Gastroenterology*, *11*(19), 2906–2911.

Zulewski, H., Abraham, E. J., Gerlach, M. J., Daniel, P. B., Moritz, W., Muller, B., … Habener, J. F. (2001). Multipotential nestin-positive stem cells isolated from adult pancreatic islets differentiate ex vivo into pancreatic endocrine, exocrine, and hepatic phenotypes. *Diabetes*, *50*(3), 521–533.

SUPPORTING INFORMATION

Additional supporting information may be found online in the Supporting Information section at the end of the article.

How to cite this article: Srivastava A, Dadheech N, Vakani M, Gupta S. Pancreatic resident endocrine progenitors demonstrate high islet neogenic fidelity and committed homing towards diabetic mice pancreas. *J Cell Physiol*. 2018; 1–13. https://doi.org/10.1002/jcp.27568

Stem Cell Research & Therapy

RESEARCH Open Access

Direct lineage tracing reveals Activin-a potential for improved pancreatic homing of bone marrow mesenchymal stem cells and efficient ß-cell regeneration in vivo

Nidheesh Dadheech[1,2], Abhay Srivastava[1], Mitul Vakani[1], Paresh Shrimali[1], Ramesh Bhonde[3] and Sarita Gupta[1*]

Abstract

Background: Despite the potential, bone marrow-derived mesenchymal stem cells (BMSCs) show limitations for beta (ß)-cell replacement therapy due to inefficient methods to deliver BMSCs into pancreatic lineage. In this study, we report TGF-ß family member protein, Activin-a potential to stimulate efficient pancreatic migration, enhanced homing and accelerated ß-cell differentiation.

Methods: Lineage tracing of permanent green fluorescent protein (GFP)- tagged donor murine BMSCs transplanted either alone or in combination with Activin-a in diabetic mice displayed potential ß-cell regeneration and reversed diabetes.

Results: Pancreatic histology of Activin-a treated recipient mice reflected high GFP^+BMSC infiltration into damaged pancreas with normalized fasting blood glucose and elevated serum insulin. Whole pancreas FACS profiling of GFP^+ cells displayed significant homing of GFP^+BMSC with Activin-a treatment (6%) compared to BMSCs alone transplanted controls (0.5%). Within islets, approximately 5% GFP+ cells attain ß-cell signature (GFP^+ Ins^+) with Activin-a treatment versus controls. Further, double immunostaining for mesenchymal stem cell markers $CD44^+$/GFP^+ in infiltrated GFP^+BMSC deciphers substantial endocrine reprogramming and ß-cell differentiation (6.4% Ins^+/GFP^+) within 15 days.

Conclusion: Our investigation thus presents a novel pharmacological approach for stimulating direct migration and homing of therapeutic BMSCs that re-validates BMSC potential for autologous stem cell transplantation therapy in diabetes.

Keywords: Bone marrow mesenchymal stem cells, Activin-a, Lineage tracing, ß-cell differentiation

* Correspondence: saritagupta9@gmail.com
[1]Molecular Endocrinology and Stem Cell Research Laboratory, Department of Biochemistry, Faculty of Science, The M.S. University of Baroda, Vadodara, Gujarat, India
Full list of author information is available at the end of the article

Introduction

Stem cell-derived β-cells present a clear proof-of-concept for cell-based diabetes medication. After "Novacell protocol," substantial progress has been made in generating stem cell-derived ß-cells from embryonic stem (ES) cells, induced pluripotent stem (iPS) cells, or adult progenitor cells [1–3]. BMSCs, however, show great promise for diabetes mitigation both in rodents and newly diagnosed individuals with type-1 diabetes [4–7]. Previous studies have shown that rodent BMSCs spontaneously differentiate into endocrine pancreatic cells [8–10]. The mechanism, however, remains largely unknown to state whether BMSCs can transdifferentiate into β-cells in vivo or are required to support paracrine interplay for existing β-cell growth and differentiation?

Most studies addressing the contribution of BMSCs in β-cell survival or regeneration have used transplantation of naive BMSC, while some others have used genetic tag, i.e., GFP for monitoring transplanted cells [11, 12]. An early study by Hess et al. demonstrated the blood glucose-lowering effect within a week after intravenous infusion of GFP-tagged allogenic BMSCs into STZ-induced diabetic mice [4]. The authors reported as low as 0.5% frequency of donor GFP$^+$BMSC to reach the pancreas while fewer differentiate into insulin-producing cells within the host islets. In another similar study, only 1% allogeneic chimerism of repopulated BMSCs were shown to reach recipient pancreas and reverse diabetes in NOD mice [12]. Ianus et al. also showed that infused BMSCs can differentiate into insulin-producing islet cells when transplanted into lethally irradiated mice [8]. Interestingly, few other groups replicating similar studies with BMSCs reported no evidence for such an anti-diabetic effect after BMSC infusion [11, 13, 14].

The migration of BMSCs to colonize in degenerating pancreas appears to be the key for stimulating β-cell regeneration [15, 16]. Moreover, a method to stimulate pancreatic migration and trans-differentiation into β-cells limits their scope in cell therapy. It has been extensively demonstrated that the CXCR4stromal-derived factor-1 axis is crucial for BMSC migration and homing. Modulating the expression of the CXCR4 gene in BMSC could alleviate their tissue-specific homing [17, 18]. The use of chemical/biological modulators such as TGF-β family member protein Activin-a is shown to support differentiation of BMSCs [3, 19, 20]. Furthermore, Activin-a induces definitive endoderm differentiation by stimulating CXCR4 expression in ES/iPS cell-derived ß-cells and regulate migration to enhance homing [21–23].

We, therefore, used a lineage tracing approach in STZ-induced diabetic mice to demonstrate the potential of Activin-a in stimulating migration, improving pancreatic homing and efficient endogenous ß-cell differentiation.

Material and methods

Animals

Animal protocols were approved and performed as per Committee for the Purpose of Control and Supervision on Experiments on Animals (CPCSEA) and our Institutional Animal Ethics Committee (IAEC, MSU Baroda) (License no: 938/PO/a/06/CPCSEA) guidelines. We used male Balb/c mice, 6–8 weeks old, weighing 25–30 g and housed at 26 °C with 12 h light-dark cycle and food/water ad libitum.

Diabetes induction and blood glucose measurement

Diabetes was induced by 5 days multiple low dose streptozotocin (STZ) injections (70 mg/kg b wt). Fasting blood glucose was monitored with Accu-Chek Glucometer.

Isolation and purification bone marrow-derived mesenchymal stem cells

BMSCs were isolated from the tibia and femur bones of 4-week-old balb/c mice by modifying the protocols adapted from Zhu et al. and Hsiao et al. using differential trypsinization steps [24, 25]. For a more detailed protocol, please refer to supplementary methods.

Generation of permanently labeled GFP$^+$BMSC

One hundred thousand donor BMSCs were transfected with pPB-eGFP (1 μg) and pCYL43-PBase (2 μg) DNA vector (a gift from Sanger Institute, UK; for map, see supplementary figure-1) using lipofectamine 2000 (Invitrogen) in 1:3 volume ratio. Following transfection, stable GFP-expressing clones were selected on puromycin antibiotic at 300 μg/ml for the first 2 days and 900 μg/ml for the next 7 days. GFP$^+$ BMSCs colonies were hand-picked using 3.2 mm clonal discs (Sigma Aldrich, USA) and FACS sorted for enriched GFP$^+$ cells (see supplementary methods for cloning and purification strategy).

Flow cytometry

Live BMSCs at p#25 or single islet cells were acquired on BD Aria-III flow cytometer for GFP$^+$ cell quantification. For immunocharacterization, formalin-fixed BMSCs or islet cells were stained for MSC surface markers (CD34, CD44, CD90, CD45, CD117, Vimentin, and SMA) and endocrine differentiation antibodies (CD49b and PDX1). Cells were fixed in 4% formalin (30 min on ice), Triton-X100 permeabilized, and stained with primary labeled antibodies overnight at 4 °C for key MSCs and endocrine differentiation markers (see Table 1 for details). Data were acquired on BD Aria-III sorter using DIVA software and later analyzed with FlowJo software (FlowJo, USA).

In vitro differentiation of BMSC into islet-like clusters

GFP$^+$BMSCs were assessed for in vitro islet differentiation and formation of ILCC using Activin-a (20 ng/ml) as described previously [26, 27].

Table 1 List of primary antibodies

Sr. no.	Antibody	Company and catalog no.	Isotype IgG	Mono/polyclonal Ab	Mol. weight (KDa)	Application	Dilution
1	Nestin	Sigma#N5413	Rabbit	Poly	177	Western	1:1000
2	Pdx-1	BD#554655	Mouse	Mono	40	Western/IF	1:1000/1:200
3	Neurogenin-3	Sigma #SAB1306585	Rabbit	Poly	23	Western/IF	1:1000
4	β-Actin	BD#612657	Mouse	Mono	42	Western	1:10000
5	Nestin-PE	BD#561230	Mouse	Mono	177	IF	1:100
6	Insulin	CST#4590	Rabbit	Poly	6	IF	1:100
7	Glucagon	Sigma#G 2654	Mouse	Mono	3.48	IF	1:100
8	Somatostatin	Sigma #SAB4502861	Mouse	Poly	12	IF	1:100
9	CD90.2-FITC	BD#55302	Rat	Mono	~ 20	Flowcytometry/IF	1:10/1:500
10	CD44-PE	BD#553134	Rat	Mono	82	Flowcytometry/IF	1:10/1:500
11	CD34-FITC	BD#553733	Rat	Mono		Flowcytometry	1:10
12	CD45-APC	BD#559864	Rat	Mono		Flow cytometry	1:10
13	CD117-PE	BD#553869	Rat	Mono		Flowcytometry	1:10
14	CD49b	BD#554999	Rat	Mono		Flowcytometry	1:10
15	Vimentin	Sigma#C9080	Mouse	Mono	53	IF	1:400
16	Smooth muscle actin	Sigma#F3777	Mouse	Mono	42	IF	1:250
17	C-Peptide	CST#4593	Rabbit	Mono	5	IF	1:100

Transplantation of GFP-labeled BMSCs

For lineage tracing, one million GFP$^+$BMSCs were pre-incubated with Activin-a (2.5 μg/ml) for 30 min prior to the transplants and then injected intravenously into STZ-induced diabetic recipient mice, followed by daily Activin-a injections (25 μg/kg b wt) for 15 days post-transplantation. Diabetic STZ treated mice (control) did not receive donor GFP-labeled BMSC and Activin-a treatment, while a group of recipient mice received only donor GFP$^+$BMSC without Activin-a treatment, served as BMSC control.

Tissue preparation and immunohistochemistry

Pancreatic tissues from all mice at day 30 post diabetes induction were harvested, formalin-fixed, and sliced in 5 μm sections while BMSC for immunocytochemistry were fixed in 10% formalin overnight. For histology, tissue sections were deparaffinized with grading xylene and ethanol grades and rehydrated in water. Both tissues or cells were permeabilized and blocked with 4% donkey serum (Sigma Aldrich, USA) for 1 h at RT, followed by primary antibodies (see Table 1 for details) incubation overnight at 4 °C. The next day, cells were washed and labeled with secondary antibodies (see Table 2 for details) for 30 min at RT. Nuclei were marked with DAPI and mounted with Fluoromount-G (VECTASHIELD, USA). Images were captured on LSM710 confocal microscope and analyzed using Zen10 software (Carl Zeiss, USA).

Protein extraction and Western blotting

FACS-sorted green cells and single-cell islet suspension from diabetic and recipient mice isolated islets were lysed in RIPA buffer (1% triton X-100, 1% sodium deoxycholate, 0.1% SDS, 0.15 mM NaCl, 0.01 M Sodium Phosphate, pH 7.2). Fifteen micrometers protein after bradford quantification was loaded on 12% SDS-page to transfer onto a nitrocellulose membrane. Membranes

Table 2 List of secondary antibodies

Sr. no.	Antibody	Company and catalog no.	Isotype IgG	Mono/polyclonal Ab	Application	Dilution
1	Anti-Mouse-IgG-HRP	Jackson ImmunoResearch #115-035-003	Goat	Poly	Western	1:5000
2	Anti-Rabbit-IgG-HRP	Jackson Immuno Research #111-035-003	Goat	Poly	Western	1:5000
3	Anti-Mouse-IgG-FITC	Sigma#F8771	Goat	Poly	IF	1:200
4	Anti-Rabbit-IgG-FITC	Sigma#F9887	Goat	Poly	IF	1:200
5	Anti-Mouse-IgG-CF555	Sigma#SAB4600299	Goat	Poly	IF	1:100
6	Anti-Rabbit-IgG-CF555	Sigma#SAB4600068	Goat	Poly	IF	1:100

were blocked with 1% BSA in PBS and probed with primary antibodies (see Table 1) at 4 °C overnight. The HRP-labeled secondary antibody was then probed for 30 min at RT. Membranes were finally stained with Chemiluminescence detection reagent and images were captured on the gel documentation system (GE Healthcare). Densitometric protein expression was measured from pooled cell extracts from 3 mice in duplicates, and fold changes with SD were calculated using Fiji software.

Serum insulin ELISA

Serum insulin from animals was measured using a mouse insulin ELISA kit (Mercodia Inc., USA).

Statistical analysis

All statistical analysis was performed using GraphPad Prism-6 software using either two-way ANOVA or Bonferroni test for p value calculations with > 95% confidence. Statistics is described in legends for each figure. The number of mice transplanted is limited to $N = 3$ due to the huge cost incurred for daily Activin-a injections.

Results

Derivation, generation and characterization of GFP$^+$BMSC

We isolated BMSCs from donor mice surgically by modifying the previously described protocols from Zhu et al. and Hsiao et al. [24, 25]. A homogeneous population of BMSC without hematopoietic and macrophage contamination was achieved by differential trypsinization technique [25]. To perform lineage tracing of BMSCs, we created traceable BMSCs by permanent genomic integration of GFP using piggyback transposomal elements (Fig. 1a; Suppl. Fig-1). Transfected BMSCs show a high frequency of GFP$^+$ cells with flowcytometry (90.6%). Fluorescent imaging also confirmed the presence of high GFP signals in the FACS-sorted clone (Fig. 1b, Suppl. Fig-2). We further confirmed mesenchymal markers profiling post-genetic modification and observed GFP$^+$ BMSC retained the characteristics. Transfected cells displayed positive expression for CD44 (97.6%) (Fig. 1c), CD34 (88.9%), CD90 (87.5%), CD117 (18.5%), Nestin (48.9%), Vimentin (99.5%), Smooth muscle actin (89%), and pancreatic duodenal homeobox-1 (8.67%) (Suppl. fig-3), while negative expression for CD45 (1.67%) (Fig. 1c) and CD49b (0.17%) (Suppl. fig-3). These marker expressions correspond to BMSC according to the International Society of Cellular Therapy System [28]. It has been well known that human BMSCs do not express the CD34 marker, but at least in mice, there are marked differences in the CD34 expression profile. These have been discussed widely in two independent reports confirming the presence of CD34 expression in murine BMSCs [29, 30].

In vitro ß-cell generation potential of GFP$^+$BMSC

Prior to lineage tracing experiments, we examined the ß-cell differentiation potential of genetically labeled BMSCs using Activin-a growth factor, ex vivo, as previously reported [26, 31]. Genome integrated GFP$^+$BMSC showed effective cell clustering at day 2 deciphered into islet-like aggregates by day 4 till day 7, similar to the non-transfected control BMSC (Suppl. fig-1b). After 7 days of differentiation, islet-like clusters were stained for dithizone staining and confirmed for the presence of vimentin expression (red) and insulin (green) (Fig. 1d). Further, the presence of insulin (green), c-peptide (green), glucagon (red), and somatostatin (red) along with other crucial pancreatic reprograming markers, nestin (red), pdx1 (green), neurog3 (red), and neuro-d1 (green), confirmed BMSC-islet differentiation (Fig. 1e).

Model of pancreatic injury and lineage tracing of GFP + BMSC to contribute to the new ß-cell formation

To evaluate the BMSC potential for repair and restoring lost ß-cell mass, we adopted the STZ-induced diabetic model for partial ß-cell ablation and mild hyperglycemia. As per National Institutes of Health (NIH) and the Animal Models of Diabetic Complications Consortium (AMDC C), USA, the recommended blood glucose level for diabetes induction in STZ-treated mice under a non-fasting state should be > 200 mg/dl (11.1 mmol/l), whereas for a fasted animal, it should be > 150 mg/dl (8.4 mM) [32, 33]. Hence, we injected STZ at 70 mg/kg body weight for 5 days to attain glycemia > 11 mM in a fasted condition. It has been well documented that the pancreatic transcriptional reprogramming markers are only expressed at early time points for a very short duration during the β-cell regeneration process. To study BMSC-derived β-cell regeneration, it is mandated to perform lineage tracing studies early-on, post-transplantation. Hence, we performed lineage tracing on day 30.

We designed an experimental approach to study pancreatic repair upon transplantation of donor allogeneic GFP-expressing BMSC (Fig. 2a). Fasting blood glucose more than 15 mM for 30 days and depleted serum insulin levels confirm the model establishment for ß-cell death (Fig. 2c, d) Histo-morphological assessment of pancreatic sections stained with hematoxylin and eosin (H + E) and immunohistochemistry for insulin (red) showed pancreatic injury and ß-cell damage in islets at day 30, resulting in hypoinsulinemia and hyperglycemia (Fig. 2f, g). Another set of diabetic un-transplanted representative mice ($n = 2$) was sacrificed and the pancreas was harvested solely to survey the GFP expression in pancreatic cells by flow cytometry and microscopy and found negative for GFP signals (Fig. 2e). Established hyperglycemic recipient mice were intravenously transplanted with transgenic GFP + BMSC, and blood glucose

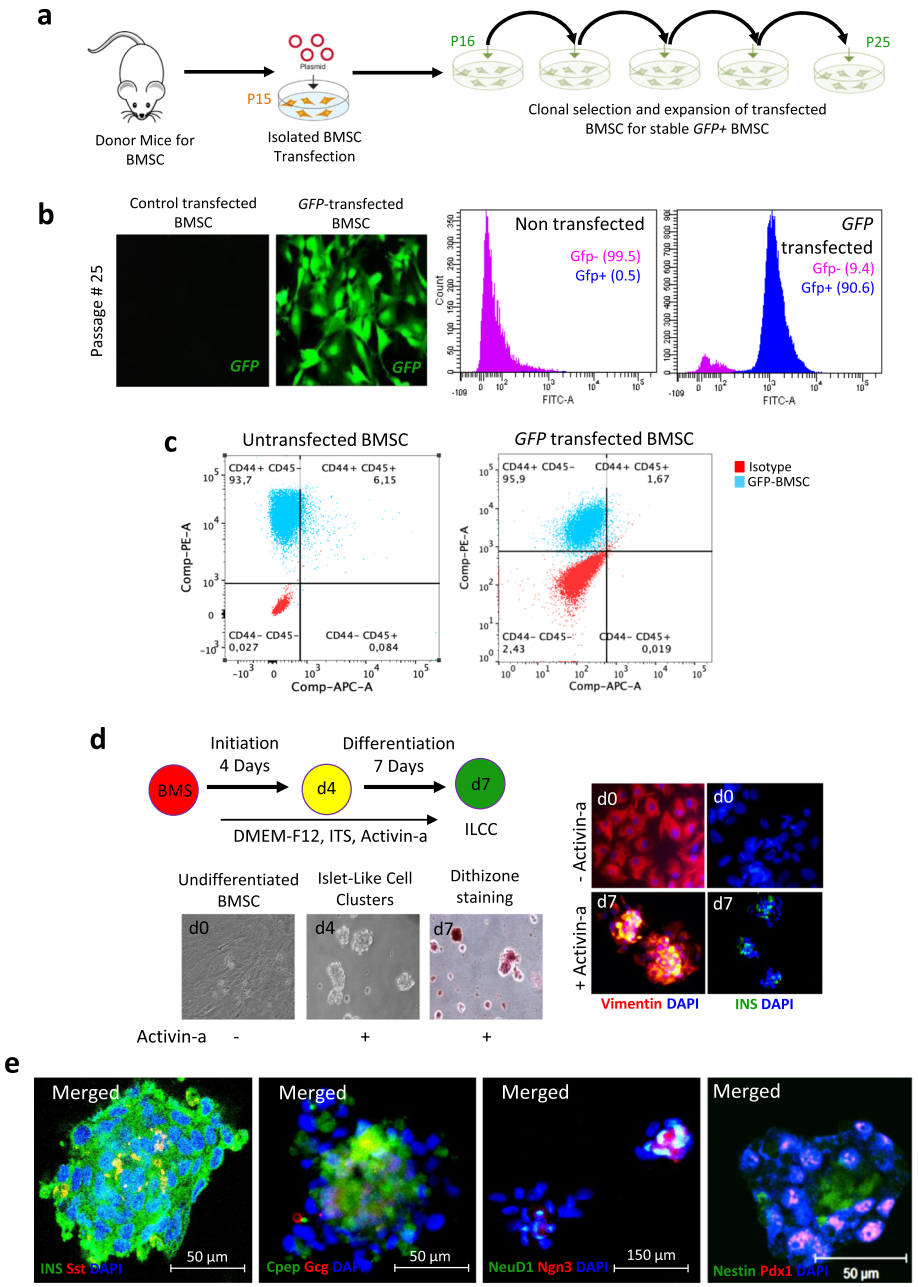

Fig. 1 Generation of GFP tagged mouse bone marrow-derived mesenchymal stem cells and differentiation into functional pseudo-islets. **a** Schematic representation for BMSC isolation and stable GFP+ clone selection. **b** Fluorescent images of stable GFP$^+$ (green) expressing BMSC and flow-cytometric quantification of sorted GFP$^+$BMSC line. **c** Immunophenotyping of mesenchymal stem cell markers in GFP$^+$BMSC in comparison untransfected BMSC using flow cytometry. **d** Schematic representation of islet differentiation protocol into functional islet-like cell clusters and representative microscopic images of GFP$^+$BMSC at days 0, 4, and 7. Immunostaining images for vimentin (red) and insulin (green) are represented at initiation and completion of differentiation steps. **e** Immunostaining images for insulin (green) and somatostatin (red); c-peptide (green) and glucagon (red); NeuroD1 (green) and Neurog3 (red), and pdx1 (red) and Nestin (green) in differentiation islet-like clusters

and serum insulin levels were measured. Control non-diabetic mice retained physiological glycemic control over the total duration of the study, while non-transplanted diabetic mice exhibited a hyperglycemic response after STZ injection with elevated blood glucose and severely depleted insulin levels (Fig. 2f, g). The data from mice transplanted with allogenic GFP$^+$BMSC without Activin-a treatment followed a similar glycemic pattern as the diabetic controls and fails to reverse diabetes. These findings coincide with the earlier similar reports where BMSC failed to reverse hyperglycemia. Additionally, in another group of our experimental design, where

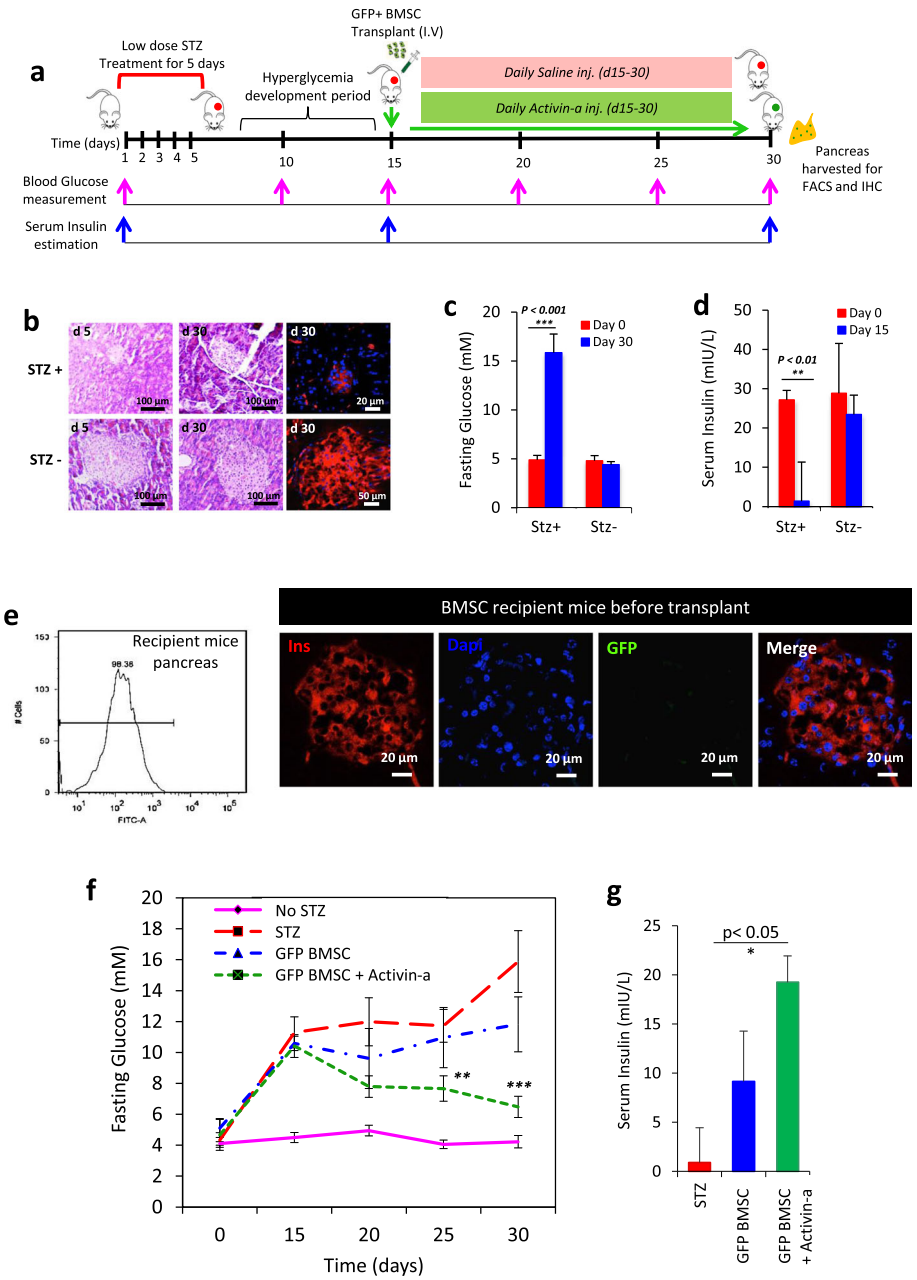

Fig. 2 Transplantation of GFP⁺BMSC into STZ induced diabetic mice model. **a** Experimental design and timeline for the development of STZ diabetic mice and assessment of pancreatic regeneration with GFP⁺BMSC in combination with Activin-a. **b** Evidence for the establishment of diabetes and pancreatic injury after STZ injections by representative pancreatic histology (H&E) and immunostaining for insulin (red). Graphical representation of fasting **c** blood glucose and **d** serum insulin levels in control and STZ treated mice. Data represent mean ± SEM with $N = 3$ mice per group. **e** Validation of GFP expression in recipient STZ treated mice pancreas using flow cytometry and immunostaining for insulin (red). Graphs represent **f** fasting blood glucose and **g** serum insulin levels in controls and donor transgenic BMSC recipient mice. Data represent mean ± SEM with $N = 3$ mice per group. All statistical analysis was performed using Graphpad Prism software using two-way ANOVA and Bonferroni test for *p* value calculations

mice transplanted with GFP⁺BMSC and also treated with Activin-a for 15 days, interestingly, we found a profound effect of this treatment on glucose-lowering and increased serum insulin levels after 30 days. We speculate that these results reflecting the reversal of diabetes in Activin-a treatment mice could be attributed to two possibilities: (1) GFP⁺BMSC contributes to a new ß-cell generation that resulted in increased insulin and

reduced blood glucose, and (2) Activin-a treatment substantially stimulate insulin biosynthesis or release from pre-existing ß-cells. To further test this, we performed lineage tracing and surveyed GFP-expressing cells in recipient mice's pancreas and liver. The aim is to survey for the evidence of transgenic BMSC contributing to ß-cell regeneration.

Activin-a treatment stimulates pancreatic migration and homing of GFP$^+$BMSC

We hypothesized that the effect on blood glucose and serum insulin levels in Activin-a treatment mice with bone marrow-derived stem cells is a result of the new ß-cell formation. To investigate this, we first examined the migration pattern and homing of GFP-expressing BMSC in diabetic control and GFP$^+$BMSC transplanted mice under the influence of Activin-a treatment. Pancreas and liver tissues harvested at day 30 from all groups of animals were digested to single-cell suspension for FACS quantification of GFP$^+$ cells. Whole pancreatic cells sorting from diabetic control and BMSC transplanted mice without Activin-a treatment displayed less than 1% (0.7 ± 0.44) GFP$^+$ cell migrating to the pancreas, whereas BMSC recipient mice treated with Activin-a presented significantly higher GFP 6 ± 0.42% expressing cells (Fig. 3a). Subsequently, no significant migration and homing were observed into the liver in all the groups (Fig. 3b), suggesting that Activin-a could only promote efficient pancreatic lineage migration of GFP$^+$ BMSC but not into the liver.

Further, to identify the specific molecular signature of pancreas migrated GFP$^+$ cells, we performed FACS profiling for GFP$^+$ cells with CD44 (mesenchymal marker) in the single-cell population. Both normal (0.12 ± 0.01%) and diabetic control (0.13 ± 0.01%) mice islet cells did not present CD44$^+$ cells, indicating that MSCs do not considerably reside within the islets. However, untreated diabetic recipient mice displayed approximately 0.31 ± 0.21%, while Activin-a treated recipient showed a significantly high number of CD44$^+$ cells (2.12 ± 0.31%), respectively, within the total cell population (Fig. 3d, Suppl. Fig-4). The fact that recipient mice received donor allogeneic BMSC, we then quantified the presence of GFP$^+$ cells specifically within the islet cell population. As expected, controls and untreated recipient diabetic mice pancreata contained an extremely low number of GFP$^+$ cells out of total islet population (control 0.75 ± 0.001%, diabetic control 0.83 ± 0.091%, and GFP-BMSC transplanted 0.51 ± 0.21%). Activin-a treated transplanted mice dramatically displayed a high frequency of GFP$^+$ cells (4.72 ± 0.87%) within the isolated islet cell population (Fig. 3e). This implied that Activin-a treatment in recipient mice could potentially stimulate efficient migration and improved homing of transplanted BMSCs to the injured pancreas.

If the donor BMSC were to contribute to new islet cell generation with Activin-a, we hypothesize that the subset of migratory GFP$^+$ cells in islets should demonstrate loss of CD44 expression without losing GFP signals. The GFP$^+$CD44$^-$ cells thereby present evidence of donor BMSC cell trans-differentiation into new islet cells. To do this, we FACS analyzed the dual stained (GFP/CD44) islet cells in each group. Again, no dual-stained cells in both controls were detected. A tiny fraction of undifferentiated GFP$^+$CD44$^+$ cells (0.13 ± 0.01%) was observed in untreated donor BMSC recipient mice. Similarly, Activin-a treated recipients demonstrated 3.67 ± 0.13% GFP$^+$CD44$^-$ (differentiated) and only 0.57 ± 0.07% GFP$^+$CD44$^+$ (undifferentiated) cells (Fig. 3c, e). The extent of differentiation of donor BMSC could be calculated by subtracting the frequency of undifferentiated cells GFP$^+$CD44$^+$ from the total GFP$^+$ cells quantified within the islets. We observed 25% of cells (0.13 out of 0.51%) of donor GFP$^+$BMSC in untreated and 88% cells (4.15% out of 4.72%) of donor GFP$^+$BMSC in Activin-a treated BMSC transplanted animals undergo trans-differentiation (Fig. 3f, Suppl. Fig-5). These observations collectively indicate that despite the potential, due to the fairly low migration of transplanted donor BMSC into the injured pancreas, not enough BMSCs could deliver and transdifferentiate into new insulin-producing cells which ultimately accounts for donor BMSC failure to mitigate hyperglycemia in control BMSC alone, recipients. On the other side, Activin-a treatment in conjunction with BMSC infusion in the recipient mice demonstrated this proof-of-concept for BMSC transdifferentiation.

Although BMSC in untreated animals holds the similar potential to produce new islet cells, however, due to the fairly low migration of transplanted donor BMSC into damaged islets, not enough BMSC deliver new insulin-producing cells and ultimately fails donor BMSC to reverse hyperglycemia in non-treated animals, unlike Activin-a treated ones.

Transplanted GFP$^+$ donor BMSC gives rise to β-cells in injured pancreas revealing evidence of β-cells neogenesis with Activin-a treatment

To investigate the endogenous β-cell regeneration, we compared the total number of insulin+ cells and GFP-expressing insulin cells in the pancreas. In our experimental model for lineage tracing using GFP$^+$BMSC as shown in Fig. 4a, at day 30, GFP$^-$Ins$^+$ cells would denote endogenous β-cell regeneration while the dual-positive GFP$^+$Ins$^+$ cells would confirm trans-differentiation of transplanted bone marrow-derived cells. Immunohistochemistry in diabetic control mice did not display any GFP-expressing cells but reduced insulin immunopositive region depicted β-cells damaged by STZ treatment (Fig. 4b). Further, occasional scattered GFP$^+$ cells were

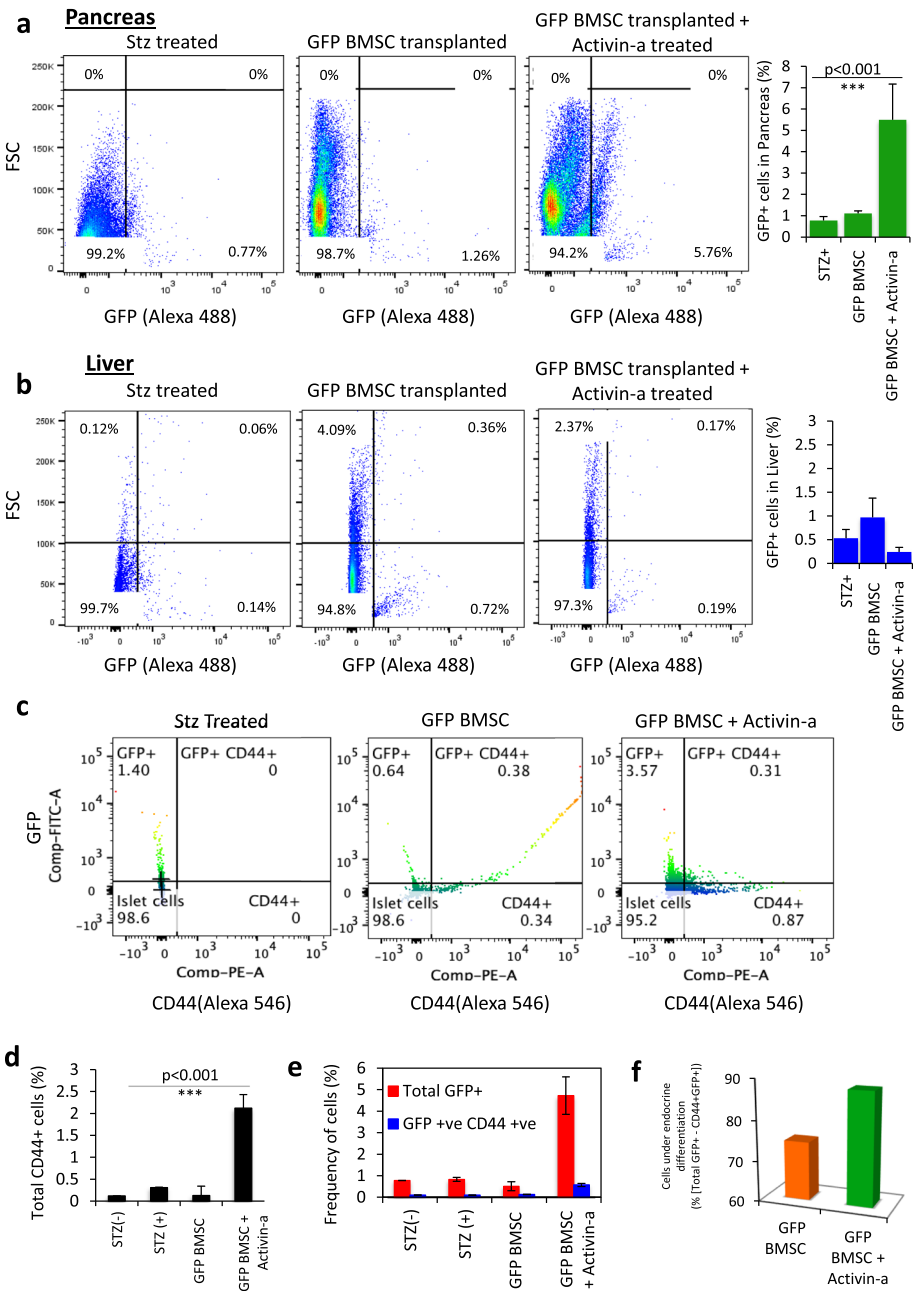

Fig. 3 Quantification of GFP$^+$BMSC in recipient mice pancreas and liver tissues. FACS analyses dot plots representing percentage population migrating to the **a** pancreas and **b** liver tissues in diabetic and donor BMSC recipient mice. Graphs present quantification of the mean frequency of GFP$^+$ cells in both pancreas and liver tissues in all groups of animals. Data represent mean ± SEM with $N = 3$ mice per group. **c** Immunophenotyping of CD44 and GFP-expressing cells in FACS sorted total pancreatic cell suspension. Graphs representing quantification of **d** total CD44$^+$ cells; **e** CD44$^+$GFP$^+$ dual population in harvested mice pancreas. **f** Graph showing quantification for the extent of endocrine differentiation in migratory donor BMSCs by reduced CD44 expression. This is calculated by subtracting CD44$^+$GFP$^+$ dual population from the total GFP$^+$ population. Data represent mean ± SEM with $N = 3$ mice per group. All statistical analyses were performed using Graphpad Prism software using two-way ANOVA and Bonferroni test for *p* value calculations

observed in the acinar region of untreated BMSC transplanted mice but devoid of insulin co-expression reflected the presence of undifferentiated BMSCs within islets. Moreover, in Activin-a-treated recipient mice, we could find a high ratio of GFP$^+$ cells in acinar, ducts, and islet regions. These animals presented 8.7 ± 0.46% GFP$^+$ cells, of which 6.4 ± 0.30% were GFP$^+$ β-cells per section of pancreatic tissue (Fig. 4c). We recorded the GFP-expressing cells infiltrated in large-sized islets co-expressing insulin as well as small clusters or β-cell

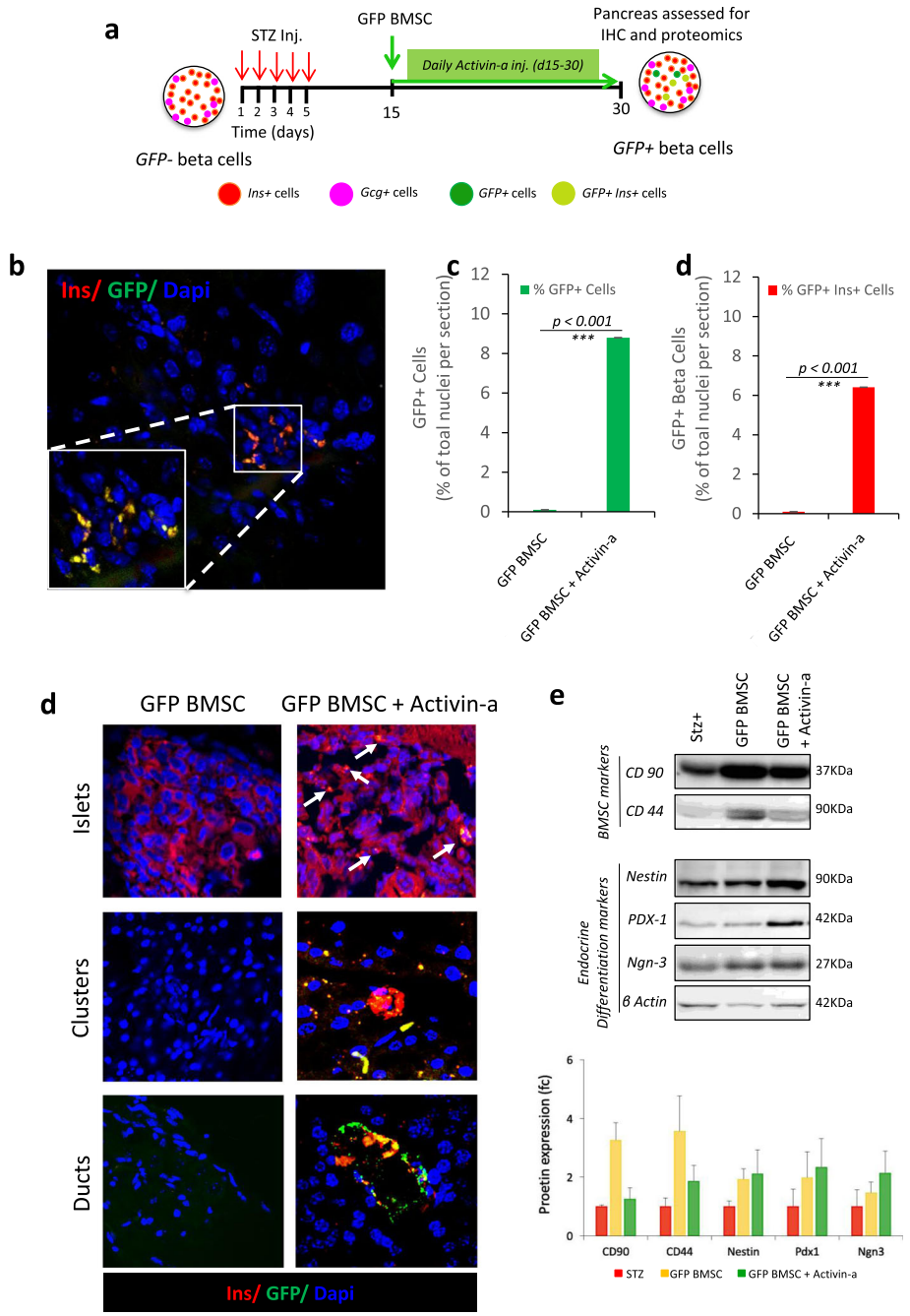

Fig. 4 In vivo lineage tracing of transplanted GFP^{+}BMSC in recipient mice pancreas. **a** Schematic representation of the experimental model to lineage trace GFP + BMSC contributing to new ß-cell generation. **b** Representative image from Activin-a treated GFP + BMSC recipient mouse pancreas showing GFP-labeled ß-cells by co-immunostained for GFP (green) with insulin (red). Nuclei were stained with Dapi (blue). The graph displays quantification of **c** total GFP+ cells and **d** GFP+ ß-cells within the islets of regenerating the pancreas. Data represent mean ± SEM with $N = 3$ mice per group. All statistical analyses were performed using Graphpad Prism software using two-way ANOVA and Bonferroni test for p value calculations. **e** Representative confocal microscopic images of immunostaining for insulin (red) and GFP (green) representing infiltration of transplanted GFP + BMSC in mature islets and ductal regions. Small clusters of GFP+ ß-cell present evidence for de novo BMSC-derived ß-cell formation from the transplanted BMSC. Nuclei were stained with Dapi (blue). **f** Proteomic characterization by western blotting and densitometric quantification of key pancreatic endocrine differentiation transcription factors from FACS sorted islet cells of 3 pooled representative mice pancreas, depicting evidence of new ß-cell differentiation markers. Chemiluminescence signals were exposed for 1–2 min and images were captured on the Gel Documentation system (GE Healthcare) and analyzed with ImageJ software. A single cropped area of key proteins from each condition is represented, while the graph represents densitometry quantification for each protein with standard deviation from 3 pooled mice cell extracts in duplicates

aggregates (Fig. 4d, Suppl. Fig-6). Interestingly, the entire cells in these clusters were found to be GFP positive along with insulin co-immunostaining, representing an index of β-cell neogenesis.

Activin-a-mediated Neurogenin-3 re-activation suggests the mechanism of trans-differentiation into GFP$^+$BMSC-derived β-cells

Using FACS-sorted single GFP$^+$β-cells from BMSC controls and Activin-a treated BMSC recipient mice pancreas, we investigated the mechanism of new β-cell formation by protein expression. Western blot analysis for key mesenchymal stem cells (CD90 and CD44) and β-cell differentiation markers (Nestin, Pdx1, and Neurog3) suggested neuroendocrine reprogramming in GFP$^+$ cells with Activin-a treatment. FACS-sorted green cells demonstrate high expression of CD90 in Activin-a-treated animals compared to STZ-treated diabetic controls. Correspondingly, CD44 remains fairly undetectable in diabetic control and Activin-a-treated groups Vs untreated BMSC recipients, suggesting lineage transformation of GFP$^+$BMSC into endocrine cells with Activin-a treatment. Increased protein expression of nestin, pdx1, and neurog3 in Activin-a treated BMSC recipients provides clear evidence for pancreatic endocrine cell reprograming with sequential activation of β-cell transcription factors. Neurog3 re-activation in GFP$^+$BMSC deciphers mechanism of trans-differentiation into new β-cells (Fig. 4e, Suppl. Fig-7).

Discussion

Over two decades, several studies presented shreds of evidence for generating β-cells from BMSC [34, 35]. Despite the BMSC potential, the underlying mechanism that governs critical signals for migration and homing of BMSC remains elusive. Lack of evidence and efficacy in migration for β-cell regeneration remained questionable.

Hess et al. reported a lowering of blood glucose levels and 0.5–2% GFP$^+$ cells reaching the pancreas [4]. Subsequently, others have reported no significant trans-differentiation of BMSC into insulin-producing cells, in vivo [14]. Our recent study suggests that permanently GFP-expressing BMSCs can efficiently reverse chemical-induced hyperinsulinemia and hyperglycemia. Using an endocrine cell-differentiating agent, Activin-a, we were now able to force prominent migration and colonization of GFP$^+$BMSCs into the injured pancreas. We believe that pre-incubation of BMSCs with Activin-a and enhanced CXCR4 expression in infused BMSCs could potentially accelerate the pancreatic migration and triggers endocrine differentiation for β-cell trans-differentiation. Our results redefined significant migration of GFP$^+$BMSC (~ 6%) into diabetic pancreas with Activin-a treatment, compared to 0.5–1% homing in BMSC transplanted/diabetic controls.

Wang et al. in 2006 reported that transplantation of GFP$^+$BMSCs into neonatal mice displayed 40% cell migration into exocrine while only a few contributes to the endocrine compartment [36]. We further redefine this with Activin-a that improves the absolute homing of BMSC specifically into endocrine (islets) fraction. Flow analysis of GFP and CD44 dual markers (Fig. 3e) and insulin/GFP imaging (Fig. 4b, d) confirm this observation. Other reports raised the concern of BMSC contributing to the development of fibrosis [37–39]; however, we did not observe this. We anticipate this could be potentially an outcome of crude bone marrow population infusion (including hematopoietic cells) while we have used more enriched and characterized and BMSC populations.

The presence of GFP+ β-cells within islets and small β-cell clusters in Activin-a treated mice confers endogenous pancreatic regeneration by BMSC transdifferentiation with daily Activin-a injections. We believe this is attributed to key endocrine transcriptional reprogramming initiation with Activin-a treatment. Protein expression profiling from FACS sorted green cells display concrete evidence for new β-cell generation and reveal a new mechanism of transdifferentiation by sequential activation of β-cell differentiation markers, precisely via neurogenin-3 re-activation in migrated GFP$^+$BMSCs.

Our method of endogenous pancreatic regeneration using BMSCs and differentiation growth factors like Activin-a could substantially influence a newer paradigm of cell therapy for diabetes in a wider diabetic population using GMP grade autologous BMSCs transplantation.

Conclusion

Our study concludes Activin-a potentiation in migration, homing, and β-cell differentiation of transplanted BMSCs. This novel pharmacological approach for stimulating direct migration and homing of therapeutic BMSCs reignites the scope for autologous BMSC transplantation therapy to treat diabetes.

Supplementary information

Supplementary information accompanies this paper at https://doi.org/10.1186/s13287-020-01843-z.

Additional file 1: Supplementary Figure 1. (a) Vector map depicting pPBGFP and pCyL43 Pbase plasmids for genomic-integrating and constitutively expressing GFP in transfected BMSC. (b) Islet differentiation stages and immunostaining representative images. **Supplementary Figure 2.** (a) Pictorial representation of BMSC clone selection strategy using flowcytometry, (b) FACS profiling, gating and sorting parameter images for positive GFP-BMSC clone, (c) Gating strategy and analysis used for population selection with doublet discrimination before BMSC surface immunophenotyping FACS quantification, and (d) representative FACS graphs for confirming cell viability and death using propidium iodide staining and fluorescent image of GFP (green) co-labelled with dapi nuclear staining. **Supplementary Figure 3.** Comparative immunophenotyping characterization of unmodified and genetically modified BMSCs with key mesenchymal, hematopoietic and pancreatic endocrine cell markers with

flow-cytometry. **Supplementary Figure 4.** Comprehensive flow cytometric quantification of percentage (a) total CD44 population and; (b) GFP population and within the injured pancreas in controls non-recipients and treated BMSC recipients with and without Activin-a treatment. **Supplementary Figure 5.** Comprehensive flow cytometric quantification of percentage GFP^+CD44^+ expressing dual population in FACS sorted single islet cell suspension. **Supplementary Figure 6.** (a) Immunocytochemical images from islet-like structures differentiated from GFP^+BMSC. (b) pancreatic immunohistochemical sections from GFP^+BMSC and GFP^+BMSC + Activin-a treated animals. **Supplementary Figure 7.** Unedited western blot images for mesenchymal stem cells and pancreatic differentiation transcription factors.

Additional file 2:. Supplementary Methods.

Abbreviations

BMSC: Bone marrow-derived mesenchymal stem cells; GFP: Green fluorescent protein; ESC: Embryonic stem cells; iPSC: Induced pluripotent stem cells; STZ: Streptozotocin; FACS: Flowcytometry

Acknowledgements

We also thank Dr. MM Panicker, NCBS, India, and Wellcome trust sanger institute, UK, for proving us the piggyBac plasmids for creating GFP-labeled BMSC.

Authors' contributions

Conceived and designed the experiments: ND, SG. Performed the experiments: ND, AS, MV, PS. Analyzed the data: ND, RRB, SG. Contributed reagents/materials/analysis tools: ND, RRB, SG. Wrote the paper: ND, SG. SG is the guarantor of this work and, as such, had full access to all the data in the study and takes responsibility for the integrity of the data and the accuracy of the data analysis. The authors read and approved the final manuscript.

Funding

This work was supported by the Department of Biotechnology, Government of India, New Delhi, India, for funding the project (grant no. BT/PR3564/BRB/10/975/2011) and DBT-MSUB-ILSPARE programme (Grant no. BT/PR14551/INF/22/122/2010) for establishing a high-end central instrumental facility for microscopy and flow cytometry at Maharaja Sayajirao University, Baroda, India.

Availability of data and materials

All relevant data are within the paper and its Supporting Information files.

Ethics approval and consent to participate

This research finding has been approved by the ethics committee of The MS University of Baroda, India.

Consent for publication

Not applicable.

Competing interests

The authors declare no conflict of interest for this study.

Author details

[1]Molecular Endocrinology and Stem Cell Research Laboratory, Department of Biochemistry, Faculty of Science, The M.S. University of Baroda, Vadodara, Gujarat, India. [2]Department of Surgery, Alberta Diabetes Institute, University of Alberta, Edmonton, AB, Canada. [3]Dr. D. Y. Patil Vidyapeeth, Pimpri, Pune, Maharashtra, India.

Received: 7 January 2020 Revised: 7 June 2020
Accepted: 20 July 2020 Published online: 30 July 2020

References

1. Ramiya VK, Maraist M, Arfors KE, Schatz DA, Peck AB, Cornelius JG. Reversal of insulin-dependent diabetes using islets generated in vitro from pancreatic stem cells. Nat Med. 2000;6(3):278–82.
2. Phadnis SM, Joglekar MV, Dalvi MP, Muthyala S, Nair PD, Ghaskadbi SM, et al. Human bone marrow-derived mesenchymal cells differentiate and mature into endocrine pancreatic lineage in vivo. Cytotherapy. 2011;13(3):279–93.
3. D'Amour KA, Bang AG, Eliazer S, Kelly OG, Agulnick AD, Smart NG, et al. Production of pancreatic hormone-expressing endocrine cells from human embryonic stem cells. Nat Biotechnol. 2006;24(11):1392–401.
4. Hess D, Li L, Martin M, Sakano S, Hill D, Strutt B, et al. Bone marrow-derived stem cells initiate pancreatic regeneration. Nat Biotechnol. 2003;21(7):763–70.
5. Xie QP, Huang H, Xu B, Dong X, Gao SL, Zhang B, et al. Human bone marrow mesenchymal stem cells differentiate into insulin-producing cells upon microenvironmental manipulation in vitro. Differentiation. 2009;77(5):483–91.
6. Sordi V, Piemonti L. The contribution of hematopoietic stem cells to beta-cell replacement. Curr Diab Rep. 2009;9(2):119–24.
7. Banerjee M, Bhonde RR. Autologous bone marrow transplantation/mobilization: a potential regenerative medicine for systemic degenerative disorders and healthy living. Med Hypotheses. 2007;68(6):1247–51. https://doi.org/10.1016/j.mehy.2006.09.069.
8. Ianus A, Holz GG, Theise ND, Hussain MA. In vivo derivation of glucose-competent pancreatic endocrine cells from bone marrow without evidence of cell fusion. J Clin Invest. 2003;111(6):843–50.
9. Zhao M, Amiel SA, Ajami S, Jiang J, Rela M, Heaton N, et al. Amelioration of streptozotocin-induced diabetes in mice with cells derived from human marrow stromal cells. PLoS One. 2008;3(7):e2666.
10. Luo L, Luo JZ, Xiong F, Abedi M, Greer D. Cytokines inducing bone marrow SCA+ cells migration into pancreatic islet and conversion into insulin-positive cells in vivo. PLoS One. 2009;4(2):e4504.
11. Choi JB, Uchino H, Azuma K, Iwashita N, Tanaka Y, Mochizuki H, et al. Little evidence of transdifferentiation of bone marrow-derived cells into pancreatic beta cells. Diabetologia. 2003;46(10):1366–74.
12. Zorina TD, Subbotin VM, Bertera S, Alexander AM, Haluszczak C, Gambrell B, et al. Recovery of the endogenous beta cell function in the NOD model of autoimmune diabetes. Stem Cells. 2003;21(4):377–88.
13. Beilhack GF, Scheffold YC, Weissman IL, Taylor C, Jerabek L, Burge MJ, et al. Purified allogeneic hematopoietic stem cell transplantation blocks diabetes pathogenesis in NOD mice. Diabetes. 2003;52(1):59–68.
14. Lechner A, Yang YG, Blacken RA, Wang L, Nolan AL, Habener JF. No evidence for significant transdifferentiation of bone marrow into pancreatic beta-cells in vivo. Diabetes. 2004;53(3):616–23.
15. Ohtake K, Saito T, Satoh Y, Kenjo A, Kimura T, Asawa S, et al. Bone marrow traffic to regenerating islets induced by streptozotocin injection and partial pancreatectomy in mice. Transplant Proc. 2008;40(2):449–51.
16. Tessem JS, Jensen JN, Pelli H, Dai XM, Zong XH, Stanley ER, et al. Critical roles for macrophages in islet angiogenesis and maintenance during pancreatic degeneration. Diabetes. 2008;57(6):1605–17.
17. De Becker A, Riet IV. Homing and migration of mesenchymal stromal cells: how to improve the efficacy of cell therapy? World J Stem Cells. 2016;8(3):73–87. https://doi.org/10.4252/wjsc.v8.i3.73.
18. Katoh M, Katoh M. Integrative genomic analyses of CXCR4: transcriptional regulation of CXCR4 based on TGFbeta, Nodal, Activin signaling and POU5F1, FOXA2, FOXC2, FOXH1, SOX17, and GFI1 transcription factors. Int J Oncol. 2010;36(2):415–20.
19. Hill CS. TGF-beta signalling pathways in early Xenopus development. Curr Opin Genet Dev. 2001;11(5):533–40.
20. Florio P, Luisi S, Marchetti P, Lupi R, Cobellis L, Falaschi C, et al. Activin A stimulates insulin secretion in cultured human pancreatic islets. J Endocrinol Investig. 2000;23(4):231–4.
21. Zhong W, Lai Y, Yu T, Xia ZS, Yuan YH, Ouyang H, et al. Wnt and Nodal signaling simultaneously induces definitive endoderm differentiation of mouse embryonic stem cells. Romanian J Morphol Embryol. 2017;58(2):527–35.
22. Wang Z, Li W, Chen T, Yang J, Wen Z, Yan X, et al. Activin A can induce definitive endoderm differentiation from human parthenogenetic embryonic stem cells. Biotechnol Lett. 2015;37(8):1711–7. https://doi.org/10.1007/s10529-015-1829-x.
23. Yasunaga M, Tada S, Torikai-Nishikawa S, Nakano Y, Okada M, Jakt LM, et al. Induction and monitoring of definitive and visceral endoderm differentiation of mouse ES cells. Nat Biotechnol. 2005;23(12):1542–50. https://doi.org/10.1038/nbt1167.
24. Zhu H, Guo ZK, Jiang XX, Li H, Wang XY, Yao HY, et al. A protocol for isolation and culture of mesenchymal stem cells from mouse compact bone. Nat Protoc. 2010;5(3):550–60.
25. Hsiao FS, Cheng CC, Peng SY, Huang HY, Lian WS, Jan ML, et al. Isolation of therapeutically functional mouse bone marrow mesenchymal stem cells

within 3 h by an effective single-step plastic-adherent method. Cell Prolif. 2010;43(3):235–48.
26. Dadheech N, Srivastava A, Paranjape N, Gupta S, Dave A, Shah GM, et al. Swertisin an anti-diabetic compound facilitate islet neogenesis from pancreatic stem/progenitor cells via p-38 MAP kinase-SMAD pathway: an in-vitro and in-vivo study. PLoS One. 2015;10(6):e0128244.
27. Dadheech N, Srivastava A, Belani M, Gupta S, Pal R, Bhonde RR, et al. Basal expression of pluripotency-associated genes can contribute to stemness property and differentiation potential. Stem Cells Dev. 2013;22(12):1802–17.
28. Dominici M, Le Blanc K, Mueller I, Slaper-Cortenbach I, Marini F, Krause D, et al. Minimal criteria for defining multipotent mesenchymal stromal cells. The International Society for Cellular Therapy position statement. Cytotherapy. 2006;8(4):315–7. e-pub ahead of print 2006/08/23. https://doi.org/10.1080/14653240600855905.
29. Lin CS, Ning H, Lin G, Lue TF. Is CD34 truly a negative marker for mesenchymal stromal cells? Cytotherapy. 2012;14(10):1159–63. e-pub ahead of print 2012/10/17. https://doi.org/10.3109/14653249.2012.729817.
30. Sharma A, Rani R. Do we really need to differentiate mesenchymal stem cells into insulin-producing cells for attenuation of the autoimmune responses in type 1 diabetes: immunoprophylactic effects of precursors to insulin-producing cells. Stem Cell Res Ther. 2017;8(1):167. e-pub ahead of print 2017/07/14. https://doi.org/10.1186/s13287-017-0615-1.
31. Dadheech N, Soni S, Srivastava A, Dadheech S, Gupta S, Gopurappilly R, et al. A small molecule Swertisin from Enicostemma littorale differentiates NIH3T3 cells into islet-like clusters and restores normoglycemia upon transplantation in diabetic Balb/c mice. Evid Based Complement Alternat Med. 2013;2013:280392.
32. Furman BL. Streptozotocin-induced diabetic models in mice and rats. Curr Protoc Pharmacol. 2015;70(5):47 41–20. https://doi.org/10.1002/0471141755.ph0547s70.
33. Breyer MD, Bottinger E, Brosius FC 3rd, Coffman TM, Harris RC, Heilig CW, et al. Mouse models of diabetic nephropathy. J Am Soc Nephrol. 2005;16(1):27–45. https://doi.org/10.1681/ASN.2004080648.
34. Gao F, Wu DQ, Hu YH, Jin GX, Li GD, Sun TW, et al. In vitro cultivation of islet-like cell clusters from human umbilical cord blood-derived mesenchymal stem cells. Transl Res. 2008;151(6):293–302.
35. Chao KC, Chao KF, Fu YS, Liu SH. Islet-like clusters derived from mesenchymal stem cells in Wharton's jelly of the human umbilical cord for transplantation to control type 1 diabetes. PLoS One. 2008;3(1):e1451.
36. Wang G, Bunnell BA, Painter RG, Quiniones BC, Tom S, Lanson NA Jr, et al. Adult stem cells from bone marrow stroma differentiate into airway epithelial cells: potential therapy for cystic fibrosis. Proc Natl Acad Sci U S A. 2005;102(1):186–91.
37. Watanabe T, Masamune A, Kikuta K, Hirota M, Kume K, Satoh K, et al. Bone marrow contributes to the population of pancreatic stellate cells in mice. Am J Physiol Gastrointest Liver Physiol. 2009;297(6):G1138–46.
38. Sparmann G, Kruse ML, Hofmeister-Mielke N, Koczan D, Jaster R, Liebe S, et al. Bone marrow-derived pancreatic stellate cells in rats. Cell Res. 2010;20(3):288–98.
39. Russo FP, Alison MR, Bigger BW, Amofah E, Florou A, Amin F, et al. The bone marrow functionally contributes to liver fibrosis. Gastroenterology. 2006;130(6):1807–21.

Publisher's Note

Research Article

Chemoprevention of breast cancer by *Psidium guajava* Linn.

Prachi D. Karia[a], Laxmi A. Patil[b], Mitul S. Vakani[c], Gaurav M. Chauhan[c], Sarita S. Gupta[c], S. P. Rathod[d], Kirti V. Patel[b*]

[a]*ITM School of Pharmacy, Dhanora Tank Road, Paldi Village, Halol Highway, Near Jarod, Vadodara, Gujarat, India*

[b]*Faculty of Pharmacy, The Maharaja Sayajirao University of Baroda,Vadodara, Gujarat, India*

[c]*Department of Biochemistry, Faculty of Science, The Maharaja Sayajirao University of Baroda, Vadodara, Gujarat, India*

[d]*Parul Institute of Pharmacy and Research, Vadodara, Gujarat, India*

Received: 20 August 2018 Revised: 9 September 2018 Accepted: 1 October 2018

Abstract

Objective: The present study was performed to investigate the chemo-preventive potential of Pulp of *Psidium guajava* (POPG) in breast cancer and elucidating it's mechanism of action by assessing its effect on key processes like apoptosis, angiogenesis and metastasis. **Materials and Methods:** The cytotoxicity assay of POPG was performed on MCF-7(ER+), MDA-MB-231(Triple negative) and MDA-MB-453 (HER2+) human breast cancer cell lines. Assessment of anticancer potential of POPG was done through measurement of growth rate, feed consumption efficiency, tumor parameters, estrogen and progesterone expressions & nucleic acid content in *in*-vivo study. The mechanism for anticancer potential was screened by *in-vitro* studies involving Migration assay (metastasis), Annexin V- FITC assay (apoptosis) and Chick Chorioallantoic Membrane assay (angiogenesis). Statistical analysis was done by ANOVA followed by bonferroni's post-hoc test. **Results:** The IC_{50} value of POPG on MCF-7 cells was significantly less than other two cell lines, indicating POPG to be more potent inhibitor of ER+ cells *in-vitro*. Confirmatory results were obtained in MNU induced mammary carcinoma. POPG attenuated tumor parameters, expression of estrogen and progesterone receptor, nucleic acid content and increased latency period. POPG prevented MCF-7 cell migration (66.67%) suggesting inhibition of metastasis. POPG significantly increased apoptotic rate, especially late apoptotic population (6.1%). The mean zone of inhibition in CAM assay was found to be 1.13±0.33 implying inhibition of neovascularization. **Conclusion:** POPG thus depicts chemoprevention of breast cancer and this could be attributed to its ability to induce apoptosis, curtail angiogenesis, prevent metastasis and is mediated through inhibition of estrogen and progesterone expression.

Keywords: Breast cancer, MCF-7 cells, methylnitrosourea, *Psidium guajava*

Introduction

Breast cancer continues to be the most frequently occurring cancer in women around the world. For women, the three most commonly diagnosed cancers are breast, lung and bronchus, and colorectal. Representing one-half of all the cases; breast cancer alone is expected to account for 30% all new cancer diagnoses in women. An estimated 41,070 breast cancer deaths will occur in 2017 (Siegel et al., 2017). In India, it is the cancer of breast alone which is expected to cross the figure of 200000 by the year 2021 (Takiar et al., 2010).

Based on the stage of diagnosis, breast cancer is treated with a multidisciplinary approach involving surgery, radiation and systemic therapy including chemotherapy or hormonal therapy (Harfindal and Helms, 2006). Surgery alone may increase the chances of relapse so combinations of chemotherapeutic agents are given. The side effects of chemotherapy depend on the individual, the drug used, the schedule and dose used. These side effects can include fatigue, risk of infection, nausea, vomiting, mouth sores, hair loss, anorexia, diarrhea and bone marrow suppression. Hormonal modifiers like Tamoxifen are given in estrogen

Address for Corresponding Author:
Dr. Kirti V. Patel
Associate Professor
Faculty of Pharmacy,
The Maharaja Sayajirao University of Baroda, Vadodara – 390001, Gujarat, India
Email: kirti.patel-pharmacy@msubaroda.ac.in

DOI:https://doi.org/10.31024/ajpp.2019.5.1.8

and progesterone positive breast cancer. The use of Tamoxifen is established but side effects like endometrial cancer and thromboembolic complexities are issue of concern. Moreover, chances of resistance development are higher. Radiation therapy causes swelling of the breast, redness and/or skin discoloration/hyperpigmentation and pain/burning in the skin.

Unfortunately, in spite of improved diagnostic skills and breakthrough in effective treatment, breast cancer continues to be the leading cause of cancer deaths among women worldwide. Cancer being a multifaceted disease should be targeted on multiple pathways. The complexity of this hyperproliferative disease requires the adoption of prevention as promising and rational way to control it. Several new studies have discovered that most patients on cancer therapy are concurrently self-medicating with one or several complementary and alternative medicines (Rockwell et al., 2005). Among Complementary and alternative medicines, natural herbal medicine is the most commonly used group of treatment. Herbal treatment is the oldest used system of medicine in the world with more than 2000 years history (Ma et al., 2011) The herbs prevent malignancy by promoting detoxification, modify the activity of precise hormones and enzymes, diminish lethal side effects and complications of chemotherapy and radiotherapy (Sakarkar and Deshmukh, 2011). Moreover, phytoconstituents resulting from the herbs such as *Vinca rosea, Taxus species, Allium sativum, Panax pseudoginseng, Taxus wallichiana, Tinospora cordifolia, Viscum album, Withania somnifera, Zingiber officinale* etc. have been used in numerous preparations to assist the body to battle cancer more efficiently and also decrease the harmful side effects of chemotherapy and radiotherapy. Vinca alkaloids, Docetaxel and Paclitaxel hold their names in FDA approved list for treatment of breast cancer. Thus, an attempt was made in the current study to identify an easily available common herb and evaluate its potential in the treatment or prevention of breast cancer. Hence, Pulp of *Psidium guajava* was selected as a plant for evaluating anticancer potency.

Psidium guajava traditionally employed intensively as folklore remedy for a wide spectrum of gastrointestinal diseases in India. *Psidium guajava* possess antibacterial, antispasmodic, anti-inflammatory, analgesic, anti-diarrheal, hepatoprotective and anti-diabetic activity (Barbalho et al., 2012). The anticancer activity of guava is proven in prostate cancer (Chen et al., 2010). Aqueous extract of leaves inhibited LNCaP cell proliferation and down-regulate expressions of androgen receptor and prostate specific antigen. Treatment with leaves also significantly diminished tumor size in a xenograft mouse tumor model (Chen et al., 2010). There is also molecular evidence that cytotoxic activities of guava may act via repression of the NF-kB pathway mainly inhibiting NF-kB transactivation level (Kaileh et al., 2007; Ojewole, 2006). The ethanol extract from guava leaf possess prostaglandin endoperoxide H synthase inhibitory activity, an enzyme responsible for synthesis of prostaglandins which play important role in inflammation and carcinogenesis (Kawakami et al., 2009). *Psidium guajava* contains myricetin (Miean and Mohamed, 2001), which is reported to be aromatase inhibitor (Paoletta et al., 2008) and anti-cancer (Lu et al., 2006) *in-vitro*. *Psidium guajava* fruits and leaves are enriched with anti-oxidative compounds that are able to suppress huge harming impacts of reactive oxygen species (ROS) which can be related to its anticancer activity (Feng et al., 2015; Thaipong et al., 2006).

In view of above mentioned facts, the present investigation was designed to evaluate the anticancer effects of *Psidium guajava* Linn. on mammary carcinoma.

Materials and Methods

Materials

MCF-7, MDA-MB-231 and MDA-MB-453 human breast cancer cell lines were procured from NCCS, Pune. Methylnitrosourea (MNU), Propidium iodide were procured from Sigma Aldrich. MTT, DMSO, Culture media, fetal bovine serum, penicillin G-streptomycin solution were procured from Himedia. Annexin V-FITC assay kit was procured from BD sciences.

Preparation of pulp of *Psidium guajava* (POPG)

Ripe fruits of *Psidium guajava* Linn**.** were collected from local market of Baroda and authenticated by senior scientist Dr**.** Geetha, Plant Breeding Department, National Research Centre for Medicinal and Aromatic Plants, Boriavi**.** All of the guavas were free from physical and pathological defects. The pulp was freshly prepared by mechanically crushing the *Psidium guajava* fruits and was standardized to maintain specific gravity in the range of 1.05 to 1.35. It was prepared in the doses of 100mg/kg, 200 mg/kg and 400 mg/kg.(Rai et al., 2007). A voucher specimen (voucher number MSUPC-016) of the same is deposited at Faculty of Pharmacy, The Maharaja Sayajirao University of Baroda, Vadodara, India.

Cell cultures

Human breast cancer cell lines MCF-7, MDA-MB-231 and MDA-MB-453 were cultured in Dulbecco's Modified Eagle's Medium (DMEM) -high glucose supplemented with 10% fetal bovine serum (FBS), 1% penicillin G-streptomycin solution at 37°C in a 5% CO_2 incubator.

MTT Assay

Cell growth inhibitory assay was performed by MTT method on human breast cancer cell lines as described

(Parvathaneni et al., 2014) with various concentrations (10-1000 µg/ml) of POPG for 24, 48, and 72 h.

Scratch Motility Assay

Anti-metastatic potential of POPG (820 µg/ml) was studied on MCF-7 cells for 24 hours by Scratch Motility Assay (Tang et al., 2013).

Annexin V- FITC apoptosis assay

Apoptosis was studied on MCF-7 cells using Annexin V-FITC/propidium iodide (PI) double staining as described with POPG (820 µg/ml) for 24 hrs (Zhu et al., 2014).

Chick Chorioallantoic Membrane (CAM) Assay

Anti-angiogenic potential of POPG was studied using Chick Chorioallantoic Membrane assay as described (Karia et al., 2018).

***In-vivo* MNU induced mammary carcinogenesis**

Nulliparous female Sprague Dawley rats were obtained from Zydus Research Centre, Ahmedabad. The animals were housed in a group of 6 rats per cage under well-controlled conditions of temperature (22 ± 2°C), humidity (55 ± 5%) and 12hrs/12hrs light-dark cycle. The animals had free access to conventional laboratory diet and distilled water *ad libitum*.

The experiment was carried out as per guidance of the Committee for the Purpose of Control and Supervision of Experiments on Animals (CPCSEA), Government of India and The Prevention of Cruelty to Animals act (PCA), 1960. All experimental protocols were approved by the Institutional Animal Ethics Committee (IAEC), Pharmacy Department, The Maharaja Sayajirao University of Baroda (MSU/IAEC/2015-16/1601).

Mammary cancer was induced by a single dose of 50mg/kg body weight of MNU, dissolved in 0.9% saline adjusted with acetic acid (pH=4) and then administered intraperitoneally. Experimental protocol was of 100 days (Jagadeesan et al., 2013).

The rats were randomly divided into 7 groups. The normal control (group 1) animals received saline. All groups except group 1 received single dose of 50mg/kg b.w; i.p MNU diluted in 0.9% saline adjusted with acetic acid at pH 4.0. Group 2 served as model control. Group 3 (Vehicle control) animals received sesame oil as per the body weight, Group 4 served as standard control and received Tamoxifen (1mg/kg b.w; s.c) (Martin et al., 1996). Group 5 To 7 were test groups and received POPG viz 100mg/kg; 200 mg/kg and 400mg/kg respectively (Rai et al., 2007). The experimental duration was for 100 days.

During experimental period, the rats were palpated for tumors every two weeks. Growth rate using formula (Final body weight/ Initial Body weight) $^{(1/Periods-1)-1}$ and feed consumption efficiency using formula (Weekly body weight gain/Weekly food consumption)*100 were calculated. At the end, animals were euthanized humanely for assessing different parameters. Tumor parameters (Parvathaneni et al., 2014) involved weight, number of tumors, volume, tumor incidence and latency period (Jagadeesan et al., 2013). Estrogen and Progesterone receptor expressions were quantified by immunohistochemistry (Parikh et al., 2005; Thordarson et al., 2001). The nucleic acids were extracted for measurement of DNA and RNA (Rengarajan et al., 2013).

Statistical analysis

All the data were expressed as mean ± SEM. The results were compared using a computer based fitting program (Prism, GraphPad version 5, GraphPad Software, Inc). Statistical difference between the means of the various groups were analyzed using ANOVA followed by post hoc Bonferroni's test with P value <0.05.

Results

Effect of POPG on cell inhibition (MTT assay) on human breast cancer cell lines

In the present study, POPG (10, 100, 200, 300, 500, 1000 µg/ml) showed decreased cell proliferation in MCF-7 human breast cancer cell line in concentration- and time-dependent manner (regression) when compared as seen by descending IC_{50} values (820 ±1.22 µg/ml, 680 ±1.34 µg/ml and 600 ±1.03 µg/ml for 24 h, 48h and 72 h respectively) (Figure 1(a)). The pattern observed for % cell inhibition in MDA-MB-453 cells was in accordance with those observed for MCF-7 cells but the % cell inhibition was comparatively weaker in case of MDA-MB-453 as depicted by IC_{50} (1000 µg/ml for 72 h) (Figure 1 (b)). The pattern obtained for % cell inhibition on MDA-MB-231 was completely different than that observed for MCF-7 and MDA-MB-453 cells. In case of MDA-MB-231 cells, the % cell inhibition was weak after 24 h as compared to 72 h. The IC_{50} value was higher than 1000 µg/ml (Figure 1 (c)). These results clearly demonstrated POPG potential to inhibit cell proliferation in MCF-7 human breast cancer cell line than in other two cell lines.

Effect of POPG on Scratch Motility Assay in MCF-7 human breast cancer cell line

Using scratch motility assay, a continuous and rapid movement was observed for all cells. The movement of cells was clearly evident in control wells at 24 hours, in which a highly confluent monolayer region gradually migrated to cell free 'scratch region'. In POPG treated well, the migration of cells was reduced and the reduction in migratory effect was found to be 66.67% (Figure 2).

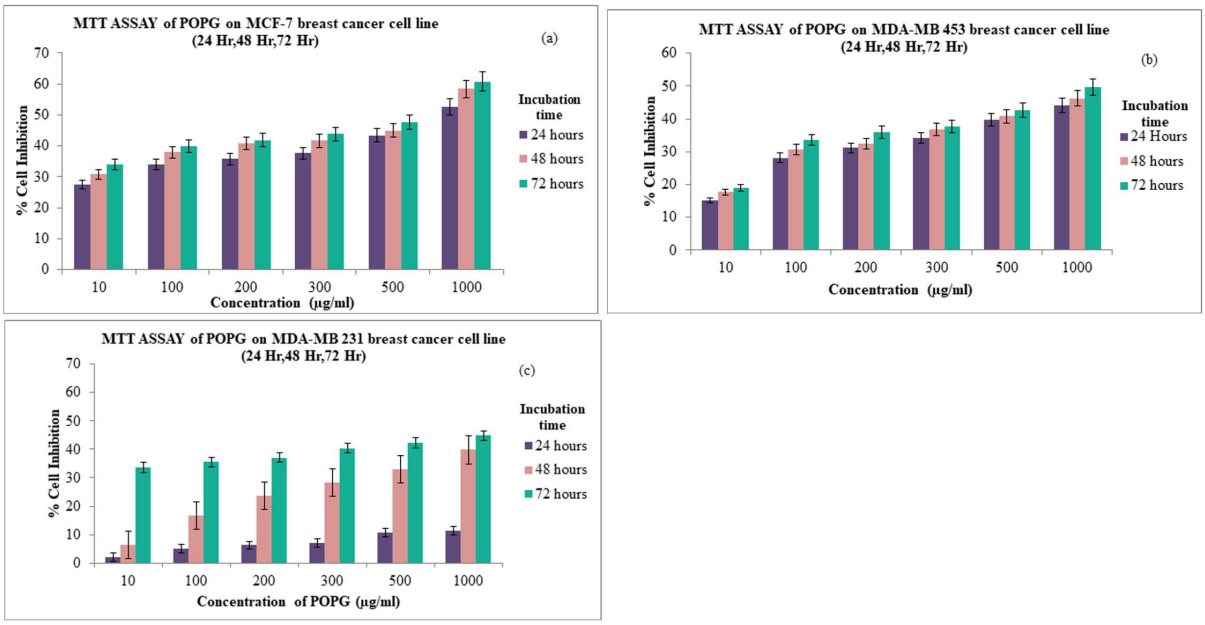

Figure 1. Effect of POPG on the cell inhibition on **(a).** ER+ MCF-7 human breast cancer cell line. **(b).** HER2+ MDA-MB-453 human breast cancer cell line **(c).** Triple negative MDA-MB-231 human breast cancer cell line. Values are expressed as mean ± SEM. (N=3)

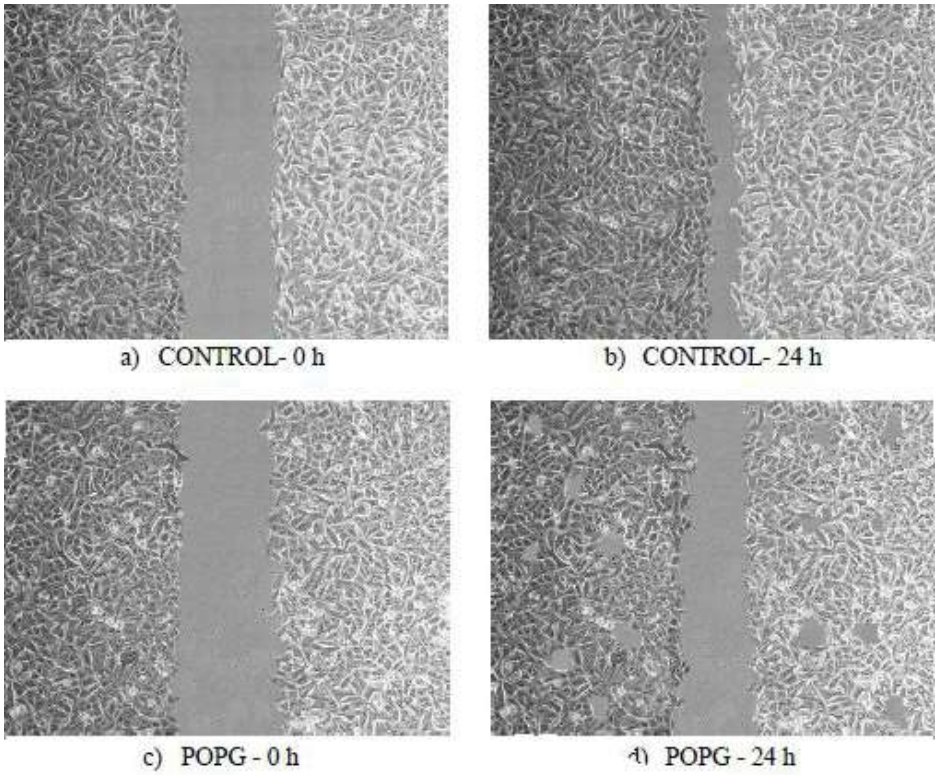

Figure 2. Effect of POPG on the cell migration (metastasis) on MCF-7 human breast cancer cell line. (a) Control- 0 h- MCF-7 cells with scratch. (b) Control 24 h- Migration of cells and restoration of monolayer in scratched area. (c) POPG- 0 h- MCF-7 cells with scratch (d) POPG 24 h- Inhibition of cell migration and less restoration of monolayer in scratched area as compared to control cells. The photographs are taken in Nikon Eclipse TS100. Magnification: 10X.

Effect of POPG on Apoptosis on MCF-7 human breast cancer cell line (Annexin V- FITC binding assay)

The results of Annexin V/PI double-staining assay demonstrated that the apoptosis of MCF-7 cells was observed after treatment with POPG for 24 h. As shown in Figure 3, after treatment with POPG, viable cell percentage was reduced to 54% which was 72.1% in control cells. The early apoptotic populations were found to be 2.5% whereas 6.1% cells were found to be in late apoptotic phase after treatment with POPG. The necrotic phase constituted 5.3% cell population. The

Table 1. Effect of POPG on Tumor parameters in MNU induced mammary carcinogenesis

Groups	Tumor Incidence	Tumor burden	Tumor multiplicity	Tumor weight (g)	Tumor volume (mm^3)	Tumor latency period (days)
Normal control	0	0	0	0	0	0
Model control	5	6	1	6.4± 1.46$^{###}$	99.29± 1.18$^{###}$	45.17±9.21$^{###}$
Vehicle control	6	6	1	6.2± 1.55	89.74± 1.18	53.23±19.41
Standard control	5	5	0.84	0.88±0.29***	2.02±6.33***	82.17±16.43**
POPG 100 mg/kg	6	6	1	3.27±0.64*	23.57± 3.45***	68.67±13.43
POPG 200 mg/kg	6	6	1	2.6±0.66**	12.04± 1.79***	71.5±15.90
POPG 400 mg/kg	5	5	0.84	1.4±0.33***	5.16± 2.54***	75±1.63*

Values are expressed as Mean ± SEM of 6 animals. Values are statistically evaluated using ANOVA analysis followed by Dunnette's Post hoc test. Significant values were compared with ###P<0.001 normal control vs. model control; *P<0.05 model control vs. all other groups; **P<0.01 model control vs. all other groups ***P<0.001 model control vs. all other groups

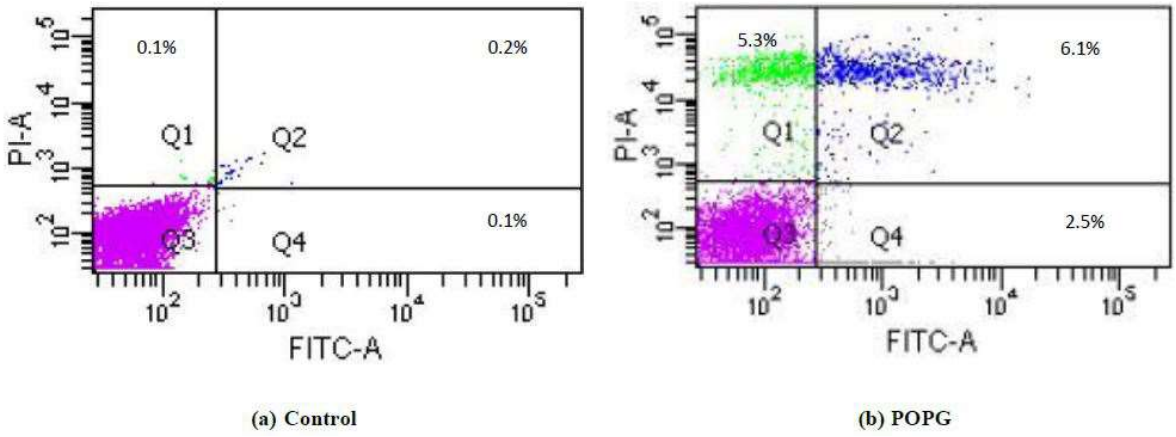

(a) Control (b) POPG

Figure 3. Effect of POPG on the apoptosis on MCF-7 human breast cancer cell line: Q1: Necrosis; Q2: Late Apoptosis; Q3: Viable cells; Q4: Early Apoptosis. (a) Control MCF-7 cells. (b) MCF-7 cells treated with POPG: Percentage of late apoptotic and necrotic population is increased. The analysis was done by FACSDiva Version 6.1.3.

untreated cells did not show any significant apoptosis.

Effect of POPG on Chick Chorioallantoic Membrane Assay in fertilized eggs

The antiangiogenic activity of POPG was investigated using a CAM assay. The increase in the blood vessel total diameter was observed in the PBS control group over the 48 h treatment and monitoring period. Starting from the first day of POPG treatment, a decrease in the vasoproliferation was observed. POPG produced a significant decrease in the development of angiogenesis in a chick embryo without any sign of thrombosis and hemorrhage over 48 h treatment and monitoring period (Figure 4). The zone of inhibition was found with 1.13±0.33 mm.

Effect of POPG on Tumor Parameters in MNU induced mammary carcinogenesis

Oral administration of SD rats bearing MNU induced mammary cancer with POPG significantly decreased the mammary cancer. The incidence rate in untreated MNU group was found to be 83.33%. The weight and volume of tumor in positive control animals were found to be 6.4±1.47 g and 99.29 ±3.19 mm^3. The

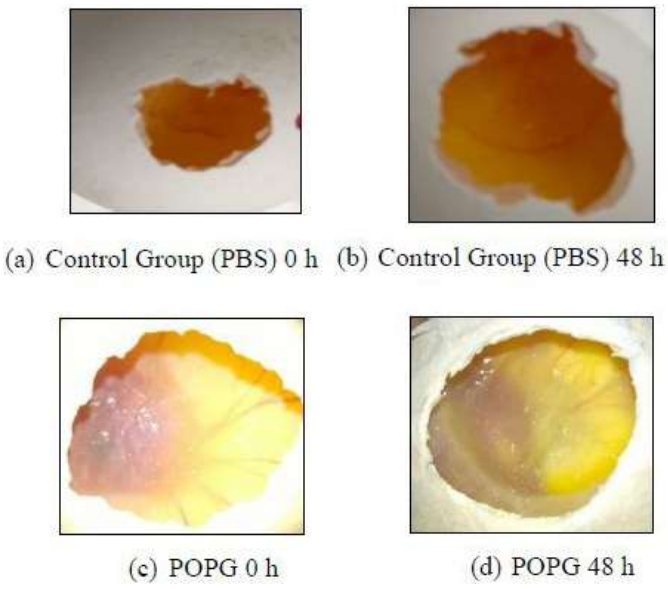

Figure 4. Effect of POPG (30µg/ml) on angiogenesis in the Chick Chorioallantoic Membrane of fertilized eggs: (a) Control group 0 h (b) Control group after 48 h- no hindrance in growth and neovascularization of CAM was observed. (c) POPG 0 h (d) POPG 48 h- Zone of inhibition with loss of blood vessels

weights and volume were significantly curtailed in all treatment groups. The latency period of cancer bearing group II was found to be 45 days. Tamoxifen (82.17±16.43; P<0.001) and all doses of POPG (100mg/kg: 68.67±13.43; 200mg/kg: 71.5±15.90 and 400mg/kg: 75±15.90) prolonged latency period. No significant changes were observed in group III vehicle control animals (Table 1).

Effect of POPG on Growth Rate in MNU induced mammary carcinogenesis

When body weight was evaluated as % growth rate, significant difference was found from 63 day. From then, the growth rate of model control animals decreased significantly (P<0.05) till the end. In vehicle control, the growth rate curve runs parallel to model control suggesting no significant difference. On treatment with POPG (100mg/kg, 200mg/kg and 400 mg/kg) and tamoxifen, the growth rate curve resembles to normal control and is significantly different from model control (Figure 5).

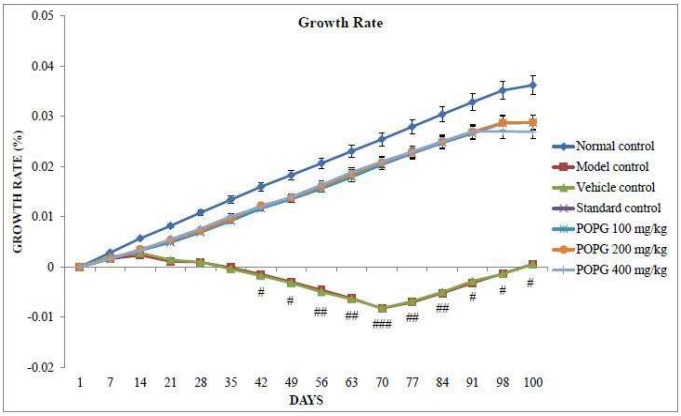

Figure 5. Effect of POPG on Growth Rate in MNU induced mammary carcinogenesis. Values are expressed as mean ± SEM of 6 animals. Values are statistically evaluated using Two way ANOVA analysis followed by Bonferroni's post hoc test. Significant values were compared with normal control vs. model control (#P<0.05, ##P <0.01, ###P<0.001)

Effect of POPG on Feed Consumption Efficiency in MNU induced mammary carcinogenesis

Food intake was calculated as food consumption efficiency. The model control animals showed decreased in feed consumption efficiency. There was no significant difference found between treated groups (Figure 6).

Effect of POPG on Estrogen and Progesterone receptor expressions in MNU induced mammary carcinogenesis

Immunohistochemical analysis revealed that the breast tumor tissue of cancer bearing group II animals expressed significantly higher number of positive stained estrogen and progesterone nuclei. The % positive stained ER and PR cells in model control were found to be 60% ± 1.03 and 73.34%± 1.29 respectively when compared to normal breast tissue (ER- 30.56% ± 0.98; PR-43.66% ± 1.38). Treatment with highest dose of POPG and Tamoxifen significantly decreased expression of estrogen and progesterone as compared to model control. The % positive stained ER and PR cells for POPG were found to be 42% ± 1.13 and 56.66% ± 2.69 respectively. The % positive stained ER and PR cells for tamoxifen were found to be 31.66% ± 0.89 and 46.66% ± 1.78 respectively (Figure 7 and 8).

Effect of POPG on Nucleic Acid contents in MNU induced mammary carcinogenesis

Within the tumor tissues of group II cancer bearing animals, the significant increased (P<0.05) levels of nucleic acids. (DNA: 5.72±1.02; RNA: 4.69±1.07) were observed when compared to group I control animals (DNA: 3.66±1.03; RNA: 2.47±1.42). Ironically, these rises were attenuated by treatment groups (P<0.05) dose dependently. The

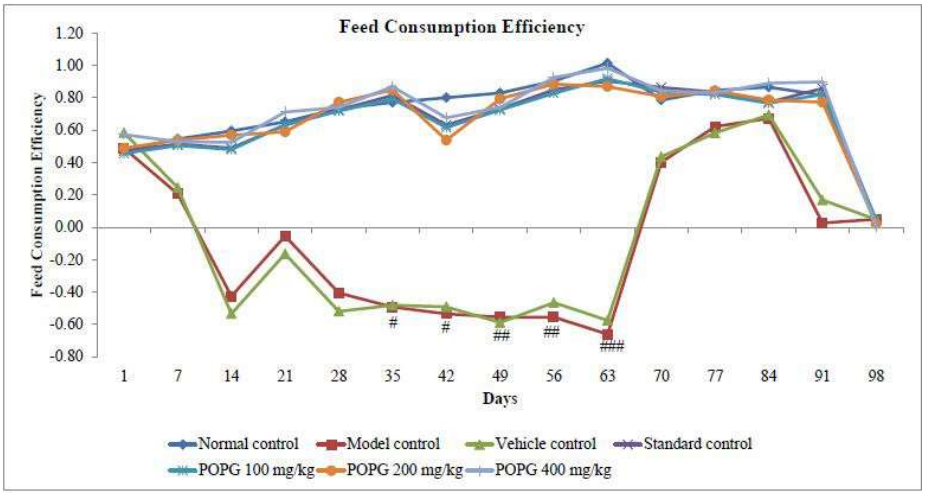

Figure 6. Effect of POPG on Feed Consumption Efficiency in MNU induced mammary carcinogenesis. Values are expressed as mean ± SEM of 6 animals. Values are statistically evaluated using Two way ANOVA analysis followed by Bonferroni's post hoc test. Significant values were compared with normal control vs. model control (# P<0.05, ##P <0.01, ###P<0.001)

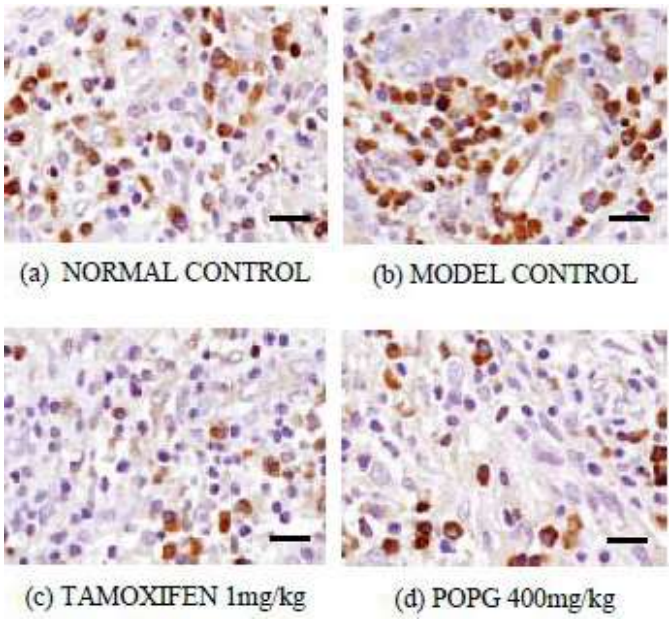

Figure 7. Effect of POPG on the expression of Estrogen in MNU induced mammary carcinogenesis. (a) Normal control (b) Model control- More positively stained brown nuclei representing higher expression levels of estrogen receptor (c) Tamoxifen- Purple hematoxylin estrogen negative stained nuclei are more in number (d) POPG- Positively stained brown nuclei are reduced. The photographs are taken in Nikon Eclipse TS100. Magnification: 10X; Scale bar: 100µm

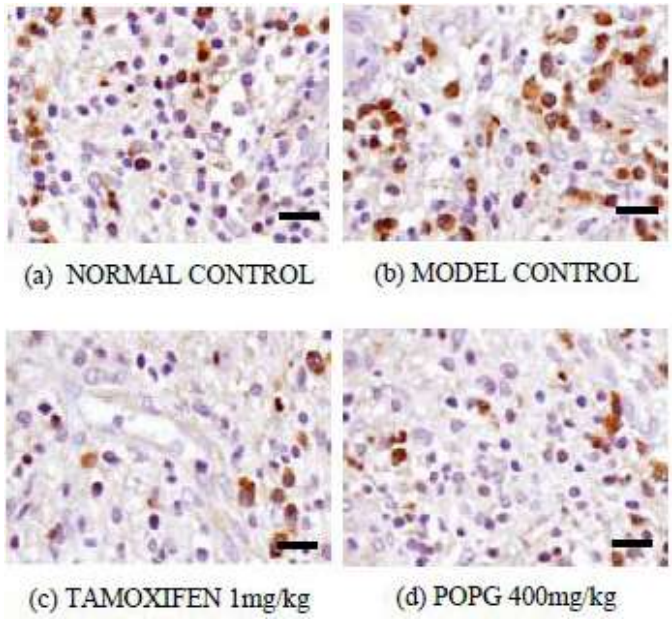

Figure 8. Effect of POPG on the expression of Progesterone in MNU induced mammary carcinogenesis. (a) Normal control (b) Model control- More positively stained brown nuclei representing higher expression levels of progesterone receptor (c) Tamoxifen- Purple hematoxylin progesterone negative stained nuclei are more in number (d) POPG- Positively stained brown nuclei are reduced. The photographs are taken in Nikon Eclipse TS100. Magnification: 10X; Scale bar: 40µm

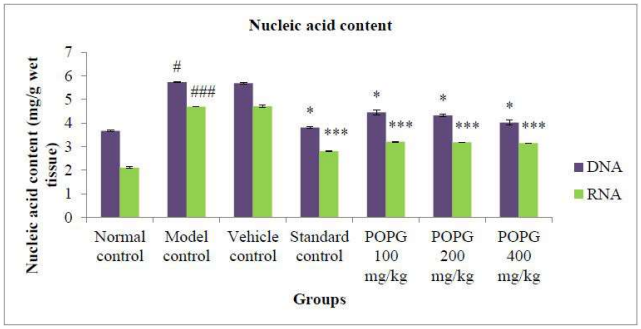

Figure 9. Effect of POPG on nucleic acid content in MNU induced mammary carcinogenesis. Each bar represents Mean ± SEM of 6 animals. Values are statistically evaluated using One Way ANOVA analysis followed by Bonferroni's post hoc test. Significant values were compared with normal control vs. model control (#P<0.05; ###P<0.001); model control vs. all other groups (*P<0.05 ***P<0.001).

percentage reduction in DNA content in Tamoxifen and POPG (100, 200, 400mg/kg) treated group were 33.50%, 22.37%, 24.69% and 29.90% respectively. The percentage reduction in RNA content in Tamoxifen and POPG (100, 200, 400mg/kg) treated group were 40.21%, 31.81%, 32.37% and 33.01% respectively (Figure 9).

Discussion

Carcinogenesis is an extremely dynamic, nonlinear process following unpredictable pathways. After immense research into its etiology, pathways and mechanisms, it still remains to be vulnerable disease. Despite the advancements in diagnosis and treatment modalities, the mortality and morbidity associated with cancer is colossal.

According to report of American Cancer Society- Cancer Facts and Figures in 2017, in female breast cancer tops the list followed by lung and colorectal. An estimated 2,52,710 new cases of breast carcinoma are expected to be diagnosed in 2017 accounting 30% of all cancer (Siegel et al., 2017).

Since antiquated times, plants and plant-derived compounds have furnished tremendous backing in conventional medication framework, and have been used as source of new potential drugs in modern pharmaceutical industries. Several new studies have discovered that most patients on cancer therapy are concurrently self-medicating with one or several complementary and alternative medicines (Rockwell et al., 2005). Approximately 60% of drugs currently used for cancer treatment have been isolated from natural products and the plant kingdom has been the most significant source.

The cancer cells acquire certain unusual capabilities like uncontrolled cell proliferation, metastasis, invasiveness due to oxidative stress, sustained angiogenesis, resistance to

apoptosis and genetic mutation (Hanahan and Weinberg, 2000). The sustained proliferation is the most defining feature. The ability of anticancer drug to inhibit cell proliferation can be explored using cancer cell lines. One such widely used cell line based assay is MTT assay. MTT Cell Proliferation and Viability Assay is a safe, sensitive, in vitro assay for the measurement of cell proliferation or, when metabolic events lead to apoptosis or necrosis, a reduction in cell viability. To estimate this property, different human breast cancer cell lines *viz.* MCF-7, MDA-MB 453 and MDA-MB-231 were used. MCF-7 is ER+ cell line, MDA-MB-453 is HER+ cell line whereas MDA-MB-231 was used as a model of triple-negative breast cancer (Holliday and Speirs, 2011). Based on present findings, the value of IC_{50} of POPG in MCF-7 cells was found to be significantly less than that of MDA-MB-231 and MDA-MB-453 cells, which indicated the higher inhibitory potency of POPG in MCF-7 cells than in other two cell lines. Furthermore, regression analysis showed that the effect of POPG was dose- and time- dependent on MCF-7 cells at highest concentration.

In course of metastasis, cancer spread beyond the place of origin into the other parts of body. Recurrence and metastasis of breast cancer after initial diagnosis and treatment are one of the major challenges for current therapeutic methods. Prevention of metastasis is very crucial for success of breast cancer therapy and survival of patients after diagnosis and treatment (Weigelt et al., 2005). Hence investigating the migration inhibition potential of POPG was undertaken and results suggested that it has potentially inhibited the migration of breast cancer cell line MCF-7. The effect might be contributed to its property to inhibit cell to cell contact.

Cell apoptosis is a normal physiological process of orderly controlled cell death for maintaining stable internal environment of the whole organism. Compounds that can induce cell cycle arrest and apoptotic cell death are generally considered to be potential anticancer drugs (Pistritto et al., 2016). The experimental data provided evidence for POPG induced apoptosis in MCF-7 human breast cancer cell line, implying a strong correlation between inhibition of cell-proliferation and apoptosis. The pathways for POPG-induced apoptosis need to be further elucidated.

Severe pathological processes such as solid tumour growth and metastasis are angiogenesis- dependent and a novel approach in cancer therapy and prevention is the use of agents with antiangiogenic activity (Samant and Shevde, 2011). Anti-angiogenesis effect was studied using Chick Chorioallantoic Membrane. In the chick embryo, the chorioallantois is formed between days 4 and 5 of development, when the outer mesodermal layer of the allantois fuses with the mesodermal lining of the chorion, and a network of blood vessels is gradually formed between the two layers. The central portion of the CAM is fully developed by day 8 to 10 at which time it becomes capable of sustaining tissue grafts, while the outskirts of the CAM are still developing and expanding until the CAM fully envelopes the embryo at day 12 of incubation (Deryugina and Quigley, 2008). In our study, we introduced filter paper disk containing POPG on Day 8 and observed it for next 48 hours. The results indicates that POPG has antiangiogenic effect, which might be phyto-constituents like lycopene which possess anti-angiogenic property (Chen et al., 2012).

To validate *in-vitro* results, mammary carcinogenesis was induced in rodents by intra peritoneal administration of N-methyl N- nitrosourea (MNU) (Macejova and Brtko, 2001). MNU is a water soluble direct alkylating carcinogen, and highly specific carcinogen for mammary gland. MNU induced mammary carcinomas are aggressive, more estrogen dependent and locally invasive. Mammary carcinomas arising from MNU- induced hyperplastic alveolar nodule contain transformed c-Ki-ras proto-oncogene with the present of specific G-35 A-35 point mutation in codon 12, which results in the substitution of normal glycine with the aspartic acid (Macejova and Brtko, 2001). With this, amplification of cyclin D1 gene, IGF2, loss of expression of the mitogenic growth factor gene, heparin binding growth factor midkine gene and mutation in the tumor suppressor p53 gene are seen in mammary tumors. Literature survey reveals that injecting 50mg/kg b.w (i.p.) MNU to nulliparous Sprague Dawley (SD) female rats induces mammary carcinoma (Jagadeesan et al., 2013; Parikh et al., 2005; Parvathaneni et al., 2014).

Our reports are in harmony to above studies. Injecting MNU (50mg/kg b.w; i.p.) to nulliparous SD female resulted in mammary tumors. Tumor was induced after 45 days post MNU injection. Five out of six rats developed mammary carcinoma suggesting 83.33% tumor incidence. Tumor burden i.e. total number of tumors in MNU injected groups was found to be 6. One rat developed two mammary tumors. Tumor multiplicity i.e. number of tumors per rat was found to be 1. Tumor weight and volume were found to be 6.4±1.47 g and 99.29 ±3.19 mm^3 respectively. The data proposed successful induction of mammary carcinomas in MNU injected rats.

Pulp of *Psidium guajava* (POPG) was used as treatment for MNU induced mammary carcinogenesis. Based on literature survey, 100mg/kg, 200 mg/kg and 400 mg/kg were selected for preventing mammary carcinogenesis (Chen et al., 2010; Gakunga et al., 2013; Ojewole, 2006; Rai et al., 2007). The results of the study have indisputably demonstrated that suppression of carcinogen-induced tumor incidence and multiplicity is caused by

administration of POPG. The latency period of tumor appearance was lengthened in POPG 400 mg/kg as compared to model control ($P < 0.05$). However, tumor incidence, multiplicity and latency period of POPG (100 mg/kg and 200 mg/kg) was not significantly different from model control. It is worthy of mention that tumor weight and tumor volume was significantly lower than model control in all treated groups. This confirms that POPG inhibit cancer cell proliferation which might be due to oncosuppressive potential of POPG.

It has been documented that there is a significant loss in the body weight and in contrast a considerable increase in the organ and as well as tumor weight in cancer conditions. It is also seen in humans possessing breast cancer. The growth rate, parameter of body weight, of the MNU injected animals was declined when compared to control groups. This may be due to the changes in energy metabolism during tumor formation and in addition an increased level of MDA also plays an important role in the initiation of tumor development and in the decrease of body weight (Rengarajan et al., 2013). Also, the feed consumption efficiency was decreased in model control but not in different experimental test groups during study period was found to be unaltered. This feature is of paramount importance because nutritional depreciation causing body weight loss may parallel a decrease in tumor volume.

Further confirmation was obtained by expression studies of Estrogen (ER) and progesterone (PR) expressions by immunohistochemistry. ER activation in breast and uterus enhances cell proliferation which is necessary for growth and maintenance of tissues (Thordarson et al., 2001). When the response to estrogens by the endocrine system is deregulated, ER activation might eventually result in tumor formation. Studies suggests that reduced levels of ER-α in the mammary gland predict low breast cancer risk. Literature revealed that MNU induces estrogen dependent tumors (Thordarson et al., 2001). Overexpression of ER can be due to binding of growth factors also like IGF-I, IGF II, EGF and TGF. PR-B is required for normal mammary gland development; PR+ cells in the mammary gland may interact primarily with stromal components to mediate proliferative signaling of nearby or neighboring PR-null cells via the action of locally acting growth factors. Both the rapid actions and the transcriptional activity of PR-B contribute to breast cancer cell proliferation in response to progesterone. Our findings are in line with previous studies demonstrating that MNU injected rats showed increased expression levels of ER and PR (Thordarson et al., 2001). These levels were significantly reduced in both standard and treatment group (POPG 400 mg/kg). The effect might be contributed to decreasing levels of endogenous hormones and cytokine levels. It also possesses NF-Kb (Choi et al., 2008) and aromatase inhibitory activity which decrease gene mutation and transcription (Duke and Beckstrom-Sternberg, 1994).

Nucleic acids damage is a sensitive indicator and a prospective biological target for many initiators of carcinogenesis. Elevation of DNA adducts formation and oxidative base lesions have been reported in the normal adjacent and tumor tissues of breast cancer patients. These findings suggest that an accumulation of DNA damage may contribute to breast carcinogenesis. Hence, the determination of DNA content plays an important role in tumorigenesis. The increased DNA content in cancer-bearing breast may be due to the increased expression of enzymes which are necessary for DNA synthesis in tumor cells with repression of many enzymes related to differentiated cell function. RNA levels were also found to be increased in the cancerous condition; the uncharacteristic increased content of DNA may lead to an increased transcription that leads to the increased RNA content of tumor cells. Jagadeesan et al. (2013) proved that diosgenin treatment to MNU induced mammary carcinoma female rats showed decrease in DNA and RNA levels. In our study, the model control animals, 56% and 90% hike in DNA and RNA levels were observed as compared to normal control.

The percentage reduction in DNA content in POPG (100, 200, 400mg/kg) treated group were 22.37%, 24.69% and 29.90% respectively. The percentage reduction in RNA content in POPG (100, 200, 400mg/kg) treated group were 31.81%, 32.37% and 33.01% respectively. The levels were brought back to be nearly the usual level, which intimate the anti-tumor property of the drugs that slow down the progression of tumor growth, since the size and weight of the tumor is well linked with the tumors DNA content in malignant conditions. The effect might be due to the intervention strategies of the POPG in nucleic acid biosynthesis which ultimately results in the inhibition on the rate of development of tumors through controlled nucleic acid biosynthesis and exhibits the tumor inhibitory effect during POPG treatment. Tamoxifen treated animals showed 33.5% and 40.21% inhibition in DNA and RNA levels as compared to model control.

In conclusion, POPG was found to be more potent cytotoxic in MCF-7 estrogen positive human breast cancer cell line than in MDA-MB-453 and MDA-MB-231. The POPG is found to be apoptotic as they increased the early and late apoptotic cell population. POPG is found to be anti-angiogenic and anti-metastatic. The results of methylnitrosourea (MNU) induced mammary carcinogenesis is in accordance to *in-vitro* cell lines studies. The cancer manifesting from MNU is Estrogen and Progesterone positive; which is more prevalent in humans also. The mammary gland differentiation, prevention of

mammary tumor induction, augmentary changes in nucleic acid & receptor status suggests chemo-preventive potential of POPG in MNU induced mammary carcinogenesis. The chemo-preventive activities are likely mediated through a number of mechanisms involving inhibition of cell proliferation, metastasis, angiogenesis, overexpression of hormones and nucleic acid content.

Conflicting interest

The Author(s) declare(s) that they have no conflicts of interest to disclose.

Source of funding: None declared

Acknowledgements

We want to thank Navli Poultry Farm for providing fertilized eggs for CAM assay; Dr. Rishit Zalawadia, Senior Manager-Discovery Biology (Pharmacology), Sun Pharma Advanced Research Company Ltd, Vadodara for his help in data analysis.

References

Barbalho S, Farinazzi-Machado F, de Alvares Goulart R, Brunnati AS, Ottoboni A, Nicolau C. 2012. *Psidium guajava* (Guava): a plant of multipurpose medicinal applications. Medicinal & Aromatic Plants, 1(104):2167-0412.

Chen KC, Peng C-C, Chiu W-T, Cheng Y-T, Huang G-T, Hsieh C-L, Peng RY. 2010. Action mechanism and signal pathways of Psidium guajava L. aqueous extract in killing prostate cancer LNCaP cells. Nutrition and Cancer, 62(2):260-270.

Chen ML, Lin YH, Yang CM, Hu ML. 2012. Lycopene inhibits angiogenesis both in vitro and in vivo by inhibiting MMP-2/uPA system through VEGFR2-mediated PI3K-Akt and ERK/p38 signaling pathways. Molecular Nutrition & Food Research, 56(6):889-899.

Choi SY, Hwang JH, Park SY, Jin YJ, Ko HC, Moon SW, Kim SJ. 2008. Fermented guava leaf extract inhibits LPS-induced COX-2 and iNOS expression in Mouse macrophage cells by inhibition of transcription factor NF-κB. Phytotherapy Research, 22(8):1030-1034.

Deryugina EI, Quigley JP. 2008. Chick embryo chorioallantoic membrane models to quantify angiogenesis induced by inflammatory and tumor cells or purified effector molecules. Methods in Enzymology, 444:21-41.

Duke JA, Beckstrom-Sternberg SM. 1994. Dr. Duke's phytochemical and Ethnobotanical Databases.

Feng XH, Wang Z-h, Meng D-l, Li X. 2015. Cytotoxic and antioxidant constituents from the leaves of Psidium guajava. Bioorganic & Medicinal Chemistry Letters, 25(10):2193-2198.

Gakunga JN, Mirianga B, Muwonge H, Sembajwe LF, Kateregga J. 2013. Antidiarrheal activity of ethanolic fruit extract of Psidium guajava (Guava) in castor oil induced diarrhea in albino rats. National Journal of Physiology: Pharmacy and Pharmacology, 3(2):191-197.

Hanahan D, Weinberg RA. 2000. The hallmarks of cancer. Cell 100(1):57-70.

Harfindal E, Helms R. 2006. Textbook of Therapeutics Drug and Disease Management, 8th End. Lippincott Williams & Wilkins, Philadelphia, pp. 2358-2377.

Holliday DL, Speirs V. 2011. Choosing the right cell line for breast cancer research. Breast Cancer Research, 13(4):215-221.

Jagadeesan J, Langeswaran K, Gowthamkumar S, Balasubramanian MP. 2013. Diosgenin exhibits beneficial efficiency on human mammary carcinoma cell line MCF-7 and against N-nitroso-N-methylurea (NMU) induced experimental mammary carcinoma. Biomedicine & Preventive Nutrition, 3(4):381-388.

Kaileh M, Berghe WV, Boone E, Essawi T, Haegeman G. 2007. Screening of indigenous Palestinian medicinal plants for potential anti-inflammatory and cytotoxic activity. Journal of Ethnopharmacology, 113(3):510-516.

Karia PD, Patel KV, Rathod SS. 2018. Breast cancer amelioration by Butea monosperma in-vitro and in-vivo. Journal of Ethnopharmacology, 217:54-62.

Kawakami Y, Nakamura T, Hosokawa T, Suzuki-Yamamoto T, Yamashita H, Kimoto M, Tsuji H, Yoshida H, Hada T, Takahashi Y. 2009. Antiproliferative activity of guava leaf extract via inhibition of prostaglandin endoperoxide H synthase isoforms. Prostaglandins, Leukotrienes and Essential Fatty Acids, 80(5):239-245.

Lu J, Papp LV, Fang J, Rodriguez-Nieto S, Zhivotovsky B, Holmgren A. 2006. Inhibition of mammalian thioredoxin reductase by some flavonoids: implications for myricetin and quercetin anticancer activity. Cancer Research, 66(8):4410-4418.

Ma H, Carpenter CL, Sullivan-Halley J, Bernstein L. 2011. The roles of herbal remedies in survival and quality of life among long-term breast cancer survivors-results of a prospective study. BMC cancer, 11(1):1.

Macejova D, Brtko J. 2001. Chemically induced carcinogenesis: a comparison of 1-methyl-1-nitrosourea, 7, 12-dimethylbenzanthracene, diethylnitroso-amine and azoxymethan models (minireview). Endocrine Regulations, 35(1):53-60.

Martin G, Melito G, Rivera E, Levin E, Davio C, Cricco G, Andrade N, Caro R, Bergoc R. 1996. Effect of tamoxifen

on intraperitoneal N-nitroso-N-methylurea induced tumors. Cancer Letters 100 (1): 227-234..

Miean KH, Mohamed S. 2001. Flavonoid (myricetin, quercetin, kaempferol, luteolin, and apigenin) content of edible tropical plants. Journal of Agricultural and Food Chemistry, 49(6):3106-3112.

Ojewole J. 2006. Antiinflammatory and analgesic effects of Psidium guajava Linn.(Myrtaceae) leaf aqueous extract in rats and mice. Methods and Findings in Experimental and Clinical Pharmacology, 28(7):441-446.

Paoletta S, Steventon G, Wildeboer D, Ehrman T, Hylands P, Barlow D. 2008. Screening of herbal constituents for aromatase inhibitory activity. Bioorganic & medicinal chemistry, 16(18):8466-8470.

Parikh RR, Gildener-Leapman N, Narendran A, Lin H-Y, Lemanski N, Bennett JA, Jacobson HI, Andersen TT. 2005. Prevention of N-Methyl-N-Nitrosourea–Induced Breast Cancer by α-Fetoprotein (AFP)–Derived Peptide, a Peptide Derived from the Active Site of AFP. Clinical Cancer Research, 11(23):8512-8520.

Parvathaneni M, Battu GR, Gray AI, Gummalla P. 2014. Investigation of anticancer potential of hypophyllanthin and phyllanthin against breast cancer by in vitro and in vivo methods. Asian Pacific Journal of Tropical Disease, 4:S71-S76.

Pistritto G, Trisciuoglio D, Ceci C, Garufi A, D'Orazi G. 2016. Apoptosis as anticancer mechanism: function and dysfunction of its modulators and targeted therapeutic strategies. Aging, 8(4):603.

Rai P, Singh S, Kesari A, Watal G. 2007. Glycaemic evaluation of Psidium guajava in rats. Indian Journal of Medical Research 126 (3):224.

Rengarajan T, Nandakumar N, Balasubramanian MP. 2013. D-pinitol prevents rat breast carcinogenesis induced by 7, 12-Dimethylbenz [a] anthracene through inhibition of Bcl-2 and induction of p53, caspase-3 proteins and modulation of hepatic biotransformation enzymes and antioxidants. Biomedicine & Preventive Nutrition, 3(1):31-41.

Rockwell S, Liu Y, Higgins SA. 2005. Alteration of the effects of cancer therapy agents on breast cancer cells by the herbal medicine black cohosh. Breast Cancer Research and Treatment, 90(3):233-239.

Sakarkar D, Deshmukh V. 2011. Ethnopharmacological review of traditional medicinal plants for anticancer activity. International Journal of PharmTech Research, 3(1):298-308.

Samant RS, Shevde LA. 2011. Recent advances in anti-angiogenic therapy of cancer. Oncotarget, 2(3):122.

Siegel RL, Miller KD, Jemal A. 2017. Cancer statistics, 2017. CA: A Cancer Journal for Clinicians 67 (1):7-30.

Takiar R, Nadayil D, Nandakumar A. 2010. Projections of number of cancer cases in India (2010–2020) by cancer groups. Asian Pacific Journal of Cancer Prevention, 11(4):1045-1049.

Tang EL, Rajarajeswaran J, Fung SY, Kanthimathi M. 2013. Antioxidant activity of Coriandrum sativum and protection against DNA damage and cancer cell migration. BMC Complementary and Alternative Medicine, 13(1):347-359.

Thaipong K, Boonprakob U, Crosby K, Cisneros-Zevallos L, Byrne DH. 2006. Comparison of ABTS, DPPH, FRAP, and ORAC assays for estimating antioxidant activity from guava fruit extracts. Journal of Food Composition and Analysis, 19(6):669-675.

Thordarson G, Lee AV, McCarty M, Van Horn K, Chu O, Chou Y-C, Yang J, Guzman RC, Nandi S, Talamantes F. 2001. Growth and characterization of N-methyl-N-nitrosourea-induced mammary tumors in intact and ovariectomized rats. Carcinogenesis, 22(12):2039-2047.

Weigelt B, Peterse JL, Van't Veer LJ. 2005. Breast cancer metastasis: markers and models. Nature Reviews. Cancer, 5(8):591.

Zhu X, Wang K, Zhang K, Zhu L, Zhou F. 2014. Ziyuglycoside II induces cell cycle arrest and apoptosis through activation of ROS/JNK pathway in human breast cancer cells. Toxicology Letters, 227(1):65-73.